

2012

# Glia Delimit Shape Changes Of Sensory Neuron Receptive Endings in *C. elegans*

Carl Procko

Follow this and additional works at: [http://digitalcommons.rockefeller.edu/student\\_theses\\_and\\_dissertations](http://digitalcommons.rockefeller.edu/student_theses_and_dissertations)

 Part of the [Life Sciences Commons](#)

---

## Recommended Citation

Procko, Carl, "Glia Delimit Shape Changes Of Sensory Neuron Receptive Endings in *C. elegans*" (2012). *Student Theses and Dissertations*. Paper 132.



**GLIA DELIMIT SHAPE CHANGES OF SENSORY  
NEURON RECEPTIVE ENDINGS IN *C. ELEGANS***

A Thesis Presented to the Faculty of  
The Rockefeller University  
in Partial Fulfillment of the Requirements for  
the degree of Doctor of Philosophy

by  
Carl Procko  
June 2012



**GLIA DELIMIT SHAPE CHANGES OF SENSORY NEURON RECEPTIVE  
ENDINGS IN *C. ELEGANS***

Carl Procko, Ph.D.

The Rockefeller University 2012

Neuronal receptive endings such as dendritic spines and sensory protrusions are structurally remodeled by experience. How receptive endings acquire their remodeled shapes is not well understood. In response to environmental stressors, including starvation, crowding and high temperature, the nematode *Caenorhabditis elegans* enters a diapause state, termed dauer, which is accompanied by remodeling of sensory neuron receptive endings. Here, we demonstrate that sensory receptive endings of the AWC amphid neurons in dauer animals remodel in the confines of a compartment defined by the amphid sheath glial cells that envelop these endings. The glia remodel concomitantly with and independently of AWC receptive endings to delimit AWC receptive ending growth. Remodeling of the glia requires the Otd/Otx transcription factor TTX-1, the C2H2 zinc finger transcription factor ZTF-16, the fusogen AFF-1, and likely the VEGFR-related protein VER-1, all acting within the glial cell. *ver-1* expression is induced by dauer entry and by cultivation at high temperature, and requires direct binding of TTX-1 and perhaps also ZTF-16 to *ver-1* regulatory sequences. Our results demonstrate that experience-induced changes in glial compartment size provide spatial constraints on neuronal receptive ending growth.

## Acknowledgements

First and foremost, I would like to acknowledge my mentor Shai for his encouragement and guidance. Shai's lab has always been an enjoyable place to work, even during periods of scientific frustration.

Within the lab, special mention also goes to Yun Lu, who performed all the electron microscopy work presented in this thesis. In addition, Aakanksha Singhvi, Elliot Perens, Grigoris Oikonomou, Maya Tevlin, Max Heiman, Menachem Katz and Taulant Bacaj shared reagents and data.

All members of the lab have contributed to the helpful and enjoyable work environment; particular thanks go to my travel and political sparring partner Taulant, Max for scientific advice, and Grigoris for enjoying beer, BBQ and nachos. Thanks also to my baymate Margherita and lab technicians Limor, Melanie and Sharon.

I would like to acknowledge my thesis committee members, past and present, for discussion and comments: Cori Bargmann, Fred Cross and Leslie Vosshall. Thanks also to my external member, Piali Sengupta, and the Dean's Office for their support.

Of course, I must also thank all the friends and family who have contributed to making my life in New York as rewarding as it has been. What kind of week would it be without our regular sushi night (Cat, Doeke, Doro, Ellina, Grigoris, Holger, Nicolai) or regular bouts of cards and tennis (Boo, John, Yun)? Final mention goes to my immediate family in the United States: my twin brother Erik for his competition and bickering, my cat Grizzly for keeping me well-groomed, and my beautiful wife Andrea, who has had to put up with my shortcomings more than any other.

## Table of Contents

<b>Acknowledgements</b> .....	iii
<b>Table of Contents</b> .....	iv
<b>List of Figures</b> .....	vi
<b>List of Tables</b> .....	viii
<b>Chapter 1: Introduction</b> .....	1
Organisms respond developmentally to environmental stress .....	2
Environmental sensory organs in animals are composed of neurons and glia .....	5
Glia are important for neuronal dendrite shapes .....	10
The nematode <i>Caenorhabditis elegans</i> responds developmentally to environmental stress .....	16
The amphids sense the environment in <i>C. elegans</i> .....	21
The <i>C. elegans</i> amphids as a model of neuron-glia interactions .....	27
Amphid dendrite endings and glia shapes are remodeled in <i>C. elegans</i> dauer larvae .....	32
Does plasticity of dendrite receptive ending shapes depend on glial plasticity? .....	33
<b>Chapter 2: Glia delimit shape changes of sensory neuron receptive endings</b> .....	37
Summary .....	38
Results .....	39
Loss of <i>daf-7</i> /TGF- $\beta$ promotes dauer remodeling of AWC neurons .....	39
AMsh glia fusion is dependent on AFF-1 and is not reversible .....	41
AMsh glia remodeling is independent of AWC expansion .....	48
<i>ttx-1</i> is required in AMsh glia for glia remodeling .....	52
Proper remodeling of AWC neurons requires glia .....	60
Discussion .....	63
<b>Chapter 3: Transcription in glia depends on dauer and environmental temperature</b> .....	66
Summary .....	67
Results .....	68
<i>ttx-1</i> promotes AMsh glia remodeling by inducing <i>ver-1</i> /RTK expression .....	68
<i>ver-1</i> exhibits temperature-dependent expression in dauers and non-dauers .....	77
Discussion .....	88
The VEGFR-related gene <i>ver-1</i> is required for glia remodeling .....	88
<i>ttx-1</i> regulates cell shape in thermoresponsive cells .....	89
<i>ver-1</i> transcription can be used as a tool for finding genes required for glia remodeling .....	92
<b>Chapter 4: Transcriptional regulators of the receptor tyrosine kinase <i>ver-1</i> are required for AMsh glia remodeling</b> .....	93
Summary .....	94

Results.....	95
Mutants with reduced <i>ver-1</i> reporter expression generally fall into 3 complementation groups.....	95
The C2H2 zinc finger factor <i>ztf-16</i> is required for <i>ver-1</i> expression .....	101
<i>ztf-16</i> functions within glia to regulate <i>ver-1</i> .....	108
ZTF-16 regulates the <i>ver-1</i> promoter through a site distinct from that bound by TTX-1 .....	113
<i>ztf-16</i> function is required in glia for AMsh glia fision in dauer animals.....	115
Discussion.....	120
<b>Chapter 5: Conclusions and future directions</b> .....	124
Glia are required for dendrite morphological plasticity .....	125
Glia can respond to environmental and developmental cues.....	127
Identifying glial factors required for morphological plasticity.....	130
What is the physiological purpose of amphid remodeling?.....	132
Amphid sensory organ remodeling as a model of nervous system plasticity .....	134
<b>Chapter 6: Experimental Procedures</b> .....	135
Strains .....	136
Germline transformation and transgene integration .....	137
Microscopy .....	137
Mutagenesis and mapping .....	138
Dauer selection .....	138
Cytoplasmic mixing assay to score AMsh glia fusion .....	139
Thermotaxis assays .....	139
Chemotaxis assays .....	140
Electrophoretic mobility-shift assays (EMSAs) .....	140
RNAi of <i>aff-1</i> and <i>eff-1</i> .....	141
Cell ablations .....	141
Statistics.....	142
Plasmid construction and isolation of cDNAs.....	142
<b>Appendices</b> .....	146
<b>Appendix 1:</b> Attempted rescue of the AMsh glia fusion defect of <i>ver-1</i> mutants.....	147
<b>Appendix 2:</b> The guanylyl cyclases GCY-8 and GCY-23 are not directly activated by temperature .....	151
<b>Appendix 3:</b> Null alleles of <i>ttx-1</i> may be lethal.....	154
<b>Appendix 4:</b> <i>fkh-9</i> may set a baseline for glial <i>ver-1</i> promoter:: <i>gfp</i> expression.....	159
<b>Appendix 5:</b> Dauer animals are repelled by isoamyl alcohol and benzaldehyde .....	172
<b>Appendix 6:</b> <i>ttx-1</i> likely functions in AFD to regulate dauer exit of <i>daf-7(e1372)</i> mutants.....	174
<b>References</b> .....	176

## List of Figures

Figure 1.1: Organisms are adapted to life in specific environments .....	3
Figure 1.2: Glia affect guidance of dendrite growth.....	13
Figure 1.3: The life cycle of <i>Caenorhabditis elegans</i> .....	17
Figure 1.4: A schematic drawing of the two amphid sensory structures in <i>C. elegans</i> .....	22
Figure 1.5: A model for glial involvement in dendrite extension of <i>C. elegans</i> sensory neurons.....	29
Figure 1.6: AWC neuron receptive endings and AMsh glia remodel in dauer larvae.....	34
Figure 2.1: AWC neuron receptive endings and AMsh glia remodel in dauer animals ....	40
Figure 2.2: Scoring AMsh glia fusion by cytoplasmic mixing.....	42
Figure 2.3: AMsh glia fusion is dependent on the <i>aff-1</i> fusogen.....	43
Figure 2.4: Cytoplasmic mixing of GFP between fused AMsh glia.....	46
Figure 2.5: Remodeling of AMsh glia persists in dauer-recovered adults .....	47
Figure 2.6: Changes in AMsh glia shape correlate with AWC neuron remodeling .....	49
Figure 2.7: Changes in AWC shape are not required for AMsh glial fusion .....	50
Figure 2.8: <i>ttx-1</i> is required for AMsh glia remodeling in dauers .....	54
Figure 2.9: <i>ttx-1</i> is expressed in glia .....	55
Figure 2.10: Glial expression of TTX-1 is not required for AFD morphology or AFD-mediated thermotaxis behavior .....	58
Figure 2.11: <i>ttx-1</i> is required for remodeling of AMsh glia .....	61
Figure 2.12: The AWC neuron cilia are constrained by the ensheathing AMsh glia .....	62
Figure 3.1: Dauer-induced expression of <i>ver-1</i> is dependent on <i>ttx-1</i> .....	69
Figure 3.2: Mutations in <i>ver-1</i> affect glia remodeling in dauers .....	71
Figure 3.3: TTX-1 can bind directly to the <i>ver-1</i> promoter .....	74
Figure 3.4: TTX-1 directly regulates glial and AFD genes .....	75
Figure 3.5: <i>ver-1</i> promoter:: <i>gfp</i> has temperature-dependent expression in AMsh and PHsh glia.....	78
Figure 3.6: Effect of temperature and dauer on other AMsh glia reporters .....	80
Figure 3.7: TTX-1 is required continuously for temperature-dependent expression of <i>ver-1</i> in AMsh glia.....	85
Figure 3.8: TTX-1 is required continuously for AFD morphology .....	86
Figure 3.9: <i>old-2</i> , a <i>ver-1</i> -related tyrosine kinase gene, is also expressed in AMsh glia ..	90

Figure 4.1: Mutations in the <i>Otx</i> -type transcription factor <i>ttx-1</i> reduce <i>ver-1</i> promoter:: <i>gfp</i> expression .....	98
Figure 4.2: Mutations in the RING finger and B-box domain factor <i>tam-1</i> reduce <i>ver-1</i> promoter:: <i>gfp</i> expression .....	100
Figure 4.3: Temperature- and dauer-induced expression of <i>ver-1</i> is reduced in <i>ns171</i> mutants .....	103
Figure 4.4: <i>ns171</i> mutants have wild-type AFD sensory ending morphology and thermotaxis behavior .....	104
Figure 4.5: The C2H2 zinc finger gene <i>ztf-16</i> is required for <i>ver-1</i> expression .....	105
Figure 4.6: ZTF-16 is expressed in glia and localizes to the nucleus .....	110
Figure 4.7: ZTF-16 regulates expression from the <i>ver-1</i> promoter through a site independent of the TTX-1 binding site .....	114
Figure 4.8: ZTF-16 may bind directly to the <i>ver-1</i> promoter .....	116
Figure 4.9: <i>ztf-16</i> function is required for AMsh glial remodeling in dauer animals .....	118
Figure A1.1: VER-1::GFP localizes as puncta .....	149
Figure A2.1: GCY-8 and GCY-23 are not directly activated by temperature .....	152
Figure A3.1: <i>ttx-1(ns260)</i> heterozygous animals express low <i>ver-1</i> promoter:: <i>gfp</i> .....	155
Figure A3.2: Glial and AFD-specific expression of <i>ttx-1</i> cDNA fail to rescue <i>ns260</i> lethality .....	156
Figure A4.1: <i>ns198</i> mutants have increased <i>ver-1</i> promoter:: <i>gfp</i> reporter intensity .....	160
Figure A4.2: <i>ns198</i> does not affect <i>vap-1</i> promoter:: <i>dsRed</i> expression in AMsh glia .....	162
Figure A4.3: <i>ns198</i> mutants have wild-type thermotaxis behavior .....	163
Figure A4.4: Mutations in <i>fkh-9</i> increase <i>ver-1</i> promoter:: <i>gfp</i> expression .....	165
Figure A4.5: <i>fkh-9</i> is a glia-expressed nuclear factor .....	167
Figure A4.6: Mutations in <i>fkh-9</i> do not affect dauer-induced glia remodeling .....	169
Figure A4.7: A mutation in the linker histone <i>his-24</i> causes a weak increase in <i>ver-1</i> promoter:: <i>gfp</i> expression .....	170
Figure A5.1: <i>daf-7(e1372)</i> dauer animals are repelled by isoamyl alcohol (IAA) .....	173
Figure A6.1: <i>ttx-1</i> likely functions in AFD to regulate dauer exit of <i>daf-7(e1372)</i> mutants .....	175

## List of Tables

Table 3.1: A summary of <i>ver-1</i> promoter deletion studies .....	73
Table 3.2: Effects of mutations in genes controlling thermotaxis, neuronal morphology, dauer, and the heat-shock/UPR pathways on <i>ver-1</i> promoter:: <i>gfp</i> expression .....	81
Table 3.3: TTX-1 acts in glia, and not AFD, to control temperature-dependent <i>ver-1</i> expression .....	83
Table 3.4: . Restoring <i>ttx-1</i> expression to <i>ttx-1(p767)</i> mutant adults using a heat-inducible promoter rescues <i>ver-1</i> expression .....	84
Table 4.1: Alleles that reduce <i>ver-1</i> promoter:: <i>gfp</i> expression generally fall into one of three complementation groups .....	97
Table 4.2: <i>ztf-16</i> acts in glia to control <i>ver-1</i> expression .....	112
Table 6.1: List of plasmids generated in this work .....	143
Table A1.1: Attempted rescue of the AMsh glia fusion defect of <i>ver-1(tm1348)</i> mutant dauer animals .....	148
Table A4.1: Mutations in the <i>fkh-9</i> gene increase <i>ver-1</i> promoter:: <i>gfp</i> expression .....	161

# **Chapter 1**

Introduction

## **Organisms respond developmentally to environmental stress**

Organisms are adapted to life in particular environments (Figure 1.1). As an environment changes, the organism senses the change and responds to optimize metabolism and growth. Extreme environmental stress poses an additional problem: how to survive and maximize reproductive success in unfavorable conditions that may otherwise be lethal. Accordingly, many organisms have evolved developmental strategies to persist under high stress conditions.

In response to environmental insults, some organisms enter a specialized, stress-resistant state. Such a state permits both the temporal avoidance of the environmental insult, and also the dispersal of the organism from one environment to another. For example, in response to nutrient depletion some species of bacteria become stress-resistant endospores. Endospores are metabolically-inactive cellular structures, with a thick, multi-layered protein coat and a dehydrated core (Nicholson et al., 2000). Specialized endospore proteins, called  $\alpha/\beta$ -type small acid soluble spore proteins (SASPs), are synthesized during sporulation and bind to the DNA, generating a protective, conformational change. These developmental changes in the bacterium confer resistance to environmental stressors, including temperature, DNA-damaging ultraviolet radiation, and noxious chemicals (Nicholson et al., 2000). These developmental changes are reversible: upon return to a favorable environment the endospore will germinate and return to vegetative growth. Endospores have incredible longevity; indeed, the endospores of a *Bacillus* species have been recovered from an extinct symbiotic bee host preserved in amber over 25 million years ago (Cano and Borucki, 1995)!



**Figure 1.1. Organisms are adapted to life in specific environments.** In hot springs, a thermal gradient is generated between where the water emerges to where it is cooled at the pool's edge. Different microbial communities grow along this gradient and produce dramatic changes in color; a result of the different ratios of chlorophyll and carotenoid pigments of the different microorganisms. The rate of photosynthesis and growth of a microbial species is optimized for the temperature in which it grows (Brock, 1967; Brock and Brock, 1966; Ward et al., 1998). (Grand Prismatic Spring, WY, U.S.A.)

Another strategy employed by organisms to escape a temporal period of stress is to generate stress-resistant offspring. For example, in response to changes in water temperature many fresh and saltwater sponges reproduce asexually to generate gemmules. Gemmules are comprised of metabolically-repressed cells that are packaged into collagenous glass capsules. These packages are resistant to environmental insults such as freezing and desiccation (Loomis, 2010). In gemmules of the sponge species *Eunapius fragilis*, the synthesis of sorbitol may serve as a cryoprotectant and also to generate a high osmotic pressure, which represses germination. The return to a favorable environment triggers the synthesis of sorbitol dehydrogenase, in turn relieving osmotic pressure and permitting germination and the differentiation of the encapsulated cells into a new sponge (Loomis, 2010; Loomis et al., 2009). This strategy ensures the genetic success of the organism during freezing winters and summer droughts.

In response to high temperature and low water availability, many animals also enter a developmental period of metabolic arrest known as estivation. Land snails, for example, have evolved annual cycles of estivation during unfavorable environmental periods. Estivation even allows some species to survive in arid environments that may not see rainfall within a given year (Schmidt-Nielsen et al., 1971). Estivation is marked by a dramatic reduction in metabolic rate (Schmidt-Nielsen et al., 1971) and the generation of an epiphragm, a protective calcium carbonate membrane that seals off the inside of the shell to the environment (Arad et al., 1989). Estivating land snails are resistant to desiccation and high temperatures, and can survive prolonged periods of stress.

Vertebrates, including mammals, are also known to enter periods of estivation when food is limiting and when challenged with a hot, dry environment. Most species of lungfish undergo seasonal estivation when the water level of their environment is reduced. The African lungfish *Protopterus annectens* excavates a burrow in the mud, and secretes a mucous from epithelial mucous glands to generate a protective cocoon that prevents water loss from the dormant animal (Secor and Lignot, 2010). Similarly, estivating amphibians reduce metabolism to increase survival time on endogenous energy stores, and some species will also generate a cocoon to prevent desiccation (Secor and Lignot, 2010). These animals can survive many months at a time waiting for water levels to return. Hibernating and estivating mammals also reduce metabolism to conserve energy, and switch from carbohydrate to lipid metabolism during the period of dormancy (Melvin and Andrews, 2009).

Together, these examples illustrate the importance of environment on organism development and the need for an organism to respond appropriately to survive and reproduce in non-ideal conditions.

## **Environmental sensory organs in animals are composed of neurons and glia**

In animals, many stressors and other environmental cues are detected by specialized sensory organs, which regulate both developmental and behavioral responses to the environment. Generally, sensory organs are composed of dedicated sensory

neurons, which are responsible for collecting environmental information and converting it into an electrical signal, and their associated glia, or glia-like cells.

Glia are intimately associated with neurons and are the most abundant cell type of the mammalian brain. Like neurons, they exhibit vast morphological complexity and specialization (Awasaki et al., 2008; Cajal, 1911; Doherty et al., 2009). Broadly defined, glia are non-neuronal cells that are closely associated with neurons, and which are lineally related (Shaham, 2005). Glia form an integral part of the nervous system: they secrete trophic factors required for neuronal survival (Meyer-Franke et al., 1995), they can provide a framework for neuronal migration and patterning (Rakic, 1971; Rakic, 1972), they form the myelin sheath around axons required for fast nerve impulses, they modulate neuronal communication at synapses (Panatier et al., 2006; Robitaille, 1998), and they can affect neuron shapes and dendritic morphologies (see below). Although the purpose of glia in brain development and function has received much attention, the role of these cells in sensory organs has been little studied.

For example, sensory neurons of the vertebrate olfactory epithelium are associated with glia-like sustentacular cells. The epithelium consists of stratified cell layers: the sustentacular cell bodies are located apically, while the sensory neurons are located beneath these. Basal to these layers are the progenitor cells that give rise to both the sensory neurons and the sustentacular support cells (Leung et al., 2007). Sustentacular cells share properties with glia: they electrically isolate the neuronal sensory dendrites (Breipohl et al., 1974), they exhibit phagocytic activity following neuronal cell death (Suzuki et al., 1996), and electrically-coupled sustentacular cells have the capacity for glia-like intercellular calcium waves (Hegg et al., 2009). It is likely that

these glia-like cells also serve a neuroprotective role. Specifically, they express high levels of detoxifying proteins such as cytochrome *P450* and *glutathione S-transferase* (Rodriguez et al., 2008). Furthermore, *Notch2* receptor mRNA is detectable in sustentacular cells but not olfactory neurons, and conditional knockout of the receptor in the epithelium results in altered sustentacular cell morphology and gene expression. This is accompanied by a disruption of the laminar structure of the epithelium and increased neuron degeneration in the postnatal mouse (Rodriguez et al., 2008).

Interestingly, sustentacular cells may also play an active role in regulating odor sensitivity of the olfactory sensory neurons. In response to hunger, animals typically have heightened sensitivity to odors, perhaps as a strategy to locate food in a complex environment (Aime et al., 2007). Compared to satiated animals, the sustentacular cells of starved *Xenopus laevis* tadpoles have higher levels of *diacylglycerol lipase  $\alpha$* , which synthesizes the intercellular signaling molecule 2-AG (Breunig et al., 2010). CB1 cannabinoid receptors, which respond to 2-AG, are expressed in the associated sensory neurons and localize to the dendrites (Czesnik et al., 2007). Inhibition of 2-AG synthesis to mimic the fed state increases the odor threshold required for neuron firing, while a CB1 agonist lowers the threshold of odor sensitivity (Breunig et al., 2010). These findings suggest that glia-like sustentacular cells modulate the activity of their associated sensory neurons by altering 2-AG release depending on the hunger state of the animal.

Likewise, supporting cells of the mammalian ear may contribute to hearing sensitivity. Deiters' cells form a scaffold that supports the sensory outer hair cells of the cochlea, and express the glial marker *glial fibrillary acidic protein (GFAP)*, suggesting they are glia (Rio et al., 2002). Following high-intensity sound exposure, Deiters' cells

are displaced towards the outer hair cells (Flock et al., 1999). This movement correlates with a loss of sensitivity of the cochlea to a test tone. Continued acoustic overstimulation results in damage to the outer hair cells; therefore, the displacement of the Deiters' cells and corresponding loss in hearing sensitivity may represent a protective mechanism against acoustic assault (Flock et al., 1999).

Glia are also associated with sensory neurons in the vertebrate eye. In the retina, both Müller glia and retinal pigmented epithelial (RPE) cells make contacts with photoreceptor cells. One purpose of these glia may be neural regeneration. In response to acute damage or destruction of photoreceptor cells by high-intensity light, Müller glia re-enter the cell cycle and dedifferentiate to produce embryonic retinal progenitor cells. These cells can subsequently form new photoreceptors, neurons or glia (Bernardos et al., 2007; Fischer and Reh, 2001). In addition, the cylindrical shape and orientation of Müller glia in the direction of incoming light might serve to guide light directly to the associated photoreceptor cells, perhaps improving the signal-to-noise ratio of an image (Franze et al., 2007).

RPE cells also make contact with photoreceptors, ensheathing the outer segment of the photoreceptor cell. RPE cells regulate the availability of the retinal chromophore, which is required for light detection by photoreceptors, as well as nutrient availability and ion homeostasis in the subretinal space to ensure correct photoreceptor function and excitability (Strauss, 2005). In addition, RPE cells play a critical role in reducing photo-oxidative stress within the photoreceptor cell. The high levels of light encountered by photoreceptors can lead to the buildup of reactive products from photo-oxidative reactions, causing retinal degeneration. RPE cells protect the photoreceptors by filtration

of light through RPE cell pigments, and the expression of antioxidants and detoxifying agents (Kevany and Palczewski, 2010). As a further measure to prevent the buildup of reactive photo-oxidative products, photoreceptor cells continually shed and regenerate about 10% of their outer segment volume every day. The outer segment is loaded with membranous discs of photosensitive pigment. These discs are assembled at the segment base and continually displaced along the segment as more discs are synthesized. At the end of the outer segment the oldest discs most likely to have accumulated damaging reactive species are detached from the photoreceptor cell, and the membranous debris is phagocytosed and degraded by the ensheathing RPE cell (Steinberg et al., 1977; Young and Bok, 1969). In animals where the phagocytic function of RPE cells is defective, the membranous debris shed by the photoreceptors accumulates in the subretinal space and results in retinal degeneration and loss of vision (Bok and Hall, 1971).

In addition, vertebrate RPE cells are required to regenerate the retinal chromophore isomer bound to the photosensitive pigments that absorb light. Photon absorption by the pigment results in the conversion of 11-*cis*-retinal to all-*trans*-retinal in the photoreceptor cell. The RPE cell is essential for regenerating 11-*cis*-retinal from all-*trans*-retinal, and makes the molecule available again to the photoreceptor for use in another transduction cycle (Baehr et al., 2003).

Together, these fledgling observations suggest that the role of glia in sensory organs is diverse: they secrete factors required for sensory function and neuroprotection, they can regenerate neurons after tissue damage, they act as phagocytic cells to remove neuronal debris, and they can regulate neuron function in response to animal state.

## **Glia are important for neuronal dendrite shapes**

Although glia have been shown to be important for sensory neuron function, there have been few reports describing a role of glia in sensory neuron morphology. Sensory cells and other neurons display enormous diversity in shape; the most prominent morphological feature being their complex and highly stereotyped dendritic arbors (Cajal, 1911; Gao, 2007). This diversity is in no small part a result of each dendrite's unique task: to gather information from specific synaptic partners or from the environment, and to transmit this information to the axon. Although knowledge of the roles of glia in regulating sensory dendrite shape is lacking, numerous studies have explored glia-dendrite interactions in non-sensory systems.

Some of the signals controlling dendritic arbor shapes are neuron intrinsic. For example, the nuclear protein HAMLET is transiently expressed in external sensory neurons of *Drosophila* during the initial phases of dendrite outgrowth, and *hamlet* mutants display altered dendritic branching patterns (Moore et al., 2002). In the nematode *Caenorhabditis elegans*, mutations that disrupt intrinsic activity of the transmembrane fusogen EFF-1 result in excessive and disorganized branching of PVD mechanosensory neuron dendrites, suggesting that EFF-1 may function to dictate membrane shape and curvature of the growing neurites (Oren-Suissa et al., 2010). However, extrinsic signals seem to play important roles as well. External signals may be (1) systemic (Woolley et al., 1990), (2) may emanate from other neurites, as in the case of activity-dependent dendritic shape determination (Parrish et al., 2007) or dendritic tiling of *da* neurons of *Drosophila* (Grueber et al., 2002; Matthews et al., 2007), or (3) may be provided by glia.

Glia are well positioned to regulate dendritic morphology as they are not only in close proximity to neurons but also ensheath neuronal processes and synapses. For example, glia have been implicated in directing process orientation in the developing vertebrate brain. Neurons generated by subventricular zone radial glia stem cells often contain a single process, resembling a dendrite (Cajal, 1911; Hatten, 2002), which is dynamically remodeled as neurons migrate to populate the brain. Neuronal migration is guided in part by the radial glia to which migrating neurons adhere and upon which they travel (Rakic, 1971; Rakic, 1972). The dendrite-like processes that emanate from these migrating neurons are oriented along the radial glial tracks, suggesting specific adhesion. The basis of the adhesion is not well understood; however, astrotactin, a neuronal protein suggested to promote neuron-glia adhesion, is required for granule neuron migration and process adhesion in the cerebellum (Fishell and Hatten, 1991). In the neocortex, recognition and adhesion of migrating neurons to radial glia requires integrins (Anton et al., 1999) and the gap junction proteins connexin 26 and connexin 43 (Elias et al., 2007).

Glia-derived cues are known to play important roles in axon guidance, affecting the shapes of axons by defining axonal extension paths (Chotard and Salecker, 2004). Recent evidence suggests that these same glia-derived axon guidance cues can also act on dendrites (Kim and Chiba, 2004). For example, the extracellular matrix (ECM) protein Slit is expressed by specialized midline glia of the *Drosophila* central nervous system (Rothberg et al., 1988; Rothberg et al., 1990) and acts to repel axon growth cones that express the Slit receptor Robo (Battye et al., 1999; Kidd et al., 1999). In *robo* mutants, the dendrites of some neurons inappropriately migrate towards or cross the midline (Furrer et al., 2003), and proper guidance of these dendrites requires cell autonomous

expression of Robo (Figure 1.2) (Furrer et al., 2003). In *C. elegans*, ventral cephalic sheath (CEPsh) glia that ensheath the nerve ring, a dense neuropil analogous to the brain of higher organisms, express the chemotropic protein Netrin/UNC-6. In *unc-6* mutant animals (Wadsworth et al., 1996) or in animals lacking CEPsh glia (Yoshimura et al., 2008), axon paths are severely disrupted, demonstrating a role for these glial cells in axon guidance. RIA nerve ring neurons possess a single neurite whose proximal end is postsynaptic, resembling postsynaptic sites on dendrites. In *unc-6* mutants this neurite also exhibits severe guidance defects, and fails to navigate towards the CEPsh glia (Colon-Ramos et al., 2007). Thus, glia can contribute to dendrite guidance via the secretion of chemotropic factors.

In addition, all dendrites possess receptive structures that receive information, either from other neurons at synapses or, in the case of sensory neurons, from the environment. For example, in the mammalian brain dendrites receive information at most excitatory synapses through specialized structures termed dendritic spines, which appear as small protrusions on the dendrite process. Dendritic spines can be remodeled by environmental experience (Holtmaat and Svoboda, 2009), and changes in spine shape are correlated with neuronal function and synaptic strength (Bourne and Harris, 2008). Likewise, the shapes of sensory neuron dendritic endings are important, as mutations that affect sensory cilia morphology perturb the ability of a neuron to respond correctly to environmental stimuli (Perkins et al., 1986). These sensory receptive endings are also morphologically malleable (Mukhopadhyay et al., 2008). The dendritic receptive structures that receive information at synapses and those that receive environmental input share many similarities in function, shape and molecular components (Shaham, 2010).

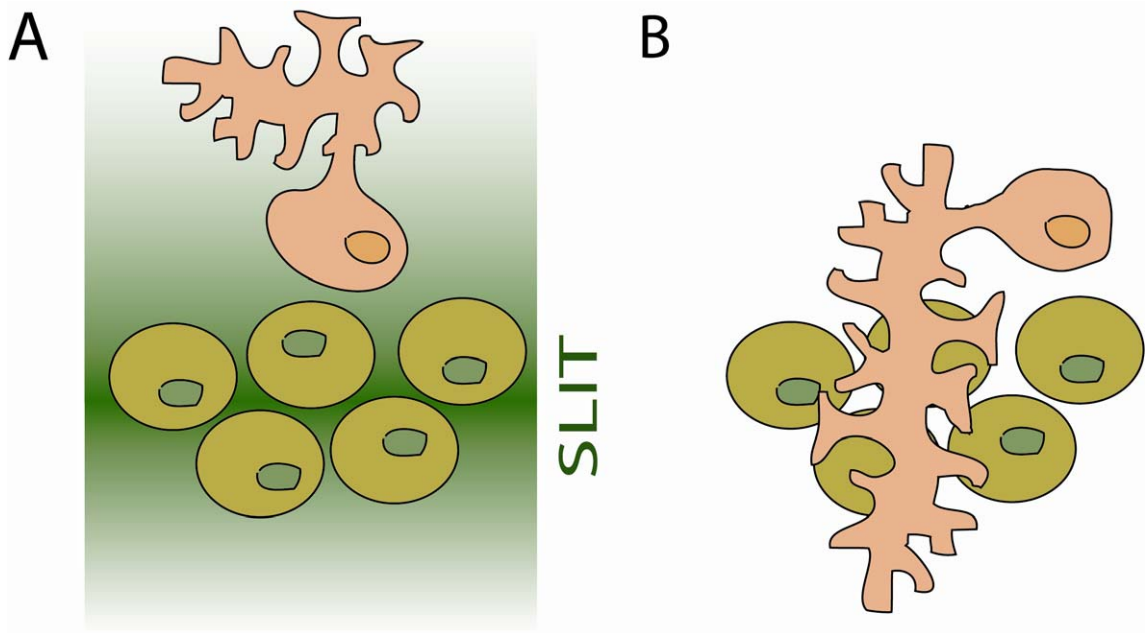


**Figure 1.2. Glia affect guidance of dendrite growth.** (A) In *Drosophila*, midline glia (green) secrete the guidance molecule SLIT, shown as a dark green gradient in the extracellular environment. The dendrites of the RP2 motor neuron (orange) are repelled from the midline. The RP2 axon is not shown. (B) Same as (A), except in a SLIT receptor mutant background (*robo*). In these animals, the neurons no longer perceive SLIT (indicated by a loss of green shading). The RP2 dendrites inappropriately move towards and cross the midline (Furrer et al., 2003).

Intriguingly, both structures are frequently ensheathed by glia (Shaham, 2010; Spacek, 1985; Ventura and Harris, 1999).

Studies of cultured purified mammalian retinal ganglion cell (RGC) neurons have been particularly informative in uncovering details of glia-neuron interactions during synapse formation, as these neurons form far fewer synapses when cultured *in vitro* in the absence of glia than in their presence (Ullian et al., 2001). A recent study suggests that physical contact between RGC neurons and astrocytic glia may allow these neurons to become competent for synapse formation. Glia-neuron contact reduces dendritic localization of the axonal protein neurexin (Barker et al., 2008), which reduces synapse formation when expressed in postsynaptic structures (Taniguchi et al., 2007). Synapse formation between RGC neurons is further induced by secretion of the ECM molecule thrombospondin (TSP) from glia (Christopherson et al., 2005). TSP interacts postsynaptically with the Ca<sup>2+</sup> channel subunit  $\alpha 2\delta$ -1 on neurons (Eroglu et al., 2009).

Studies in *C. elegans* also provide evidence for roles of non-neuronal cells in determining the locations of synapses. The presynaptic HSN neurons form synapses onto the postsynaptic VC neuron to create part of the circuit controlling egg-laying behavior in the animal. The positions of these synapses is determined not by the neurons, but by guidepost epithelial cells (Shen and Bargmann, 2003). These guidepost cells express the transmembrane, immunoglobulin superfamily protein SYG-2, which interacts with and localizes the SYG-1 immunoglobulin protein on the HSN neurons (Shen and Bargmann, 2003; Shen et al., 2004). Synapses form where SYG-1 is localized (Shen and Bargmann, 2003). Similarly, *C. elegans* CEPsh glia may affect the location of synapse formation between the presynaptic interneuron AIY and its postsynaptic partner RIA. The Netrin

receptor DCC/UNC-40 is expressed in AIY and localizes near the site where the CEPsh glia contact the neuron and secrete Netrin/UNC-6 (Colon-Ramos et al., 2007).

In addition to regulating the formation and localization of the receptive structures on dendrites, glia also affect the shapes of these structures. During development of the mammalian cerebellum, the extension of processes from Bergmann glia is intimately correlated with changes in Purkinje cell dendritic spine shapes (Lippman et al., 2008), suggesting that glia might influence spine shape dynamics. One way they may do this is via ephrin-Eph signaling. The astrocytic glia that ensheath hippocampal excitatory synapses express ephrin A3, while the receptor EphA4 is expressed in neurons and localizes to dendritic spines (Murai et al., 2003). When EphA4 is activated by adding exogenous ephrin A3, the dendritic spines retract (Murai et al., 2003). By contrast, mice lacking either ligand or receptor tend to exhibit elongated dendritic spines (Carmona et al., 2009; Murai et al., 2003). The analysis of *EphA4* mutant mice suggests that the consequences of these spine shape abnormalities may include defects in hippocampus-dependent learning (Carmona et al., 2009).

Dendrite guidance, as well as the formation, placement, and shapes of dendritic receptive structures, can all be affected by glia, suggesting that these cells play key roles in shaping the nervous system. The implications of these studies are profound, as in all nervous systems neuronal shape determines circuitry, and the shapes of receptive structures affect signal strength. Thus, exploration of glial roles in controlling neuron shape and activity is essential for understanding how the nervous system is put together and how it functions. To address these issues, the soil-dwelling nematode *C. elegans*

may provide a unique *in vivo* setting for determining the roles of glia in regulating dendrite morphology and function.

## **The nematode *Caenorhabditis elegans* responds developmentally to environmental stress**

In addition to the organisms described above, the nematode *C. elegans* provides another striking example of an animal that enters an alternative developmental program in response to environmental stressors. Under favorable conditions, *C. elegans* grow rapidly, progressing through four larval stages (L1 through L4) in only a few days to become egg-laying adults. This is termed reproductive growth. By contrast, in an unfavorable environment *C. elegans* enter a protective, developmentally-arrested larval stage after the second larval transition, termed dauer, from the German for “enduring” larva (Figure 1.3) (Cassada and Russell, 1975).

A number of morphological changes occur in dauer animals to enable them to persist in a harsh environment. For example, the cuticle is altered, having a thicker outer cortex and an additional striated underlayer compared to non-dauer animals, and radial shrinkage of the body circumference occurs (Cassada and Russell, 1975). Movement of dauers is suppressed (Cassada and Russell, 1975), while feeding ceases and metabolism is altered for long-term survival (Holt and Riddle, 2003). These morphological changes confer on the animal extreme longevity and increased resistance to environmental challenges, such as resistance to desiccation, dilute acid, hypertonic solutions, temperature extremes outside of the optimum growth range of 15-25°C, and detergents,

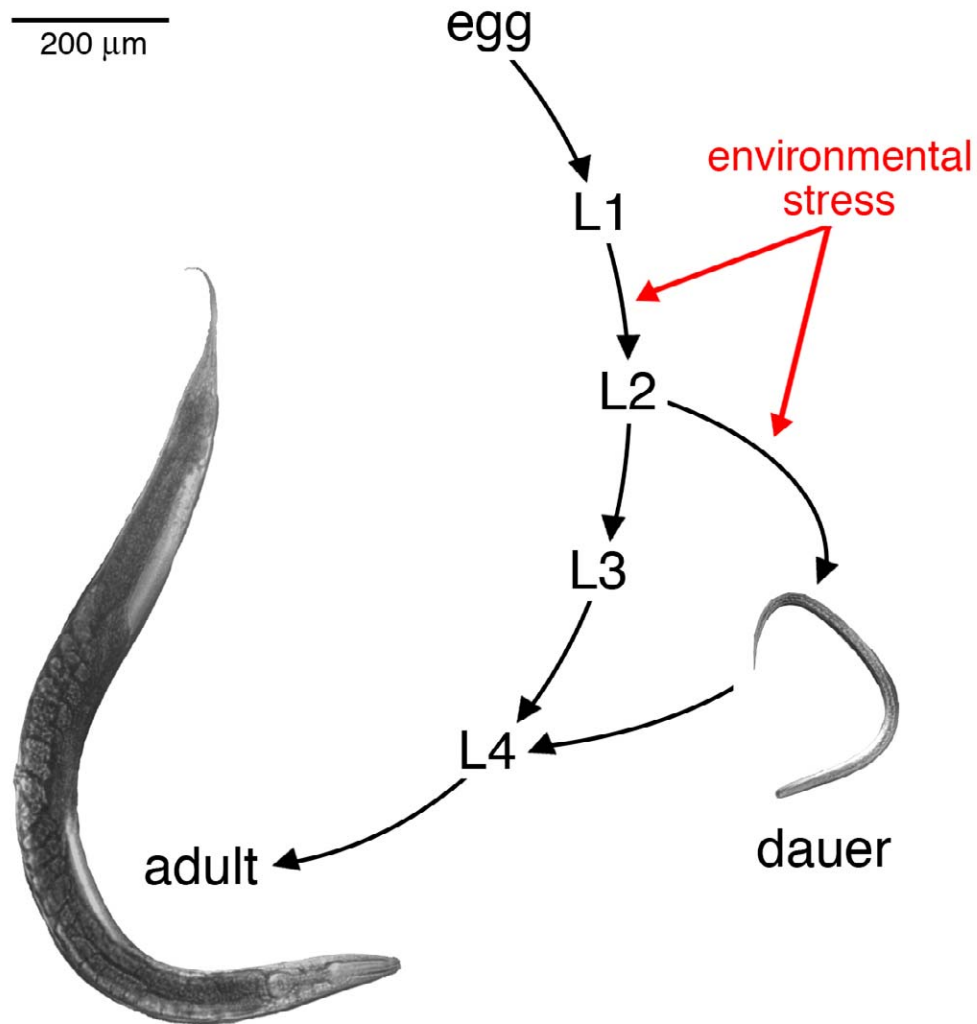


**Figure 1.3. The life cycle of *Caenorhabditis elegans*.** During reproductive development, *C. elegans* progresses through four larval stages, L1 to L4, before becoming an egg-laying adult. In an unfavorable environment, *C. elegans* will instead enter a diapause larval state, termed dauer, after the second molt. The environmental signals that regulate dauer entry are sensed during the first and second larval stages, marked in red (Golden and Riddle, 1984a). When environmental conditions become favorable, *C. elegans* will exit the dauer state and become fertile adults.

as measured by increased resistance to sodium dodecyl sulfate (SDS) (Cassada and Russell, 1975). When environmental conditions improve, the animal resumes feeding and proceeds with development, becoming a fertile adult (Figure 1.3). Thus, similar to bacterial endospores, the dauer state likely provides a means of temporal escape from a harsh environment and a dispersal form between environments.

Dauer entry in *C. elegans* is promoted by high population density, low food abundance and high temperature (Cassada and Russell, 1975; Golden and Riddle, 1984a). *C. elegans* measure population density by the levels of dauer pheromone in the environment, a complex mixture of chemicals secreted constitutively by the animal and which constitutes the most potent dauer entry signal (Golden and Riddle, 1984a). The induction of dauer entry by pheromone is, in turn, temperature-dependent (Golden and Riddle, 1984b). The most active components of the dauer pheromone are structurally related small molecule glycosides of the sugar ascarylose, termed ascarosides (Butcher et al., 2007). These are perceived through multiple receptors, one pair of which is the guanosine-5'-triphosphate (GTP)-binding protein (G-protein)-coupled receptors (GPCRs) SRBC-64 and SRBC-66, that are expressed specifically in a pair of environmental sensory neurons and function together to mediate responses to dauer pheromone (Kim et al., 2009).

Dauer pheromone and environmental stressors that induce dauer entry are perceived by specialized sensory neurons in the head of the animal (Bargmann and Horvitz, 1991b) (see below). Due to the organism-wide morphological and metabolic changes that occur in dauer animals, it is necessary that these neurons communicate this information about the environment to other tissues. These systemic changes in

physiology are promoted through two major neuroendocrine pathways: insulin/insulin-like growth factor (IGF) and transforming growth factor- $\beta$  (TGF- $\beta$ ) signaling pathways (Kimura et al., 1997; Ren et al., 1996). In both pathways, when hormone levels are high animals proceed with reproductive development. When either hormone is low, the dauer state is promoted.

The TGF- $\beta$ -related hormone DAF-7 is expressed in the ASI amphid sensory neurons, and animals carrying mutations in the *daf-7* gene (for *dauer formation-7*) enter dauer constitutively in otherwise favorable environments (Ren et al., 1996). Transcription of *daf-7* is coupled to environmental stimuli that induce dauer; for example, transcription is inhibited by pheromone and high temperature, and reduced in dauer animals (Ren et al., 1996; Schackwitz et al., 1996). While TGF- $\beta$ /DAF-7 is expressed only in a specific sensory neuron, its receptor, the DAF-1/DAF-4 receptor kinase, is expressed broadly (Estevez et al., 1993; Georgi et al., 1990). Likewise, although a number of insulin/IGF-like peptides exist in worms, one of these, DAF-28, is expressed in the ASI and ASJ amphid sensory neurons, and a *daf-28* transcriptional reporter is regulated by sensory stimuli that induce dauer entry (Li et al., 2003). Mutations in the *daf-28* gene result in transient dauer arrest. DAF-28, and possibly other insulin-like peptides, acts through the insulin receptor-like tyrosine kinase DAF-2 to inhibit dauer entry (Kimura et al., 1997). Like the receptor for DAF-7/TGF- $\beta$ , the insulin receptor DAF-2 is broadly expressed, predominantly in the nervous system. In addition, other sensory neurons that detect environmental stressors can modulate the production of dauer hormone ligands from ASI and ASJ (Bargmann and Horvitz, 1991b; Kim et al., 2009). Thus, through both TGF- $\beta$ /DAF-7 and insulin/DAF-28 neuroendocrine pathways,

sensory neurons can communicate information about the environment systemically to affect dauer development.

TGF- $\beta$ /DAF-7 and insulin receptor/DAF-2 pathways converge onto the nuclear hormone receptor (NHR) DAF-12. Like other NHR genes, *daf-12* codes for a transcriptional regulator with a variable amino terminus, a conserved DNA-binding domain, a variable hinge region, and a conserved carboxy terminal ligand-binding domain (Antebi et al., 2000). A transcriptional reporter for *daf-12* is expressed in most cells of the animal, with peak expression in the second larval stage when the commitment to dauer is made (Antebi et al., 2000). Loss of function mutations in *daf-12* cause a dauer-defective phenotype that is epistatic to the dauer-constitutive phenotypes of *daf-7* and some *daf-2* alleles (Larsen et al., 1995; Riddle et al., 1981). These findings are consistent with a model in which DAF-12 integrates signals from the TGF- $\beta$  and insulin/IGF-like neuroendocrine pathways (Fielenbach and Antebi, 2008). According to this model, both TGF- $\beta$ /DAF-7 and insulin/IGF-like neuroendocrine pathways induce the synthesis of a secondary endocrine signal in downstream cells: the DAF-12 ligands. These ligands are dafachronic acid steroid hormones, which are secreted and act systemically on all DAF-12 expressing cells (Motola et al., 2006). DAF-12 bound to its ligand promotes reproductive development; whereas, in an unfavorable environment, TGF- $\beta$ /DAF-7 and insulin/DAF-28 signaling is low, and consequently dafachronic acid synthesis is reduced and the unbound DAF-12 receptor instead regulates gene transcription to specify dauer development (Fielenbach and Antebi, 2008).

Dauer entry reflects a developmental decision made by the *C. elegans* larva to maximize reproductive success in a given environment. How the animal perceives and

interacts with its environment is mediated by sensory neurons and, in the case of dauer development, their effects on neuroendocrine signaling pathways.

## **The amphids sense the environment in *C. elegans***

Like vertebrates and other animals, *C. elegans* sense the environment through organs composed of specialized sensory neurons and glia. In *C. elegans*, most environmental signals are detected by neurons of the bilateral amphid sensilla. The amphids are required for many behavioral responses, such as movement in response to tastants and odorants (Bargmann et al., 1993; Bargmann and Horvitz, 1991a), nose touch responses (Kaplan and Horvitz, 1993), and temperature seeking behavior (Mori and Ohshima, 1995), as well as for dauer development in response to environmental stress (Bargmann and Horvitz, 1991b; Perkins et al., 1986).

Each amphid consists of 12 neurons, each of which extends a single unbranched dendrite from the cell body to the anterior nose-tip, a length of ~100  $\mu\text{m}$  (Figure 1.4) (Ward et al., 1975). Here, the dendrites terminate in specialized cilia, the shape of which are important for sensory responses (Perkins et al., 1986). These ciliated sensory endings are sites where cell-surface receptors, ion channels, and signal transduction machinery are localized (Shaham, 2010). The morphologies of amphid neuron sensory endings can be simple or complex. For example, the ASI neurons, which secrete endocrine signals in response to environmental stressors that induce dauer (see above), have a single, microtubule-based cilium (Ward et al., 1975). By contrast, the dendrites of AWC and AFD amphid neurons terminate in more elaborate structures.

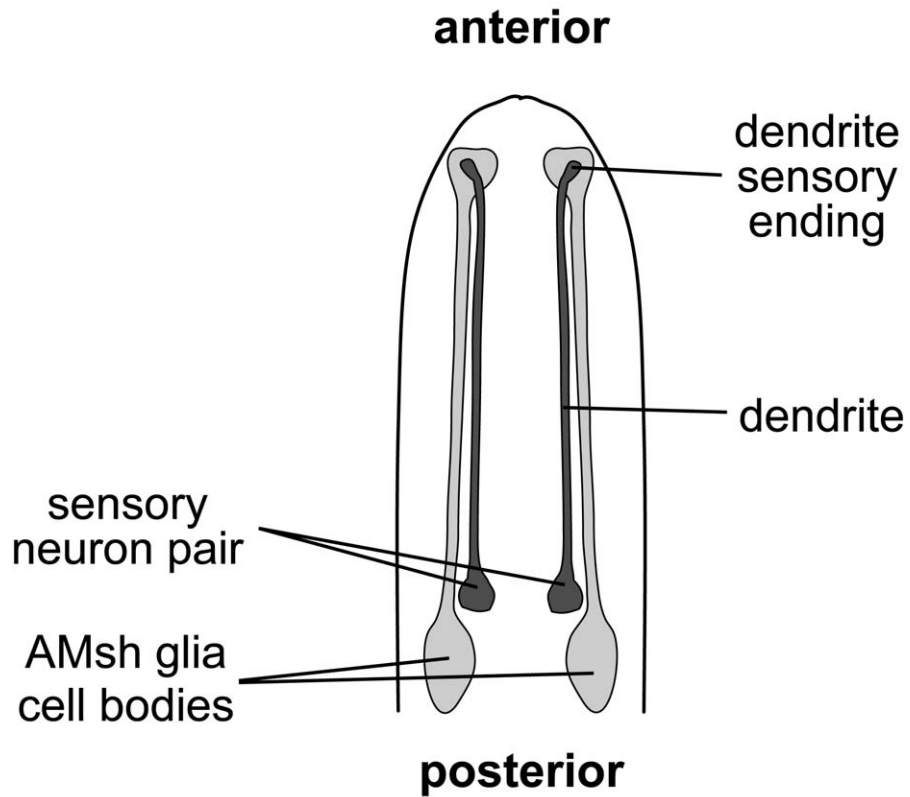


**Figure 1.4.** A schematic drawing of the two amphid sensory structures in *C. elegans*. Each neuron is bilateral (left and right); for simplicity, only a single neuron pair is shown (dark shading, cell bodies marked). Each of these neurons extends a dendritic process ~100  $\mu\text{m}$  long anteriorly to the nose-tip, where the dendrite terminates in a specialized sensory ending. Associated with these neurons are a pair of amphid sheath (AMsh) glial cells (light shading), that also extend a process to the nose and there ensheath the neuronal sensory endings. Not to scale.

The AWC dendrite ending has a wing-like, butterfly morphology that is required for behavioral responses to odorants (Bargmann et al., 1993; Perkins et al., 1986; Ward et al., 1975). Calcium imaging experiments have shown that the neuron is activated most strongly by the removal of odorants from the environment (Chalasanani et al., 2007). This causes the release of the neurotransmitter glutamate at AWC synapses, affecting a downstream neuronal circuit that regulates animal turning behavior and ultimately results in attraction towards the odor stimulus (Chalasanani et al., 2007). In addition to responses to odorants, AWC may also have minor roles in temperature-associated behavior (Biron et al., 2008; Kuhara et al., 2008); however, it is unclear if the neuron is a direct thermosensor (Ramot et al., 2008a).

The primary temperature-sensing neuron in *C. elegans* is the AFD amphid neuron. When placed in a thermal gradient, *C. elegans* will seek the temperature at which they were cultivated, a behavior known as thermotaxis (Hedgecock and Russell, 1975). Computational studies suggest that plasticity in the memory of cultivation temperature, which is reset over the course of hours, likely serves to maintain worms at a fixed, optimal depth in the soil over daily and seasonal temperature fluctuations (Ramot et al., 2008b). Laser ablation experiments of the AFD neurons have shown that this behavior is dependent on AFD (Mori and Ohshima, 1995). Unlike AWC, the AFD sensory dendrite terminates not in a wing-like morphology but rather in microvillar finger-like projections (Ward et al., 1975). Calcium imaging experiments and the localization of sensory transduction molecules suggest that the temperature-sensing capability of the cell is localized to this sensory ending (Clark et al., 2006; Coburn and Bargmann, 1996; Komatsu et al., 1996). Consistent with this, mutant animals with

perturbed AFD sensory endings have defective thermotaxis behaviour. The endings of AFD dendrites in animals carrying a mutation in the *otd/Otx*-type transcription factor *ttx-I* adopt a default single cilium in place of the elaborate microvillar extensions. These mutant animals exhibit cryophilic behavior down a temperature gradient (Hedgecock and Russell, 1975; Perkins et al., 1986; Satterlee et al., 2001) and are hypersensitive to dauer pheromone, suggesting a role of AFD in modulating dauer responses (Golden and Riddle, 1984b). Furthermore, the exogenous expression of *ttx-I* in other sensory neurons confers on them an AFD-like morphology, suggesting that the transcription factor acts to partly specify AFD thermosensory cell fate and morphology (Satterlee et al., 2001).

Although *in vivo* patch-clamp recordings suggest that the AFD neuron is exquisitely sensitive to bidirectional changes in temperature (Ramot et al., 2008a), the molecular mechanism of how the neuron senses the temperature change is unknown. In the mammalian peripheral nervous system, environmental temperature is sensed by neurons of the dorsal root ganglia that project to the epidermis and dermis of the skin. These neurons, as well as associated keratinocyte cells, express non-selective cation channels of the transient receptor potential (TRP) channel family that are directly gated by temperature (Peier et al., 2002a; Peier et al., 2002b; Story et al., 2003; Tominaga et al., 1998). Temperature-gated TRP channels are also utilized by pit-bearing snakes to sense the infrared radiation emitted by warm-blooded prey (Gracheva et al., 2010), demonstrating conservation of TRP channel thermosensory function over diverse vertebrate species. By contrast, the bacterium *Escherichia coli* senses temperature fluctuations through a direct change in the activities of two transmembrane proteins, the chemoreceptors Tsr and Tar (Maeda and Imae, 1979; Mizuno and Imae, 1984). Tsr and

Tar also bind the attractive ligands serine and aspartate, respectively, to mediate chemotaxis behavior. This suggests that different environmental signals can be integrated at the receptor level in single-celled bacteria. Plants also sense changes in temperature, and use this information to optimize flowering and growth with the seasons and time of day. The mustard plant *Arabidopsis thaliana* may couple temperature cues directly to gene transcription via modifications in DNA chromatin structure (Kumar and Wigge, 2010). As temperature decreases, the histone variant H2A.Z is more likely to be incorporated into DNA-bound nucleosomes in place of the canonical histone H2A. Mutants that are defective in incorporating H2A.Z display a warm-temperature gene expression pattern and phenotype, suggesting that changes in H2A.Z occupancy are linked to temperature-induced gene expression changes (Kumar and Wigge, 2010). Fluctuations in gene transcription, however, would be inconsistent with the fast response times of AFD to temperature (Ramot et al., 2008a).

By contrast, the AFD neurons of *C. elegans* sense temperature by a cyclic guanine monophosphate (cGMP)–dependent pathway. Although temperature-sensitive GPCRs in *C. elegans* have not yet been found, the downstream components of the thermosensory signaling pathway within AFD include multiple redundant membrane-associated guanylyl cyclases and a cyclic nucleotide-gated cation channel (Coburn and Bargmann, 1996; Inada et al., 2006; Komatsu et al., 1996), which is consistent with a G-protein signaling pathway (Liu et al., 2010). Some precedence for a temperature-sensing GPCR is found in *Drosophila*, where the light-sensitive GPCR rhodopsin also has roles in thermotaxis behavior; however, it is unclear if rhodopsin is directly activated by temperature or via interactions with other molecules (Shen et al., 2011). In addition, the

elaborate and unique morphology of the AFD sensory ending is intriguing, and may be required either directly for temperature responses of the cell or for modulating those responses (Perkins et al., 1986; Satterlee et al., 2001). For example, the specialized morphology of the thermosensory sensilla in the beetle *Melanophila acuminata* converts temperature changes to a mechanical stimulus (Campbell et al., 2002; Schmitz and Bleckmann, 1998). As part of its natural ecology, *Melanophila* locates forest fires from great distances, where it mates and lays its eggs under the burnt bark of conifer trees, where the larvae feed. Each *Melanophila* sensilla is innervated by a single mechanosensory dendrite cilium that is enclosed within a cuticular sphere. Electrophysiology recordings are consistent with a model whereby infrared radiation is absorbed by the cuticle, resulting in expansion of the cuticular sphere and a deformation on the sensory cilium, thus converting a temperature signal to a mechanical one (Campbell et al., 2002; Schmitz and Bleckmann, 1998). It is unknown if AFD microvillar structure plays a similar role.

Associated with AFD, AWC and other *C. elegans* neurons are glial cells, which ensheath sensory endings, synapses and neuron processes (Shaham, 2006; White et al., 1986). In each amphid sensory organ, the amphid sheath (AMsh) glial cell extends a process to the nose where it ensheaths the ciliated receptive endings of the dendrites (Figure 1.4) (Ward et al., 1975). Some of these sensory endings, such as AWC and AFD, are embedded in the AMsh glia in a hand-in-glove configuration, while others project through an open channel formed by the glia and are directly exposed to the outside environment. Each of the dendrites form tight junctions with the glia to form an isolated

sensory compartment, into which the glia secretes a specialized ECM required for neuronal function (Bacaj et al., 2008; Perkins et al., 1986; Ward et al., 1975).

In addition to the amphid sensilla at the nose-tip of the animal, analogous bilateral sensory organs called the phasmids are located in the tail. These organs consist of only two neurons, again associated with a sheath glial cell, and are required for measuring nose-to-tail environmental gradients (Hilliard et al., 2002).

### **The *C. elegans* amphids as a model of neuron-glia interactions**

Despite the many possible roles of glia in controlling various aspects of nervous system function, *in vivo* studies of vertebrate glia and their roles in the nervous system have been complicated, primarily because the ablation or manipulation of glia often results in neuronal death (Cui et al., 2001; Delaney et al., 1996). By contrast, in *C. elegans*, neurons survive following glia ablations, opening a unique *in vivo* arena in which to investigate the effects of glia on neuron function and shape (Bacaj et al., 2008; Yoshimura et al., 2008). Furthermore, *C. elegans* has the advantage of facile genetics, and sensory inputs to amphid sensory neurons are well-defined and can be experimentally manipulated.

Recent studies suggest that glia are required for amphid neuronal function and morphology. For example, the correct morphogenesis of the AMsh glia channel is required for the direct access of amphid sensory neurons to the environment. One factor required in glia for channel formation is the Patched-related transmembrane protein DAF-6, which lines the channel and apical surfaces of other tubular structures (Perens

and Shaham, 2005). *daf-6* mutants have bloated channels in which the sensory cilia are bent and neuronal responses to the environment are defective (Perens and Shaham, 2005; Perkins et al., 1986). This observation suggests that *daf-6* may be required to reduce the diameter of the channel. Balancing the function of *daf-6* is a pathway involving glia-expressed *Nemo*-like kinase *lit-1*, which acts to increase channel diameter and may interact with the actin cytoskeleton at the anterior tip of the AMsh glia where the channel forms (Oikonomou et al., in press).

In addition, the process lengths of the AMsh glia and sensory dendrites are coordinated during development and may be under glial control. Although dendrite tips may often need to be told where to go by guidance cues (see above; Figure 1.2), this is not always the case. Unlike some dendrites that elongate by growing a process out of a stationary cell body, time-lapse microscopy studies demonstrate that the dendrites of *C. elegans* amphid sensory neurons develop by first anchoring the presumptive dendritic tip to the surrounding environment at the nose (Heiman and Shaham, 2009). Posterior migration of the cell body then stretches out a dendritic process (Figure 1.5A) (Heiman and Shaham, 2009). The length of the dendrite and glial processes are correlated: in mutant backgrounds where the dendrites are too short, the glial process is also truncated (Heiman and Shaham, 2009). At least one component of the dendritic-tip anchor, DYF-7, is expressed by the sensory neurons (Heiman and Shaham, 2009), suggesting that anchoring is in part determined by the neurons themselves. However, a second anchor component, DEX-1, is supplied by non-neuronal hypodermal cells surrounding the dendrite tip, raising the possibility that a number of cell types may contribute to creating the anchor.

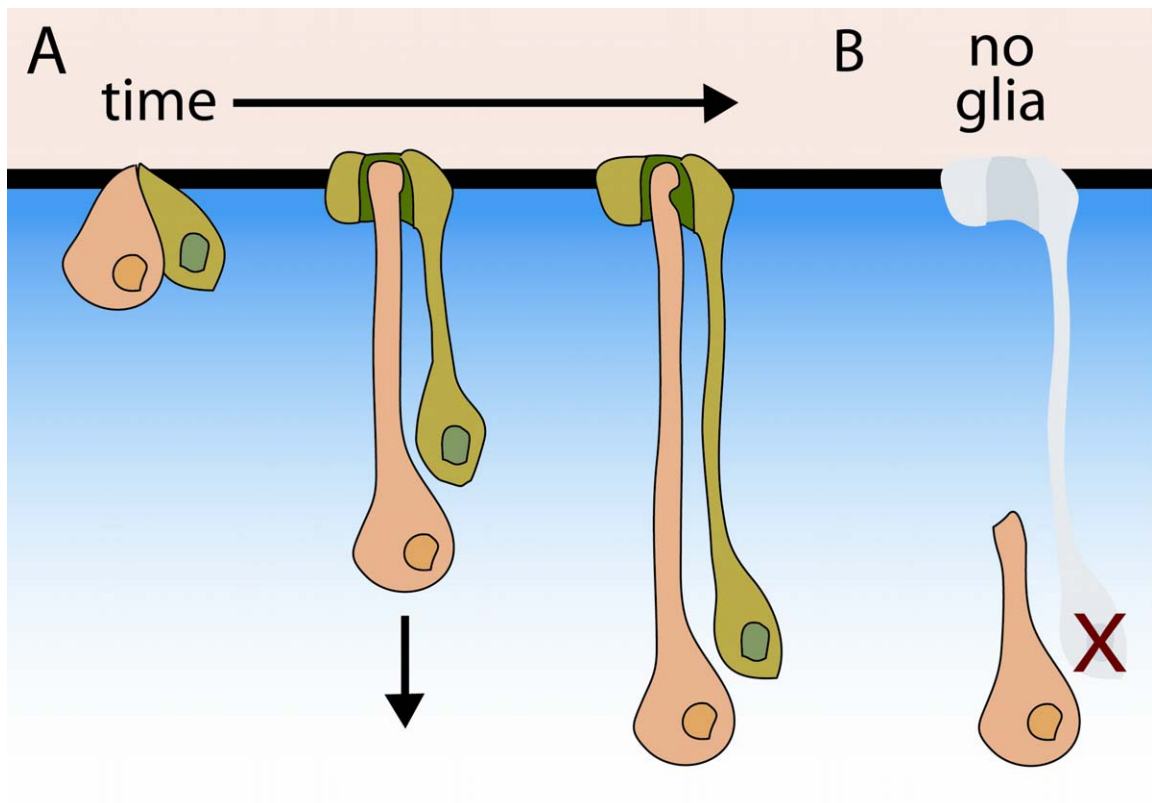


**Figure 1.5. A model for glial involvement in dendrite extension of *C. elegans* sensory neurons.** (A) The single, unbranched dendrite of a *C. elegans* amphid neuron (orange) extends a process via retrograde extension. The presumptive dendritic tip of the neuron is anchored to its local environment (black, horizontal line). The dendrite is then extended by posterior migration of the cell body (indicated by arrow). The direction of migration is likely driven by a gradient of a chemotropic factor (blue gradient). The neuron is associated with the AMsh glial cell (green), whose process ensheaths the dendritic ending and which likely develops by retrograde extension also (Heiman and Shaham, 2009). (B) When the amphid sheath glial precursor cell (Bacaj and Shaham, unpublished results) or the sheath glial precursor found in cephalic sensory structures (Ward et al., 1998; Yoshimura et al., 2008) is ablated, the dendrite of the associated sensory neuron is too short.

The DYF-7/DEX-1 anchor seems to be an example of a structurally unique ECM of diverse functions in different systems. DYF-7 is a secreted zona pellucida (ZP) domain protein localized near the tips of anchored sensory dendrites, while DEX-1 is a secreted zonadhesin (zonad) domain protein. ZP domains form the ECM surrounding vertebrate oocytes (the zona pellucida), while zonadhesin is a sperm protein required for fertilization (Monne et al., 2008). Both domains are also present in  $\alpha$ -tectorin, a major component of the tectorial membrane, a highly organized proteinaceous ECM that anchors the ciliated outer hair cells of the inner ear (Legan et al., 1997).

The observation that a single AMsh glial cell ensheaths all 12 amphid sensory neurons suggests that glia are also in a position to contribute to the common anchoring matrix. Indeed, AMsh glia express several ZP domain proteins as well as other predicted extracellular proteins that could potentially contribute to the ECM anchor (Bacaj et al., 2008). Furthermore, ablation in early development of the precursor cells of the AMsh glia results in unanchored, short dendrites (Bacaj and Shaham, unpublished results), but does not affect sensory neuron cell migration. Similarly, the dendrites of CEP sensory neurons, which are part of another *C. elegans* anterior sensory organ, are shortened when their glial precursors are ablated or when genes affecting differentiation of the associated glia are mutated (Figure 1.5B) (Yoshimura et al., 2008).

Strengthening the notion that glia contribute to the ECM required for dendrite anchoring is the observation that the ECM that tethers mechanosensory neurons in *Drosophila* is, at least in part, secreted by glia-like cells associated with these neurons (Chung et al., 2001). In type I mechanosensory organs of *Drosophila*, a sheath cell (also called the thecogen or scolopale cell in external sensory organs and chordotonal organs,

respectively) wraps the dendrite of the sensory neuron, and at the ciliated tip of the dendrite secretes a specialized ECM called the dendritic cap (Chung et al., 2001; Hartenstein and Posakony, 1989). Although the sheath cell does not express the glial marker *glial cell deficient/glial cell missing (glide/gcm)* (Van De Bor et al., 2000), it is lineally related to the sensory neuron and has been described as a glial cell (Carlson and Saint Marie, 1990; Hartenstein and Posakony, 1989; Moore et al., 2004). One of the proteins secreted by the sheath cell into the dendritic cap is No-mechanoreceptor-potential A (NompA), which, like DYF-7, is a ZP domain protein. In *nompA* mutant animals, the ciliated tips of the sensory dendrites fail to attach to nearby stimulating structures, either mechanosensory bristles or attachment cells, resulting in mechanosensory defects (Chung et al., 2001). Furthermore, in the male tail of *C. elegans*, glial structural cells secrete the ZP domain protein RAM-5, which is required for correct morphology of the ray sensory organs (Yu et al., 2000).

Together, these studies suggest that sensory organ glia may produce local ECM to which dendrite endings attach. This ECM, in turn, may play a key role in determining dendrite length. However, components of this specialized ECM may have other functions besides process anchoring. Indeed, additional studies from the *C. elegans* amphid organs suggest the involvement of glia-secreted proteins in controlling the shapes of dendritic receptive structures and function. Specifically, late-stage ablations of the AMsh glia result in changes in the morphology of the sensory endings of the ensheathed amphid neurons (Bacaj et al., 2008). These changes correlate with behavioral defects of the animals in response to environmental stimuli (Bacaj et al., 2008). The molecules contributed by the AMsh glia to maintain dendrite ending shape are not yet known;

however, the identification of a large number of glia-enriched mRNAs encoding secreted and transmembrane proteins by microarray analysis (Bacaj et al., 2008) may provide candidates for mediating shape determination.

Interestingly, like vertebrate astrocyte glia, the AMsh glia of *C. elegans* secrete a TSP-domain protein called FIG-1, which, although having no defects in sensory cilia shape, is required for sensory neuron properties and function (Bacaj et al., 2008). Sensory neurons in *fig-1* mutants are no longer able to accumulate the membrane dye DiI, suggesting the speculative possibility that the synaptogenic effects of TSP on vertebrate retinal ganglion cell neurons (Christopherson et al., 2005) may reflect a role in setting up postsynaptic architecture.

## **Amphid dendrite endings and glia shapes are remodeled in *C. elegans* dauer larvae**

The morphology and/or metabolism of many organs are altered when *C. elegans* enters the dauer state, and this includes the amphid sensilla. Electron microscopy (EM) reconstructions of the dendrite sensory endings at the nose-tip suggest that of the twelve bilateral neuron pairs, four of these are remodeled in dauer (Albert and Riddle, 1983). Two of these, the single-ciliated ASG and ASI neurons, are displaced posteriorly in the AMsh glia channel. The others, AFD and AWC, show a change not in position but rather in shape. The AFD sensory ending exhibits an increase in the number of microvillar extensions compared to non-dauer animals. By contrast, AWC exhibits an even more dramatic change: the spatially-separated wing-like cilia expand at the nose-tip, such that

the left and right AWC neurons now overlap extensively in dauers. This remodeling correlates with expansion and, remarkably, fusion of the two bilateral AMsh glia where they ensheath the AWC sensory endings (Figure 1.6) (Albert and Riddle, 1983). What regulates the morphological remodeling of the amphids in dauer animals, and how dauer-inducing signals from the environment feed into this developmental pathway are unknown.

Why do the amphid structures remodel in dauer animals? It is possible that these changes serve no functional purpose. For example, the radial shrinkage of the body in dauer animals may shift the position of the ASI and ASG cilia, and bring the AWC sensory ending pair and two AMsh glia closer together (Albert and Riddle, 1983). Alternatively, the neurons of dauer animals may respond differently to their environment, and the remodeling of their morphology may have a functional consequence. For example, these neurons may have altered sensitivity to food and other cues that would signal an improvement in their environment and the need to exit dauer to become reproductive adults. Consistent with this hypothesis, the repertoire of odorant receptors expressed in a given sensory neuron is also altered in dauer animals (Peckol et al., 2001).

## **Does plasticity of dendrite receptive ending shapes depend on glial plasticity?**

In addition to a well-established maintenance role of glia on dendrite shape (see above), could glia also be required for plasticity of dendritic receptive structures, such as sensory endings and dendritic spines? Both structures exhibit morphological plasticity;

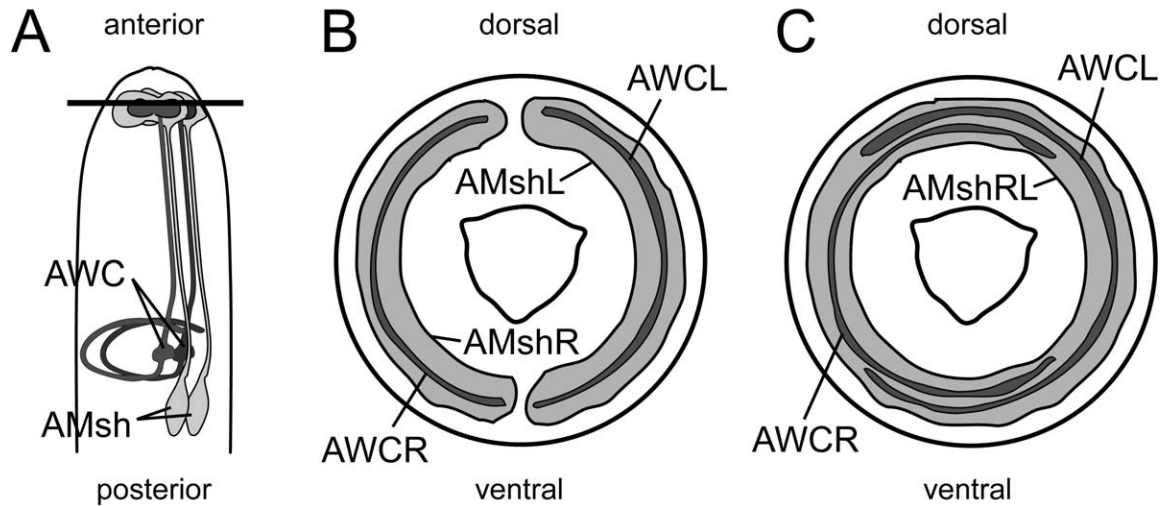


**Figure 1.6. AWC neuron receptive endings and AMsh glia remodel in dauer larvae.**

(A) A schematic of the head of the animal, showing the two bilateral AMsh glia and AWC sensory neurons (see also Figure 1.4). The horizontal line indicates the position of the transverse sections shown in (B,C). (B,C) Sections through the nose tip showing the relative positions of the AWC neuron receptive endings and the ensheathing AMsh glia in non-dauer (B) and dauer (C) animals. AMsh glia fusion may occur on either the ventral or dorsal side. In all images, left and right AWC (AWCL/R; dark shading) and AMsh glia (AMshL/R; light shading) are indicated. Adapted from Albert and Riddle, 1983; Ward et al., 1998. Not to scale.

for example, during synaptogenesis in the mouse cerebellum, dendritic spines of Purkinje cells exhibit dynamic shape changes, with spines rapidly emerging, growing, and retracting. The frequency of these shape changes decreases as development proceeds to establish a stable synaptic repertoire (Dunaevsky et al., 1999). In addition, systemic estrogen signals can affect dendritic spine number and density of adult rat hippocampal neurons (Woolley et al., 1990).

The proximity of glial processes to dendritic receptive endings and the importance of glia in maintaining receptive ending shape may suggest that glia can influence neuronal receptive ending shape plasticity and that dynamic interactions between these cellular protrusions exist. For example, in the cerebellum, Bergmann glia extend and retract processes in concert with the emergence and regression of Purkinje cell dendritic spines (Lippman et al., 2008). Similarly, during lactation in female rats the processes of hypothalamic astrocytic glia retract, and this is accompanied by synaptic remodeling of the glia-ensheathed supraoptic nucleus (SON) neurons (Theodosis and Poulain, 1993). Some glia express neurotransmitter receptors (Porter and McCarthy, 1996), and in the case of visual cortex astrocytes, exhibit tuning responses similar to nearby neurons (Porter and McCarthy, 1996; Schummers et al., 2008). Thus, glia possess machinery to gauge the environment surrounding receptive endings as well. Together, these various observations raise the intriguing but speculative possibility that extracellular cues such as systemic hormones or environmental signals received by glia may promote their shape changes, which, in turn, could affect the shapes of neurons. Furthermore, glia are already known to regulate plasticity of neuronal function; for example, sustentacular glia-like

cells in the olfactory epithelium affect the sensitivity of the sensory neurons to odorants following animal starvation (Breunig et al., 2010; Czesnik et al., 2007) (see above).

Dauer-induced AWC neuron remodeling in *C. elegans* offers unique advantages for studying receptive ending plasticity: it is inducible, reproducible, and can be studied in an organism with facile genetics and molecular biology. The fact that AWC and the other amphid neurons remodeled in dauer animals are all ensheathed by the AMsh glia, and that these glia also remodel, may indicate that the glia are required for directing some of the morphological changes in the neurons. In this thesis, I will address roles of neurons and glia in nervous system shape plasticity, using *C. elegans* dauer-induced amphid remodeling as a model of dendrite-glia interactions. In addition, I will describe a set of glial factors that are required for morphological changes of the glia in dauer animals.

## **Chapter 2**

Glia delimit shape changes of sensory neuron  
receptive endings

## Summary

Dendritic receptive endings, such as dendritic spines and sensory protrusions, are structurally remodeled by experience. How receptive endings acquire their remodeled shapes is not well understood. In *C. elegans* dauer larvae, the AMsh glia remodel concomitantly with the sensory endings of the glia-ensheathed AWC neurons. By ablating AWC, we have found that the glia remodel independently of AWC sensory ending growth. By contrast, we have used genetic perturbations in the glia to show that the AWC sensory endings remodel in the confines of a compartment defined by the AMsh glia. Our results demonstrate that stimulus-induced changes in glial compartment size provide spatial constraints on neuronal receptive ending growth.

## Results

### Loss of *daf-7*/TGF- $\beta$ promotes dauer remodeling of AWC neurons

To characterize remodeling of AWC neuron sensory receptive endings, we examined dauer animals by EM serial reconstructions. We found that in 2 of 3 animals examined, AWC receptive endings overlapped extensively. By contrast, no overlap was evident in non-dauer adults ( $n = 6$ ) (Figure 2.1A,B). These results demonstrate that AWC remodeling occurs in some but not all dauers.

Remodeling of AWC neurons could occur as a direct response to dauer pheromone, or may be a consequence of downstream systemic changes induced by pheromone. To distinguish between these possibilities, we examined animals carrying a temperature-sensitive mutation in the *daf-7* gene (Ren et al., 1996). *daf-7* encodes a TGF- $\beta$  protein thought to function downstream of pheromone reception, and likely acts to inhibit the dauer program by binding to the DAF-1/DAF-4 TGF- $\beta$  receptor complex expressed on the surfaces of many cells (Estevez et al., 1993; Georgi et al., 1990; Riddle et al., 1981) (see Chapter 1). We found that AWC remodeling still occurred in *daf-7(e1372ts)* animals induced to enter dauer at 25°C. Specifically, 2 of 3 *daf-7(e1372)* dauers examined by EM showed overlap of AWC receptive endings (Figure 2.1C), suggesting that remodeling of AWC is a downstream consequence of pheromone signaling. In addition, these results also demonstrate that *daf-7* mutants are a suitable inducible setting in which to study AWC remodeling.

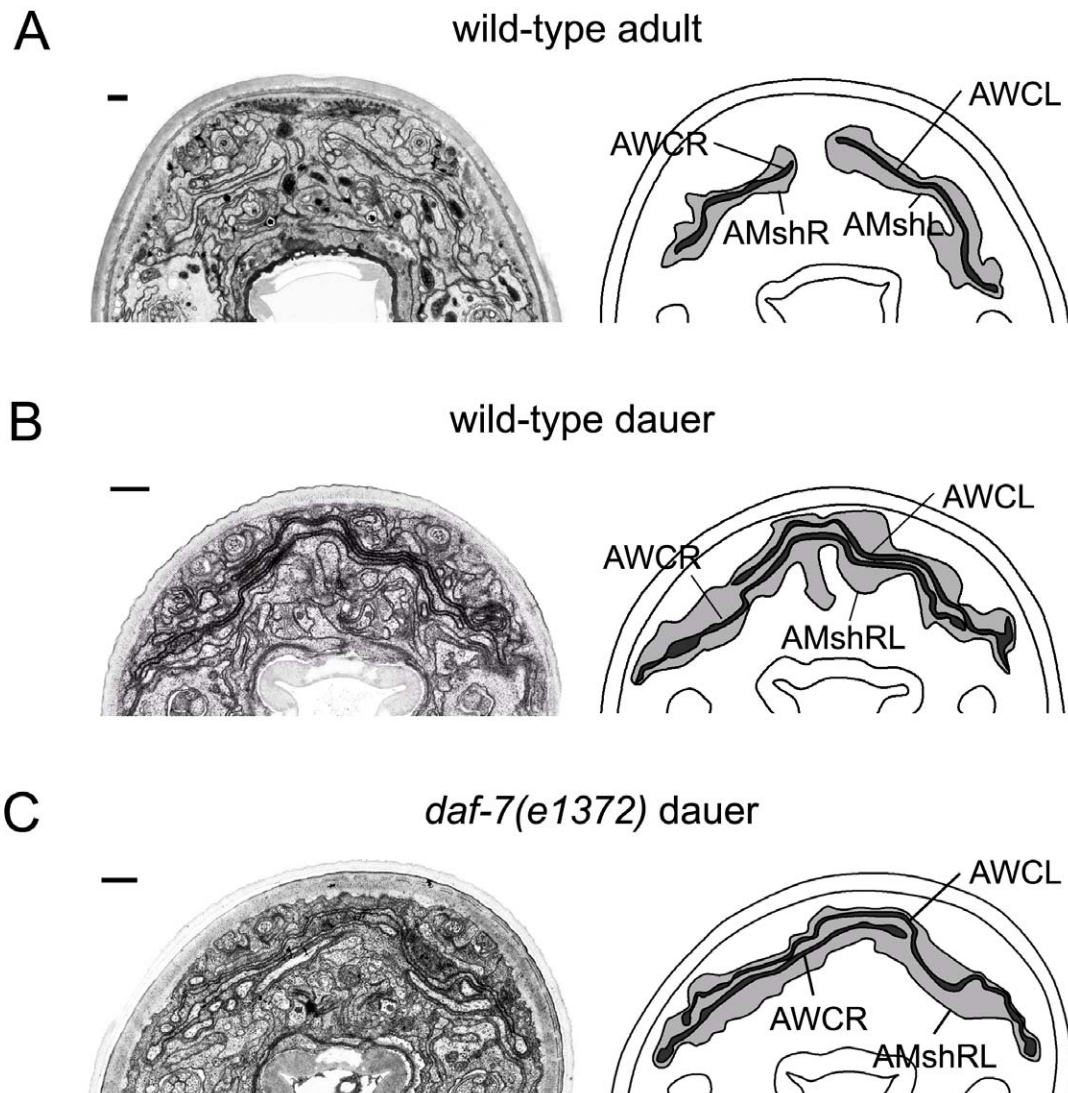


**Figure 2.1. AWC neuron receptive endings and AMsh glia remodel in dauer animals.** (A-C) Representative electron micrographs (EM) and schematic outlines of amphid sensory organs in non-dauer wild-type adults (A), wild-type dauers induced by starvation (B), and *daf-7(e1372)* dauers (C). Dorsal is up. In all schematics, left and right AWC (AWCL/R; dark shading) and AMsh glia (AMshL/R; light shading) are indicated. Scale bars, 5  $\mu$ m. See also Figure 1.6.

## **AMsh glia fusion is dependent on AFF-1 and is not reversible**

To probe the extent of AMsh glia remodeling in dauers and to quantitatively describe the process, we developed a fluorescence assay to monitor AMsh glia fusion. First- or second-stage *daf-7(e1372)* larvae expressing an AMsh glia::*green fluorescent protein (gfp)* reporter from an unstable extrachromosomal array (*nsEx1391, F16F9.3 promoter::gfp*) were selected for mosaic expression of GFP in only one of the two glial cells. These animals were then cultivated for 48 h at 25°C to induce dauer entry. The presence of GFP in both glial cells in dauers was taken as evidence of cytoplasmic mixing between the cells, indicative of cell fusion (Figure 2.2).

Four control studies suggest that our assay faithfully reports on cell fusion:

First, two independent chromosomally-integrated transgenes expressing a fluorescent reporter protein under the *F16F9.3* promoter (*nsIs142* and *nsIs143*) are constitutively expressed in both AMsh glia ( $n = 100$  animals for each line), supporting the notion that single-cell expression of animals carrying the AMsh glia::*gfp* reporter (*nsEx1391*) is a result of mosaicism of the extrachromosomal array, and not asymmetric reporter expression.

Second, we tested whether the presence of GFP in both AMsh glia required molecular mediators of cell fusion. Two *C. elegans* genes, *eff-1* and *aff-1*, encode fusogens required for somatic cell fusion in the animal (Mohler et al., 2002; Sapir et al., 2007). We found that both genes were expressed in AMsh glia (Figure 2.3A,B) (Mohler et al., 2002; Sapir et al., 2007) and localized to the apical region that undergoes fusion in dauers (Figure 2.3C,D). Furthermore, glia fusion was markedly reduced in *aff-1*(RNAi)

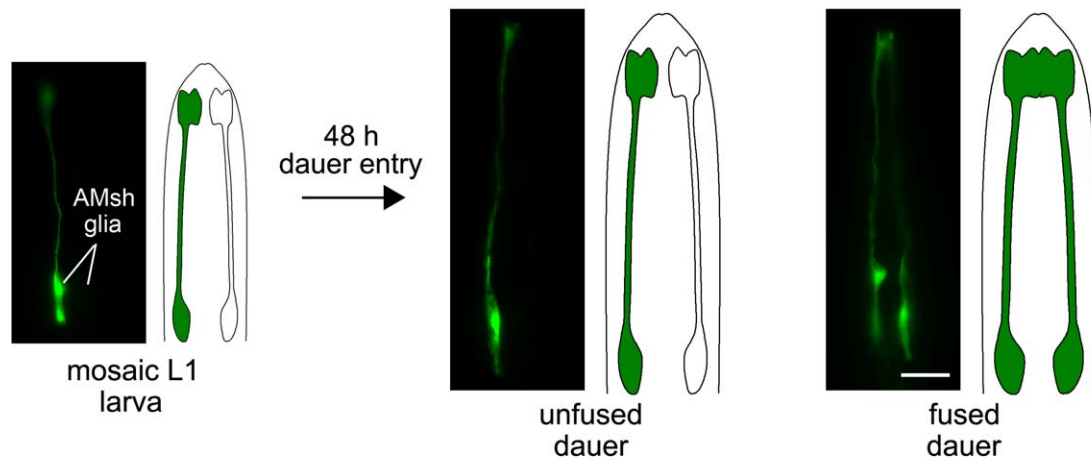


**Figure 2.2. Scoring AMsh glia fusion by cytoplasmic mixing.** Animals express an AMsh::*gfp* reporter from an unstable extrachromosomal array (*nsEx1391*). First- or second-stage mosaic larvae expressing GFP in one of the two AMsh glia were picked and cultivated for 48 h at 25°C. If the two AMsh glia fuse at the nose-tip, cytoplasmic mixing occurs and both cells fluoresce. If fusion does not occur, the animals continue to express GFP in only one of the two AMsh glia. Entry into dauer is facilitated by the temperature-sensitive, dauer-constitutive *daf-7(e1372)* allele. Examples of *daf-7(e1372)* dauers where cytoplasmic mixing has and has not occurred are shown. Scale bar, 20  $\mu$ m. Anterior is up.

**Figure 2.3. AMsh glia fusion is dependent on the *aff-1* fusogen.** (A,B) Fluorescence (left) and DIC (right) images of a wild-type adult animal carrying (A) an *aff-1* promoter::*gfp* transgene (*hyEx167*) or (B) an *eff-1* promoter::*gfp* transgene (*zzEx26*). Arrows indicate AMsh glia cell bodies. Scale bars, 20  $\mu\text{m}$ . Anterior is up. (C) Fluorescence (left) and DIC (right) images showing localization of an AFF-1::GFP fusion protein, expressed under an AMsh glia promoter (*nsEx2727*), to the nose-tip (arrow). Punctal cell body expression is also seen. Scale bar, 15  $\mu\text{m}$ . (D) Fluorescence image showing localization of an EFF-1::GFP fusion protein, expressed under an AMsh glia promoter (*nsEx2703*), to the nose-tip of a dauer animal. Dashed line is the outline of the animal. Scale bar, 20  $\mu\text{m}$ . (E) Percentage of *daf-7(e1372)* dauer animals treated with *eff-1* and *aff-1* RNAi with fused AMsh glia as assayed by cytoplasmic mixing. *P* values between columns are determined using the  $\chi^2$  test. Number of animals examined (*n*) is above each column.

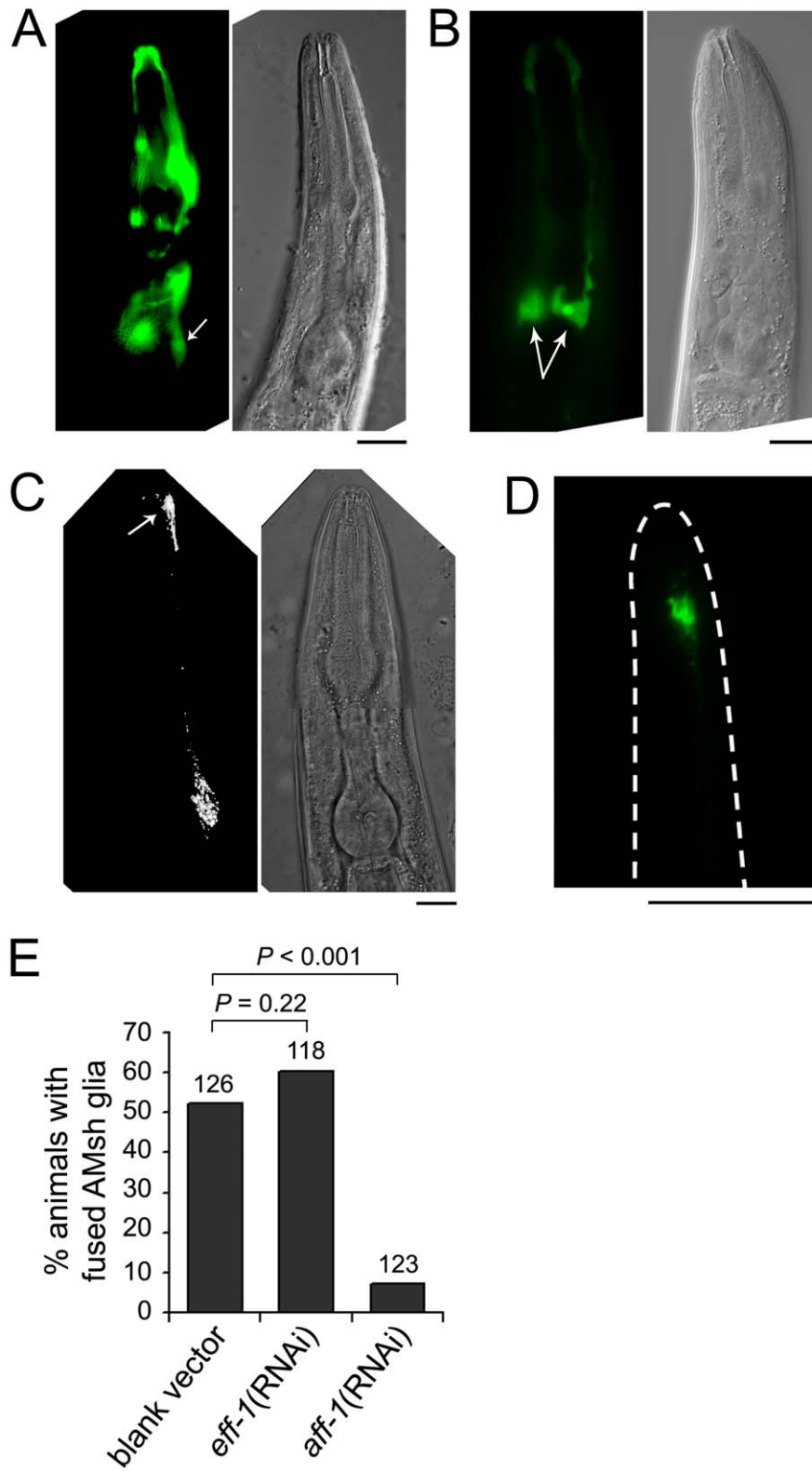


Figure 2.3. AMsh glia fusion is dependent on the *aff-1* fusogen.

dauers (Figure 2.3E), demonstrating an important role for AFF-1 protein in glia remodeling. RNAi against *eff-1* had no effect on glia fusion.

Third, EM serial reconstructions demonstrated that glia remain unfused in dauer animals expressing GFP in only one AMsh glial cell, whereas dauers expressing GFP in both AMsh glia have fused glia (see below).

Fourth, when we followed mosaic animals over time we observed that the time taken for GFP to be expressed at equal intensity in both glia took less than 2 h ( $n = 17$ ). In some of these animals, GFP fluorescence at the nose tip was stronger relative to the cell body, indicative of a cell filling with GFP at its fused anterior tip (Figure 2.4). These observations are consistent with cell fusion.

Using our validated assay, and consistent with our EM studies, we found that AMsh glia fusion was never observed in wild-type, non-dauer adult animals, whereas 51% of animals induced to enter dauer by the *daf-7(e1372)* mutation had fused AMsh glia (Figure 2.5A). To address whether remodeling of AMsh glia was reversible upon exit from the dauer state, we examined post-dauer *daf-7(e1372)* adult animals recovered by cultivation of dauers at 15°C for 7 days. While GFP perdures in amphid sheath glia for two days or less (Perens and Shaham, 2005), we found equal GFP fluorescence in both glial cells (Figure 2.5B). Furthermore, EM serial reconstruction of a single wild-type 2-day post-dauer adult revealed fused AMsh glia (Figure 2.5C; image provided by Singhvi, Lu and Shaham). Together, these results suggest that remodeling induces a permanent change in AMsh glia architecture.

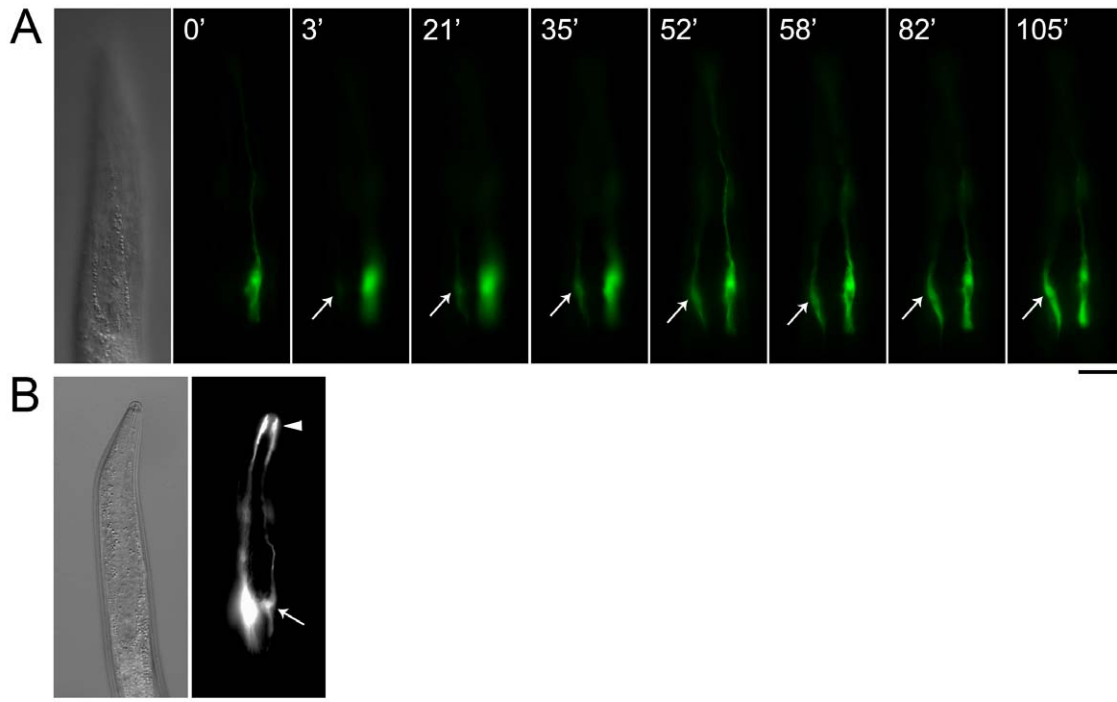


**Figure 2.4. Cytoplasmic mixing of GFP between fused AMsh glia.** (A) Fluorescence images showing cytoplasmic mixing of GFP between two AMsh glia in a *daf-7(e1372)* animal induced to enter dauer by cultivation at 25°C. The animal was initially selected for mosaic expression of an AMsh::*gfp* reporter (see Figure 2.2). Far left image, DIC. In fluorescence images, the plane of focus is at the level of the AMsh cell body which is filling with GFP, as marked by an arrow. In these images, the nose tip is out of focus. Time in minutes (') is indicated. The animal was anesthetized using 10 mM levamisole in S-basal. (B) Fluorescence image of a *daf-7* animal during cytoplasmic mixing. The AMsh glia on the right is filling with GFP. Note the greater intensity of GFP at the nose tip (arrow head) compared to the cell body (arrow) (compare with the relative GFP intensities between the anterior cell tip and cell body of the glia on the left). In (A,B), scale bar, 20  $\mu$ m. Anterior is up.

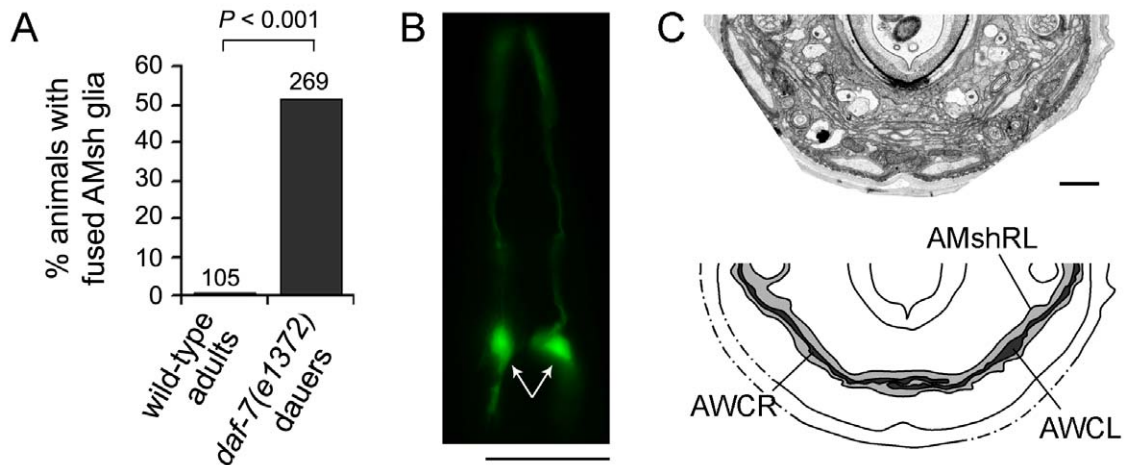


**Figure 2.5. Remodeling of AMsh glia occurs in dauer animals and persists in dauer-recovered adults.** (A) Percentage of animals with fused AMsh glia as scored by cytoplasmic mixing. Number of animals examined ( $n$ ) is above each column.  $P$  value between columns was determined using the  $\chi^2$  test. (B) Representative fluorescence image of a dauer-recovered *daf-7(e1372)* adult. First- or second-stage *daf-7* larvae with mosaic expression of an AMsh::*gfp* reporter were induced to enter dauer at 25°C and then selected for GFP fluorescence in both AMsh glia (see A and Figure 2.2). These animals were then induced to exit the dauer stage and became adults by cultivation at 15°C for 7 days. Note persistence of equal intensity *gfp* expression in both AMsh glia (arrows). Scale bar, 50  $\mu\text{m}$ . Anterior is up.  $n = 44$ . (C) Electron micrograph (EM) image (top) and schematic outline (below) of the amphid sensory organs of a wild-type, 2-day post-dauer adult. In this animal, the AMsh glia have fused on the ventral side. Scale bar, 1  $\mu\text{m}$ . Dorsal is up.

## **AMsh glia remodeling is independent of AWC expansion**

In all dauers and normally-developed adults that we examined by EM serial reconstructions, regardless of genotype, we found that overlap of AWC sensory receptive endings correlated with AMsh glia expansion and fusion (8 and 19 animals examined with and without AWC overlap, respectively; Figure 2.1; see also below). In one *daf-7(e1372)* dauer, glia expanded to allow overlap of the bilateral AWC receptive endings but did not fuse (Figure 2.6). These observations suggested to us that the remodeling of AMsh glia, with or without fusion, may be required to define a compartment into which the AWC receptive endings expand in dauers.

Changes in glial architecture to accommodate the remodeling of AWC receptive endings could be induced by the expanding AWC neurons. Alternatively, glia may independently define a compartment that limits the extent of AWC expansion. To distinguish between these possibilities, we ablated the two AWC neurons using a laser microbeam in first-stage *daf-7(e1372)* larvae that were mosaic for AMsh glia::*gfp* expression and that expressed an AWC promoter::*yellow fluorescent protein (yfp)* reporter (*oyIs45*). Ablated animals were then induced to become dauers by incubation at 25°C for 48 h, and glial fusion was monitored using the cytoplasmic mixing assay. We found that mock-ablated animals had a high rate of fusion, 89% ( $n = 36$ ), perhaps a result of the strain background (Figure 2.7A). Importantly, in animals where both AWC neurons were ablated, we saw no significant decrease in glial cell fusion (81%;  $n = 26$ ;  $P = 0.47$ , Fisher's exact test). EM serial reconstructions of ablated animals confirmed both the degradation of the AWC receptive endings and the remodeling of the glia in the absence of AWC expansion (Figure 2.7B;  $n = 2$ ).

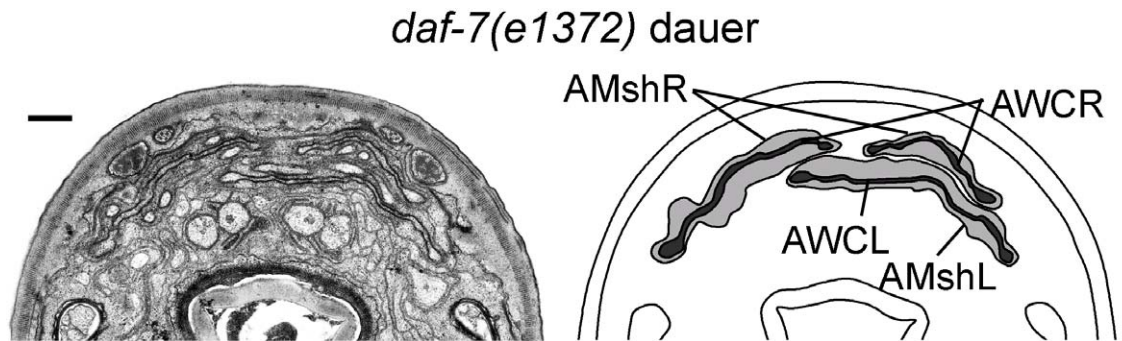
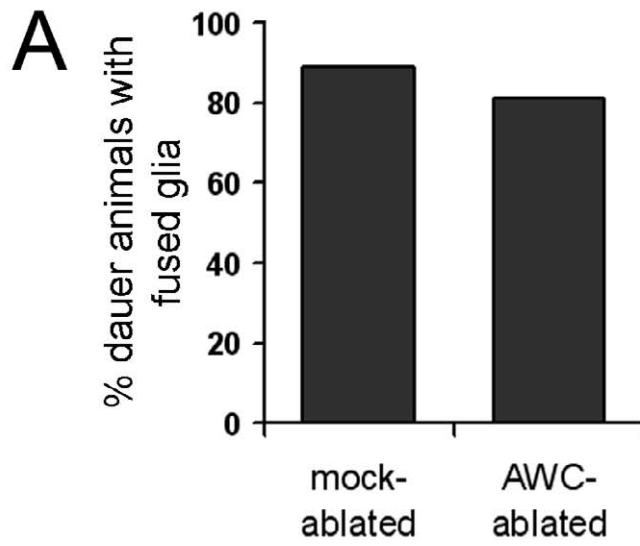


**Figure 2.6. Changes in AMsh glia shape correlate with AWC neuron remodeling.** Electron micrograph (EM) and schematic outline of the amphid sensory organs of a *daf-7(e1372)* dauer larva in which the AWC sensory endings expanded and overlapped. The AMsh glia also expanded but did not fuse. Scale bar, 5  $\mu$ m; dorsal is up. Left and right AWC (AWCL/R; dark shading) and AMsh glia (AMshL/R; light shading) are indicated.

**Figure 2.7. Changes in AWC shape are not required for AMsh glial fusion. (A)** Percentage of mock- and AWC-ablated dauer animals with fused AMsh glia as scored by cytoplasmic mixing ( $P = 0.47$ , Fisher's exact test). All animals carry the *daf-7(e1372)* mutation and AWC promoter::*yfp* reporter (*oyIs45*). **(B)** Electron micrograph (EM) (top) and schematic outline (below) of the amphid sensory organs of a *daf-7(e1372); AWC::*yfp* (oyIs45)* dauer, where both AWC neurons were ablated in the first larval stage. AMsh glia fusion was scored prior to EM analysis by assaying for glial cytoplasmic mixing. Left and right AWC (AWCL/R; dark shading) and AMsh glia (AMshL/R; light shading) are indicated. Scale bar, 5  $\mu\text{m}$ ; dorsal is up.



**B** AWC-ablated *daf-7(e1372)* dauer

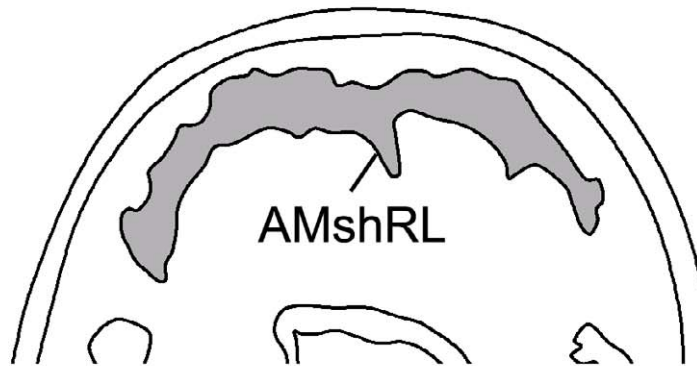
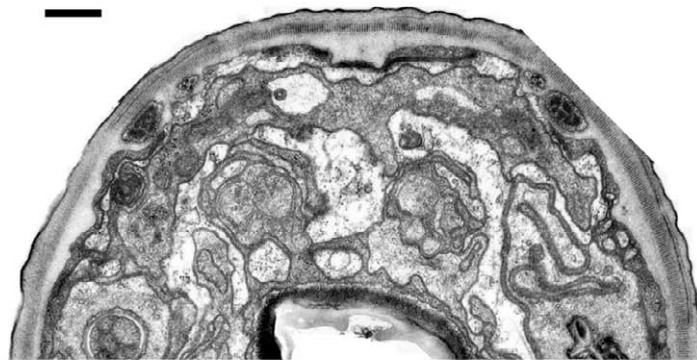


**Figure 2.7. Changes in AWC shape are not required for AMsh glial fusion.**

These results suggest that in response to external dauer signals the AMsh glia, independently of AWC neurons, define a compartment that delimits AWC receptive ending expansion.

### ***ttx-1* is required in AMsh glia for glia remodeling**

The observation that glia can remodel in the absence of AWC neurons suggests that active processes within AMsh glia may be required to promote glia remodeling and that interference with these processes should lead to defects in AWC sensory receptive ending shape. To test this prediction and to begin to characterize the molecular basis for glia remodeling, we sought fully-penetrant mutants in which glia remodeling was blocked. Importantly, since previous studies from our laboratory indicated that AMsh glia are required for maintaining AWC receptive ending shape (Bacaj et al., 2008), we aimed to identify mutants that specifically disrupt glia remodeling in dauers but in which glial shape was unperturbed in non-dauer animals. *aff-1* was unsuitable for such an analysis: RNAi knockdown of *aff-1* did not have a fully-penetrant defect in glial remodeling and *aff-1* genetic lesions had morphological abnormalities in the AMsh glia and other tissues by EM (Lu, Oikonomou and Shaham, unpublished results; see also Sapir et al., 2007). Therefore, other mutants were sought.

In the course of our studies, we had observed that the transcription of an AMsh glia-expressed gene, *ver-1*, was strongly dependent on temperature (see Chapter 3). *ttx-1* codes for an *otd/Otx* transcription factor required for temperature responses of the animal (Satterlee et al., 2001). Therefore, we analyzed the effect of the gene *ttx-1* on glia remodeling. As shown in Figure 2.8, AMsh glia fusion failed to occur in almost all *daf-*

*7(e1372); ttx-1(p767)* and *daf-7(e1372); ttx-1(oy26)* double mutant dauer animals scored using the cytoplasmic mixing assay. Thus, *ttx-1* may be a component of the glial remodeling machinery, and *ttx-1* mutants might provide a suitable genetic background in which to test the effects of AMsh glia remodeling on AWC neuron shape changes.

However, previous studies suggested that *ttx-1* is expressed specifically in the AFD thermosensory neurons of *C. elegans*. Animals carrying *ttx-1* promoter::*gfp* transgenes express GFP in AFD (Satterlee et al., 2001), and the AFD sensory receptive endings in *ttx-1* mutants lack their wild-type microvilli-like protrusions (Perkins et al., 1986). Furthermore, *ttx-1* mutants have defects in thermotaxis, an AFD-dependent behavior in which animals placed in a thermal gradient seek the temperature at which they were reared (see Chapter 1) (Hedgecock and Russell, 1975; Mori and Ohshima, 1995). *ttx-1* might, therefore, act in AFD to drive AMsh glia fusion in dauers. To test this possibility, we blocked activity in a number of amphid sensory neurons, including AFD, using a mutation in the *tax-2* gene, which encodes a subunit of a cyclic nucleotide gated channel required for thermotaxis and other sensory functions (Coburn and Bargmann, 1996; Komatsu et al., 1996). We observed no defect in the fusion of AMsh glia in *tax-2(p691)* mutants (Figure 2.8;  $P = 0.70$ ,  $\chi^2$  test), suggesting that sensory signaling in AFD was unlikely to be important for glia remodeling. These results suggested the possibility that *ttx-1* may act in AMsh glia to promote their remodeling in addition to its previously described roles in AFD.

To test this idea, we examined expression of transgenes containing *ttx-1* regulatory sequences fused to sequences encoding fluorescent reporter proteins. As shown in Figure 2.9A,B, a 7.5 kb sequence immediately upstream of the *ttx-1*

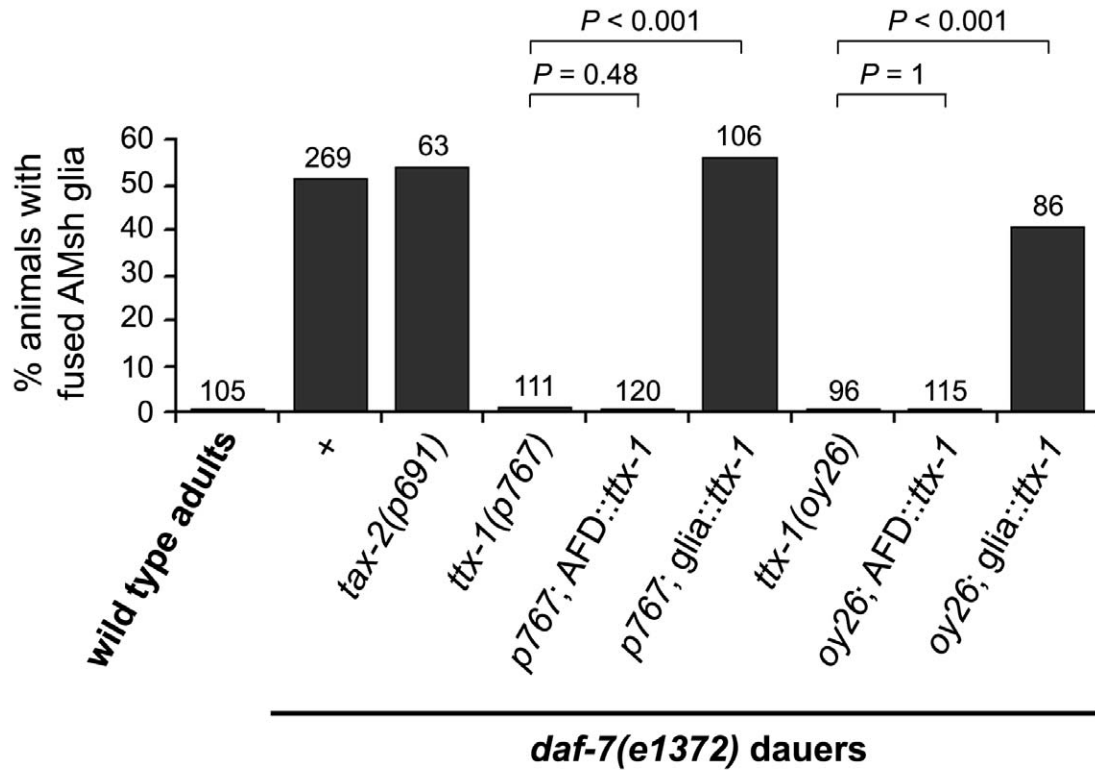


**Figure 2.8. *ttx-1* is required for AMsh glia remodeling in dauers.** Percentage of animals with fused AMsh glia as scored by cytoplasmic mixing. Strains carrying a *daf-7(e1372)* mutation are as indicated. Number of animals examined (*n*) is above each column. *P* values between columns are determined using the  $\chi^2$  test or Fisher's exact test. Transgenes expressing cell-specific *ttx-1* are *nsIs99* (AFD::*ttx-1*) and *nsIs219* (glia::*ttx-1*). The longest *ttx-1* splice form, *ttx-1a*, was used (see Chapter 3; Table 3.3). Additional glia::*ttx-1* transgenes also gave rescue of glia fusion (data not shown).

**Figure 2.9. *ttx-1* is expressed in glia.** (A) A schematic of the *ttx-1* promoter. The ATG start codon and first exon (filled narrow box) are shown, as well as 11 kb of upstream sequence (solid, horizontal line). The *ttx-1*pro1 region includes the 7.5 kb sequence upstream and adjacent to the *ttx-1* start site. The *ttx-1*pro2 region includes the 3.5 kb sequence upstream of *ttx-1*pro1. Scale bar, 2 kb. (B) Fluorescence image of an adult animal carrying a transgene containing the *ttx-1*pro1 sequence fused to *dsRed* (*nsEx1320*). Fluorescence is seen in the two AFD thermosensory neurons. (C) Fluorescence image of an animal carrying a transgene containing the *ttx-1*pro2 sequence fused to *gfp* (*nsEx1942*). Reporter expression is evident in the AMsh (arrows) and amphid socket (arrowheads) glia. (D,E) Representative fluorescence images of *vap-1* promoter::*dsRed* (*nsIs53*) expression within an AMsh glial cell at 20°C in wild-type (D) and *ttx-1*(*p767*) mutant (E) adults. Exposure time, 250 ms. In (B,C) and (D,E), scale bars, 50 μm; anterior is up.

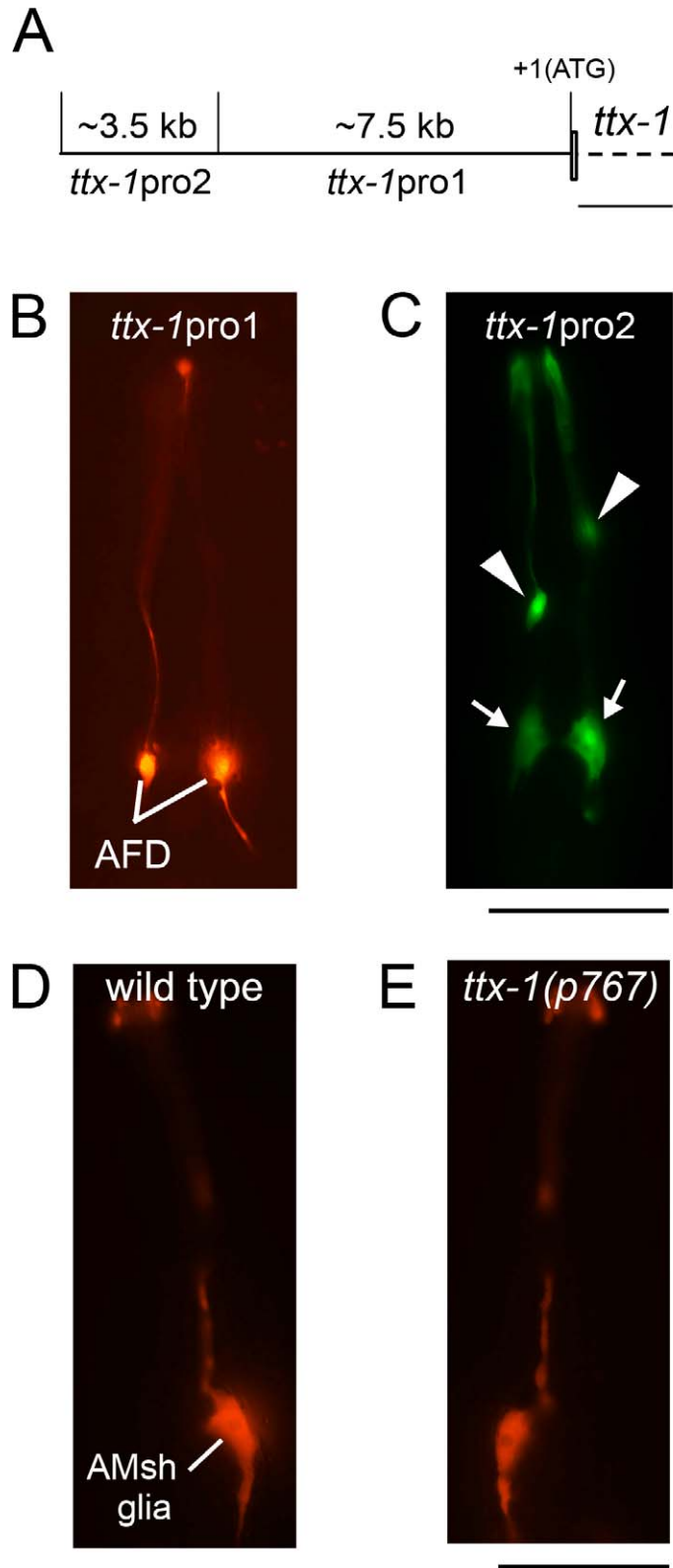


Figure 2.9. *ttx-1* is expressed in glia.

transcription start site drives reporter expression in AFD, consistent with previous observations (Satterlee et al., 2001). By contrast, a 3.5 kb sequence further upstream drives expression in AMsh and phasmid sheath (PHsh) glia, as well as in associated socket glia (Figure 2.9A,C; and data not shown). The PHsh glia are associated with the phasmid sensory organ in the tail. Furthermore, by driving *ttx-1* cDNA under cell-specific promoters (see Chapter 6 for promoter details), we observed that although expression of *ttx-1* in AFD was sufficient to confer wild-type AFD sensory ending morphology and thermotaxis to *ttx-1* mutants (Figure 2.10A-C,F-H; see also Satterlee et al., 2001), it did not rescue the AMsh glia fusion defect in dauer animals (Figure 2.8). Restoring *ttx-1* in AMsh glia, however, rescued AMsh glia fusion (Figure 2.8) but not thermotaxis or AFD morphology (Figure 2.10A,D,E,I). These results demonstrate that *ttx-1* has separable, cell-autonomous roles in the AFD thermosensory neurons and the AMsh glia.

To determine whether *ttx-1* was generally required for AMsh glia shape maintenance, we examined the morphology of these cells in non-dauer animals. We found no defects in the shape of these glia. Furthermore, expression of constitutive glial genes we examined was affected weakly or not at all by mutations in *ttx-1* (Figure 2.9D,E; and data not shown). In addition, an *aff-1* promoter::*gfp* reporter (*hyEx167*) showed GFP expression in AMsh glia of both wild-type and *ttx-1* mutants (86% of wild-type animals expressed GFP in AMsh glia, compared to 93% of *ttx-1(p767)* mutants;  $n > 40$  both genotypes), suggesting that *ttx-1* likely affects glia remodeling and fusion through the transcriptional regulation of genes other than *aff-1*.

**Figure 2.10. Glial expression of TTX-1 is not required for AFD morphology or AFD-mediated thermotaxis behavior.** (A) The number of animals with a mutant, elongated single cilium present or absent at the AFD dendrite ending at 25°C. In some mutant animals, microvilli are observable at the base of the single cilium. Representative, cell-specific *ttx-1a* rescuing arrays are shown (*nsEx875*, *nsEx877* and *nsEx930*). Equivalent rescue was obtained with splice form *ttx-1b* (see Chapter 3). (B-E) Representative fluorescence images of the AFD dendrite endings of adult wild-type (B), *ttx-1(oy26)*; AFD::*ttx-1a* (C), *ttx-1(oy26)*; AMsh::*ttx-1a* (D), and *ttx-1(oy26)*; AM+PHsh::*ttx-1a* (E) strains at 25°C. Scale bar, 5 μm. Anterior is left. In (A-E), a *gcy-8* promoter::*gfp* transgene (*oyIs17*) was used to visualize the AFD neurons. Note the presence of an aberrant single elongated cilium in (D,E). (F-I) Thermotaxis of wild-type (F), *ttx-1(p767)* mutant (G), *ttx-1(p767)*; AFD::*ttx-1a* (*nsIs99*) (H), and *ttx-1(p767)*; glia::*ttx-1a* (*nsIs219*) (I) animals. Animals were cultivated at 15°C (blue), 20°C (yellow) or 25°C (red) prior to performing each assay (see Chapter 6). The linear temperature gradient is represented by bins 1-6 on the horizontal axis, from cold (~18°C) to hot (~26°C). All values are mean +/- s.d. All animals also carry the *ver-1* promoter::*gfp* transgene (*nsIs22*). For AFD cell-specific rescues of AFD morphology and thermotaxis defects of *ttx-1* mutants (C,H) see also reference (Satterlee et al., 2001).

**A**

Genotype	AFD morphology at 25°C		
	absence of cilium	elongated single cilium	n
wild type	30	0	30
<i>ttx-1(oy26)</i>	5	24	29
<i>ttx-1(oy26); AFD::<i>ttx-1</i></i>	14	1	15
<i>ttx-1(oy26); AMsh::<i>ttx-1</i></i>	1	14	15
<i>ttx-1(oy26); AM+PHsh::<i>ttx-1</i></i>	1	17	18

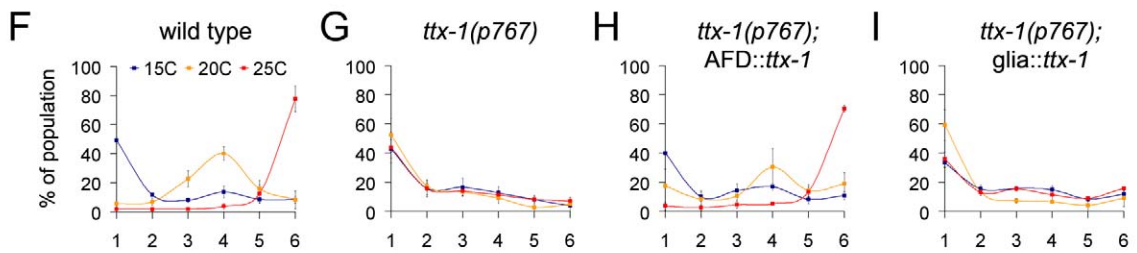
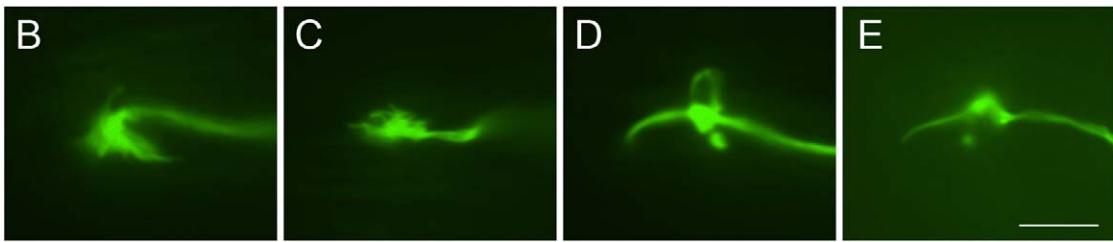


**Figure 2.10. Glial expression of TTX-1 is not required for AFD morphology or AFD-mediated thermotaxis behavior.**

Our data show that *ttx-1* has specific cell-autonomous roles in AMsh glia, supporting the idea that active glia-intrinsic processes promote glia remodeling. These results also suggest that animals lacking *ttx-1* function provide a suitable setting in which to test the effects of AMsh glia on AWC neuron remodeling.

### **Proper remodeling of AWC neurons requires glia**

To address whether remodeling of AWC receptive endings in dauer animals depends on remodeling of AMsh glia, we examined EM serial sections of *ttx-1* mutants. We first noted that *ttx-1(p767)* starvation-induced dauers as well as *ttx-1(p767); daf-7(e1372)* dauers indeed fail to show AMsh glia fusion (Figure 2.11A,B;  $n = 6$ ), verifying the results of our cytoplasmic mixing assay. Importantly, in these same animals, AWC receptive endings did not overlap extensively (Figure 2.11A,B;  $n = 6$ ,  $P < 0.016$ ). Furthermore, animals in which AMsh glia fusion was rescued by restoring *ttx-1* expression in these cells displayed a wild-type pattern of AWC overlap by EM (Figure 2.11C;  $n = 2$ ). Interestingly, in 2/6 *ttx-1* mutants we examined, AWC appeared to have expanded but, instead of projecting circumferentially around the nose as was always observed when AWC expanded in wild-type dauers, folded back on itself (Figure 2.12). It is possible that in these animals AWC attempts to expand but is constrained by the size of the compartment defined by the unfused glial cell, and therefore forms a whorl rather than extending circumferentially.

The AWC ablation and *ttx-1* studies demonstrate that AMsh glia respond to dauer signals independently of AWC to define a compartment confining AWC receptive

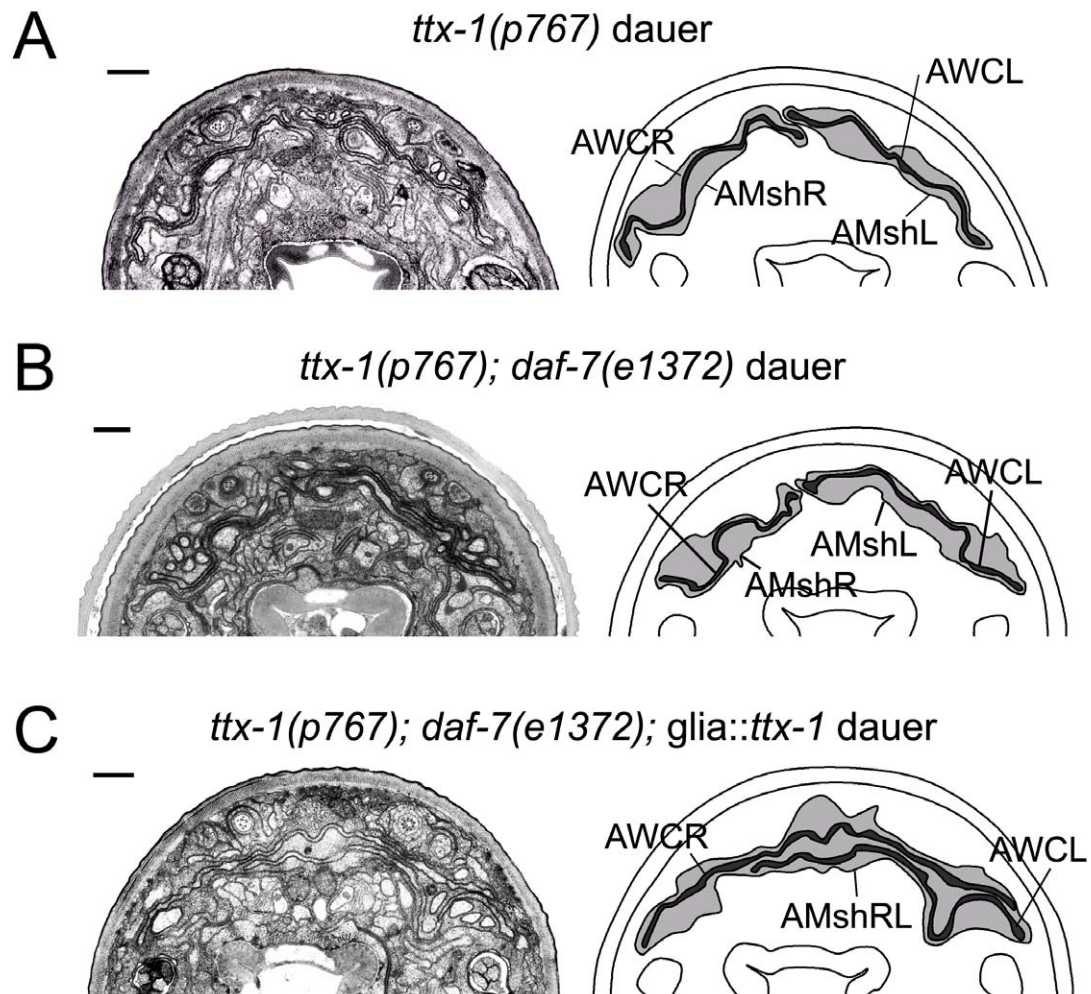


**Figure 2.11. *ttx-1* is required for remodeling of AMsh glia.** (A-C) Representative electron micrographs (EM) and schematic outlines of amphid sensory organs in *ttx-1(p767)* dauers induced by starvation (A), *ttx-1(p767); daf-7(e1372)* dauers (B), and *ttx-1(p767); daf-7(e1372); glia::ttx1 (nsIs219)* dauers with fused AMsh glia as assayed by cytoplasmic mixing prior to EM analysis (C). Left and right AWC (AWCL/R; dark shading) and AMsh glia (AMshL/R; light shading) are indicated. Scale bars, 5 μm; dorsal is up.

*ttx-1(p767); daf-7(e1372)* dauer

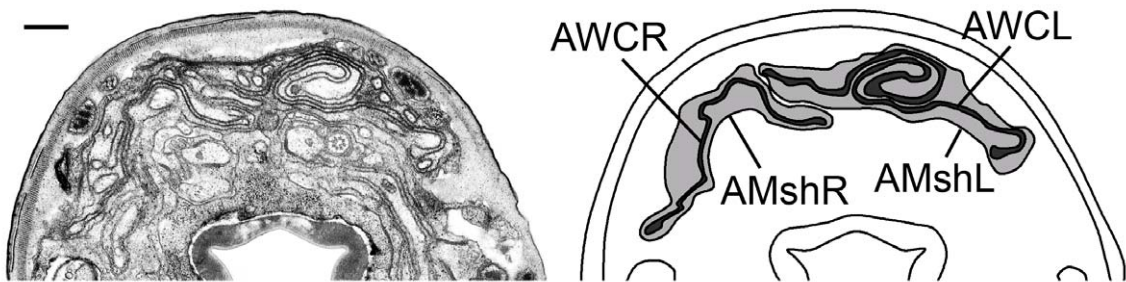


**Figure 2.12. The AWC neuron cilia are constrained by the ensheathing AMsh glia.** Electron micrograph (EM) image and schematic outline of the amphid sensory organs of a *ttx-1(p767); daf-7(e1372)* dauer animal in which an AWC neuron folded back on itself within an unfused glial process. Scale bar, 5  $\mu\text{m}$ . Dorsal is up. Left and right AWC (AWCL/R; dark shading) and AMsh glia (AMshL/R; light shading) are indicated.

endings, and that defects in glial compartment plasticity lead to defects in the morphology of AWC receptive endings.

## Discussion

The results described here show that the extent of remodeling of a glial compartment in *C. elegans* dauers restricts the shape of remodeled AWC receptive endings: when *ttx-1* function in glia is impaired the AWC sensory protrusions fail to take on their wild-type overlapping appearance. Glia or glia-like cells are intimately associated with sensory receptive endings from *C. elegans* to humans (Shaham, 2010), suggesting that the roles they play in delimiting receptive ending morphological plasticity may be conserved. Furthermore, the many similarities between sensory receptive endings and dendritic spines, which serve as receptive endings for postsynaptic neurons (Shaham, 2010), suggest the interesting possibility that glia may be in a position to define compartments that will constrain dendritic spine shape as well. Indeed, all dendritic spines examined by EM in the cerebellum are tightly ensheathed by Bergmann glia (Spacek, 1985), and most spines examined by EM in the hippocampus are ensheathed by astrocytes (Ventura and Harris, 1999). Furthermore, Bergmann glia have been shown to affect neuronal receptive ending shapes in the cerebellum (Lippman et al., 2008), and astrocytic glia affect dendritic spine morphology of hippocampal neurons via ephrin-A3/EphA4 signaling (Murai et al., 2003).

At least two possible mechanisms by which the glial compartment can delimit receptive-ending shape are possible. Glia may form an inelastic physical barrier against

expansion of neuronal receptive endings. Alternatively, glia may provide specific signals that induce receptive-ending growth or retraction. Although both mechanisms may apply, our finding that in some *ttx-1* mutants AWC attempts to remodel but forms membrane whorls confined to the space defined by the AMsh glia (Figure 2.12) is consistent with a physical barrier role for these cells. A similar role for astrocytic glia in remodeling SON neuron synapses in the mammalian hypothalamus has been proposed: the retraction of astrocytic processes from postsynaptic surfaces may facilitate the increased number of synapses that occur onto a single postsynaptic element during lactation in female rats (Theodosis and Poulain, 1993). In both of these cases, remodeling of the glia may be permissive for neuronal shape changes.

The receptive endings of the amphid AFD thermosensory neurons may also remodel in dauer animals, as the number of AFD microvilli has been reported to increase upon dauer entry (Albert and Riddle, 1983). Thus, it is possible that AMsh glia play a role in this remodeling process as well. We were unable to use *ttx-1* mutants to assess the effects of AMsh glia on AFD remodeling, as *ttx-1* also functions within AFD to control morphology.

Together, our results suggest that plasticity of dendrite receptive ending shape can depend on glial plasticity. Furthermore, we have shown that the changes in AMsh glial shape depend on the transcriptional regulator *ttx-1* and the cell fusion protein *aff-1*, both acting in the glia. Dauer entry and glial fusion were also induced by a mutation in the neuroendocrine *daf-7*/TGF- $\beta$  signaling pathway, suggesting that some signals affecting glial changes must come from sensory neurons that regulate dauer. However, it is unclear if the glia can also respond independently of neurons to dauer-inducing

environmental stressors. In the next chapter, I will describe the characterization of a glial gene, the receptor tyrosine kinase *ver-1*, and show that its transcription is regulated both by dauer entry and the stressor high temperature. Using transcriptional reporters of this gene as a tool, I will further show that temperature signals are likely independent of sensory neurons, suggesting that the glia can respond to environmental stress and may integrate this information with dauer-inducing neuroendocrine pathways.

# **Chapter 3**

Transcription in glia depends on dauer and  
environmental temperature

## Summary

Although morphological plasticity of glia has been demonstrated in some settings, little is known about the molecular mechanisms promoting glial shape changes in response to environmental or developmental cues. Here, we show that remodeling of the AMsh glia in dauer animals is affected by mutations in the *ver-1* receptor tyrosine kinase, and that *ver-1* expression is glia-specific and dependent on dauer development. In addition, *ver-1* transcription was up-regulated by an environmental stimulus that induces dauer: high temperature. *ver-1* expression required the transcription factor TTX-1, previously shown to affect AFD thermosensory neuron morphology and function. However, we found that *ver-1* expression at high temperature was independent of AFD, suggesting that the glia might respond to temperature independently of sensory neurons. Our findings suggest that glial transcription is dynamically regulated by environmental and developmental cues, and that these transcriptional changes are important for morphological remodeling of the glia.

## Results

### ***ttx-1* promotes AMsh glia remodeling by inducing *ver-1*/RTK expression**

To further elaborate the mechanism by which *ttx-1* promotes the remodeling of AMsh glia, we turned our attention to the gene *ver-1*. *ver-1* encodes a protein with similarities to the mammalian vascular endothelial growth factor receptor (VEGFR), a receptor tyrosine kinase (RTK), and was previously reported to be expressed in AMsh and PHsh glia (Popovici et al., 2002). Interestingly, we found that at 15°C, wild-type dauers induced by starvation strongly expressed a *ver-1* promoter::*gfp* reporter in AMsh and PHsh glia (Figure 3.1A,C; see also Popovici et al., 2002). However, only very weak expression of *ver-1* was detected in non-dauer adults raised under the same temperature conditions (Figure 3.1B,D). Thus, *C. elegans* AMsh glia respond to dauer signals by modifying gene expression concomitantly with induction of remodeling.

The induction of *ver-1* expression in dauers suggested to us that this gene may be involved in remodeling AMsh glia. To test this idea, we examined two strains carrying different deletions of the *ver-1* locus (Figure 3.2A) using our fluorescence fusion assay. As shown in Figure 3.2B, both strains displayed significantly reduced AMsh glia fusion. Although we have been unable to rescue this mutant phenotype (Appendix 1), the fact that two independent alleles of *ver-1* both have reduced fusion is suggestive that this gene is required for glia remodeling.

Furthermore, we found that expression of *ver-1* in glia was dependent on functional *ttx-1*, as two independent *ttx-1* alleles greatly reduced *ver-1* promoter::*gfp* expression in dauers (Figure 3.1E). To determine how TTX-1 regulates *ver-1*

**Figure 3.1. Dauer-induced expression of *ver-1* is dependent on *ttx-1*.** (A,B) Representative fluorescence images (left) and DIC and fluorescence merged images (right) of *ver-1* promoter::*gfp* (*nsIs22*) expression in one of the two AMsh glial cells of a wild-type dauer induced by starvation at 15°C (A), and in a non-dauer adult animal at 15°C (B). Exposure time for *ver-1* promoter::*gfp* was 800 ms; scale bar, 50 μm; anterior is up. (C,D) As in (A,B), except showing *ver-1* promoter::*gfp* (*nsIs22*) expression in the PHsh glia. Exposure time was 200 ms; scale bar, 50 μm; anterior is up. (E) Expression of a *ver-1* promoter::*gfp* transgene (*nsIs22*) in AMsh glia of wild-type, *ttx-1*(*oy26*) and *ttx-1*(*p767*) dauers at 15°C and 25°C. GFP expression is scored as either strong (dark green), weak (green), or absent. Note that the *ttx-1*(*oy26*) allele is temperature sensitive.

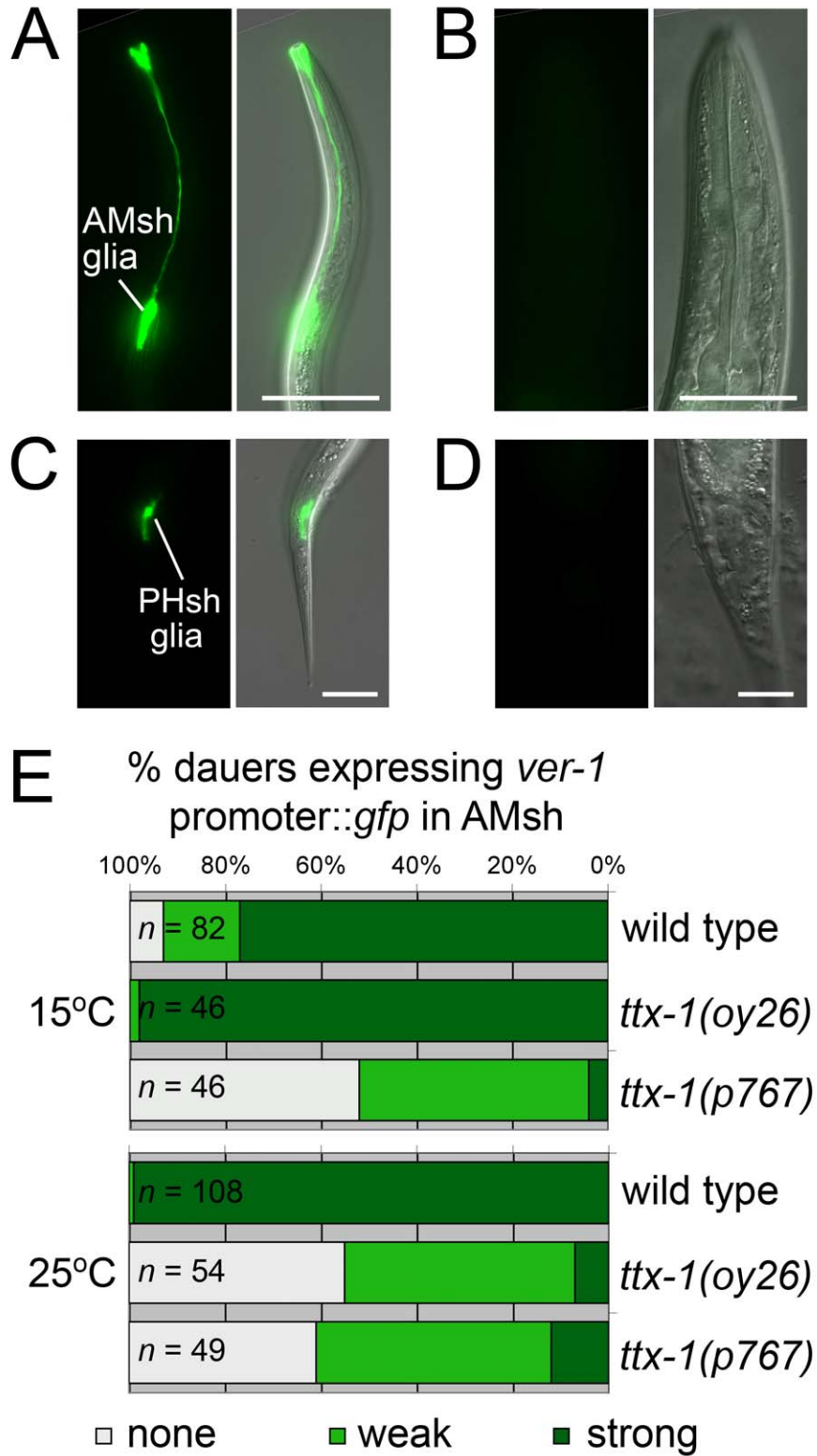
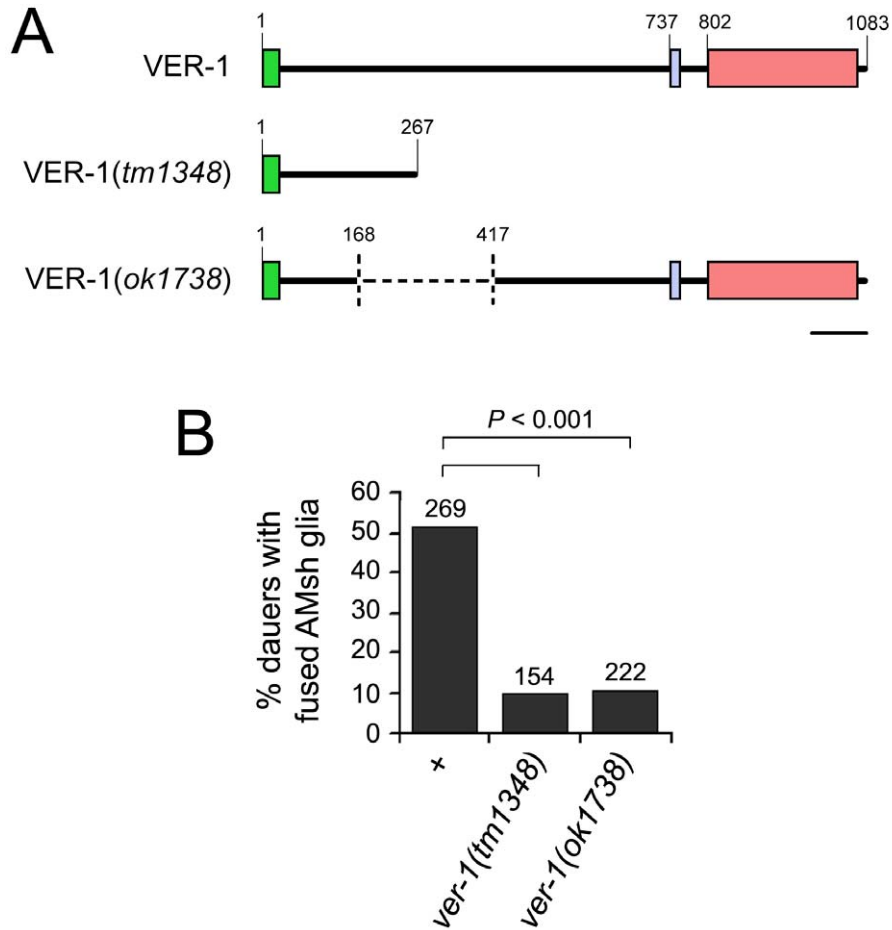


Figure 3.1. Dauer-induced expression of *ver-1* is dependent on *ttx-1*.



**Figure 3.2. Mutations in *ver-1* affect glia remodeling in dauers.** (A) A schematic of *ver-1* deletion alleles. The predicted VER-1 protein structure has an amino-terminal extracellular region (dark solid line) with immunoglobulin-like domains, flanked by a signal sequence (green box) and a single transmembrane domain (blue box). An intracellular protein kinase domain (red box) is predicted (Popovici et al., 2002). The *tm1348* allele has a frame-shift deletion that codes for a truncated protein without the transmembrane and protein kinase domains, which is followed by an additional non-homologous 21 amino acids (HSPSSETLRSETNSEKFYTFZ, not shown). A single base mutation also causes an amino acid change at position 266 (Y to C). The *ok1738* allele has an in-frame deletion (dashed line) removing part of the extracellular region. Scale bar, 100 amino acids. (B) Percentage of *daf-7(e1372)* dauer animals with fused AMsh glia as scored by cytoplasmic mixing. Number of animals examined (*n*) is above each column. *P* values were determined using the  $\chi^2$  test.

expression, we performed deletion studies of the *ver-1* promoter with the aim of identifying a minimal interval required for expression of the gene. We identified a ~90 bp interval required for *ver-1* expression in dauers (Table 3.1). Within this interval we identified a potential TTX-1 binding site based on similarity to the mammalian Otx2 binding site (Kelley et al., 2000), suggesting that *ttx-1* might directly regulate *ver-1*. Indeed, a 40 bp oligonucleotide containing this sequence bound a GST::TTX-1 homeodomain fusion protein, and alteration of the core nucleotides of the putative binding site from GGATTATC to GGGGGGTC abolished both *in vitro* binding (Figure 3.3) and *in vivo* expression of a *ver-1* promoter::*gfp* transgene (Table 3.1). Thus, *ver-1* is likely a direct TTX-1 target.

The specific requirement of *ttx-1* for both *ver-1* expression and AMsh glia remodeling in dauers suggested to us that *ttx-1* may be important for the expression of genes required for specific terminally differentiated features and/or functions of AMsh glia. To test this idea, we asked whether other glia-specific genes were also regulated by *ttx-1*. Specifically, using the BLAST algorithm to search the *C. elegans* genome, we identified within a cluster of thrombospondin (TSP)-domain encoding genes a 15-bp sequence highly similar to that surrounding the TTX-1 binding site in *ver-1* (Figure 3.4A; 14/15 residues identical). Previous studies have shown that glia secrete TSPs to regulate synaptogenesis in mammals and sensory neuron function in *C. elegans* (Bacaj et al., 2008; Christopherson et al., 2005); thus, TSP-related proteins are required for terminal/functional differentiation of glia. Transcriptional reporters for the TSP genes we studied here were expressed in either AFD neurons or AMsh glia, and were regulated by *ttx-1* (Figure 3.4B-D). This result lends support to the notion that TTX-1 is required to

**Table 3.1. A summary of *ver-1* promoter deletion studies.**

Fragment coordinates <sup>a</sup>	sheath glia GFP expression at:				regulated by <i>ttx-1</i> ? <sup>b</sup>
	15°C	25°C	dauer 15°C	dauer 25°C	
-2110 to +263 (in-frame)	–	++	++	++	yes
-2110 to +262 (-1 frame) <sup>c</sup>	–	++	nd	nd	nd
-2110 to +261 (-2 frame) <sup>c</sup>	–	++	nd	nd	nd
-2110 to -1	–	–	nd	nd	nd
+1 to +263	–	++	++	++	yes
+57 to +263	–	+	+	++	yes
+112 to +263	–	–	–	+	yes
+130 to +263	–	–	–	+	yes
+170 to +263	–	–	–	–	nd
+201 to +263	–	–	–	–	nd
+1 to +243	–	+	+	++	nd
+1 to +220	–	+	–	+	yes
+1 to +201	–	–	–	–	nd
+1 to +263 ATTA→GGGG <sup>d</sup>	–	–	–	–	nd

<sup>a</sup>The indicated fragments were fused to *gfp*, introduced into animals, and assayed for GFP expression.

“–” indicates no expression, “+” weak expression, and “++” moderate to high expression, while “nd” indicates not determined. All constructs were injected at 60 ng/μl with 60 ng/μl pRF4. Coordinates refer to positions relative to the WormBase predicted ATG start codon of *ver-1*.

<sup>b</sup>To test if a *ver-1* reporter was regulated by *ttx-1*, a single array was crossed to *ttx-1(p767)* and scored for reduced GFP intensity.

<sup>c</sup>Frame-shift reporters likely give GFP expression using the *gfp* start site rather than the *ver-1* start, and demonstrate that regulation of GFP expression by temperature and dauer is transcriptional rather than translational.

<sup>d</sup>The core ATTA nucleotides of the predicted TTX-1 binding site (GGATTATC) are at position +176.

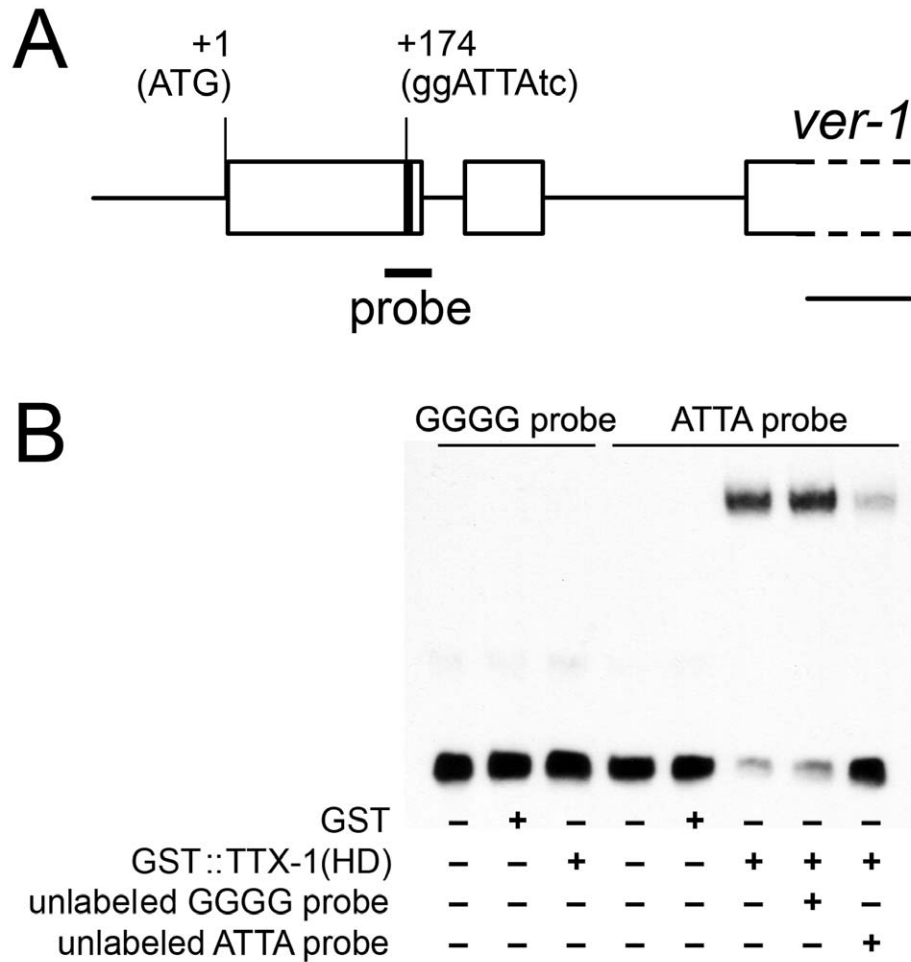


**Figure 3.3. TTX-1 can bind directly to the *ver-1* promoter.** (A) A schematic showing part of the predicted *ver-1* gene and promoter. Wormbase-predicted exons are shown as boxes, non-coding regions as a solid, horizontal line. The ATG start codon, putative TTX-1 binding site (ggATTAtc; core binding residues in capital letters), and location of the 40-bp probe used in (B) are shown. Scale bar, 100 bp. (B) Electrophoretic mobility-shift assay showing binding of either a GST control or a purified GST::TTX-1 homeodomain (HD) fusion protein to a wild-type (ATTA) or mutant (GGGG) 40 bp biotin-labeled probe from the *ver-1* promoter. Competitor, unlabeled wild-type or mutant probes were added in 200-fold excess.

**Figure 3.4. TTX-1 directly regulates glial and AFD genes.** (A) A schematic showing part of the F58F9 cosmid sequence, which includes a cluster of five thrombospondin (TSP)-domain containing genes (boxes). The gene numbers are designated by WormBase. The putative TTX-1 binding site, based on conservation with the *ver-1* promoter, is indicated (conserved residues between *ver-1* and F58F9 are 5' ACG[A/-]GATTATCGGATTCAG 3', with core TTX-1 binding residues underlined). Also shown are the *F58F9.10* and *F58F9.6* promoter regions used in expression studies. (B,C) Fluorescence images (left), and DIC and fluorescence merged images (right) showing *gfp* expression in the AFD neurons of an adult wild-type animal carrying an *F58F9.10* promoter::*gfp* transgene (*nsEx2284*) (B), or in the AMsh glia of a wild-type animal carrying an *F58F9.6* promoter::*gfp* transgene (*nsEx2330*) (C). GFP expression in AFD is indicated by arrowheads, and in AMsh glia by arrows. Expression of *F58F9.6* promoter::*gfp* in AMsh glia was rare (1/13 lines). (D) As in (C), except in a *ttx-1(p767)* mutant. (E) As in (C), except in a dauer animal. Exposure (C-E), 500 ms. Scale bar (B-E), 50  $\mu$ m. Anterior is up. All animals grown at 25°C.

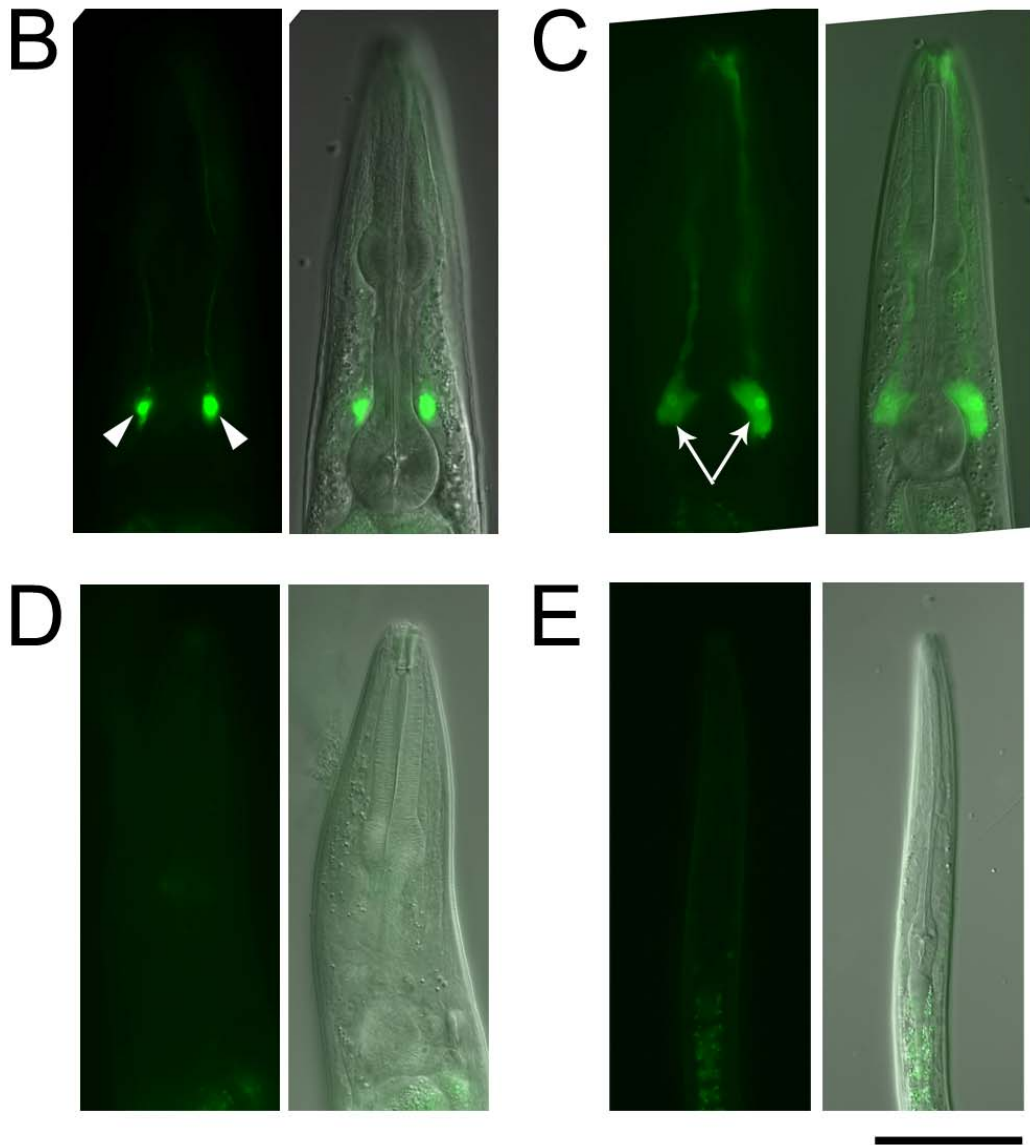
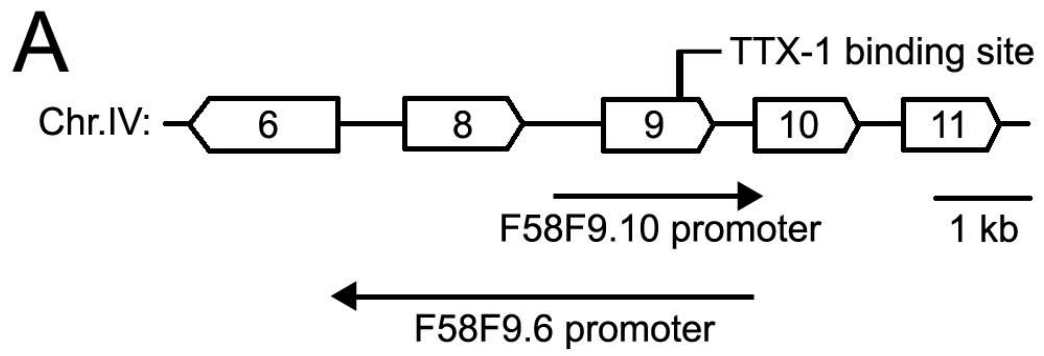


**Figure 3.4. TTX-1 directly regulates glial and AFD genes.**

directly maintain the expression of markers of both AMsh glia and AFD differentiated cell types. In addition, our observation that TSP expression within glia, unlike *ver-1*, was not dauer-dependent (Figure 3.4E) suggests that the role of TTX-1 in *ver-1* expression is likely permissive: other factors must be required to induce expression of *ver-1* in dauer animals and to confer glia *versus* AFD specificity.

Taken together, these results suggest that *ttx-1* may act to regulate AMsh glia fusion in dauer animals in part by promoting *ver-1* expression.

### ***ver-1* exhibits temperature-dependent expression in dauers and non-dauers**

Although *ver-1* expression was strongly induced by dauer entry, we also noticed induction of expression by high ambient temperature in non-dauer animals. Over a temperature range of 15-25°C, adult animals exhibited a graded increase in *ver-1* promoter::*gfp* expression intensity (Figure 3.5A,C). The increase in expression was not a general transcriptional response, as reporters for three other glial genes demonstrated only mild temperature effects and were not upregulated by dauer entry (Figure 3.6). Furthermore, neither the heat-shock nor the unfolded protein response pathways affected *ver-1* expression (Table 3.2; and data not shown), indicating that the expression pattern observed was not a result of a general stress response.

The induction of *ver-1* expression by temperature was, however, dependent on *ttx-1*, as animals containing *ttx-1* mutations failed to express the *ver-1* promoter::*gfp* reporter at high temperatures (Figure 3.5B). Restoring *ttx-1* specifically in glia rescued temperature-dependent *ver-1* expression, whereas restoring *ttx-1* in AFD neurons did not

**Figure 3.5. *ver-1* promoter::*gfp* has temperature-dependent expression in AMsh and PHsh glia.** (A) Representative DIC and fluorescence merged images (top), and fluorescence only images (below) of *ver-1* promoter::*gfp* (*nsIs22*) expression in one of the two AMsh glial cells of wild-type adult animals at 15-25°C. (B) DIC and fluorescence merged (top), and fluorescence only (below) images of *ver-1* promoter::*gfp* expression in a *ttx-1(p767)* mutant adult at 25°C. (C) As in (A), except in the PHsh glia. Scale bars (A,B), 50 µm. Scale bar (C), 20 µm. In all images, anterior is up. Exposure (A,B), 800 ms. Exposure (C), 200 ms.

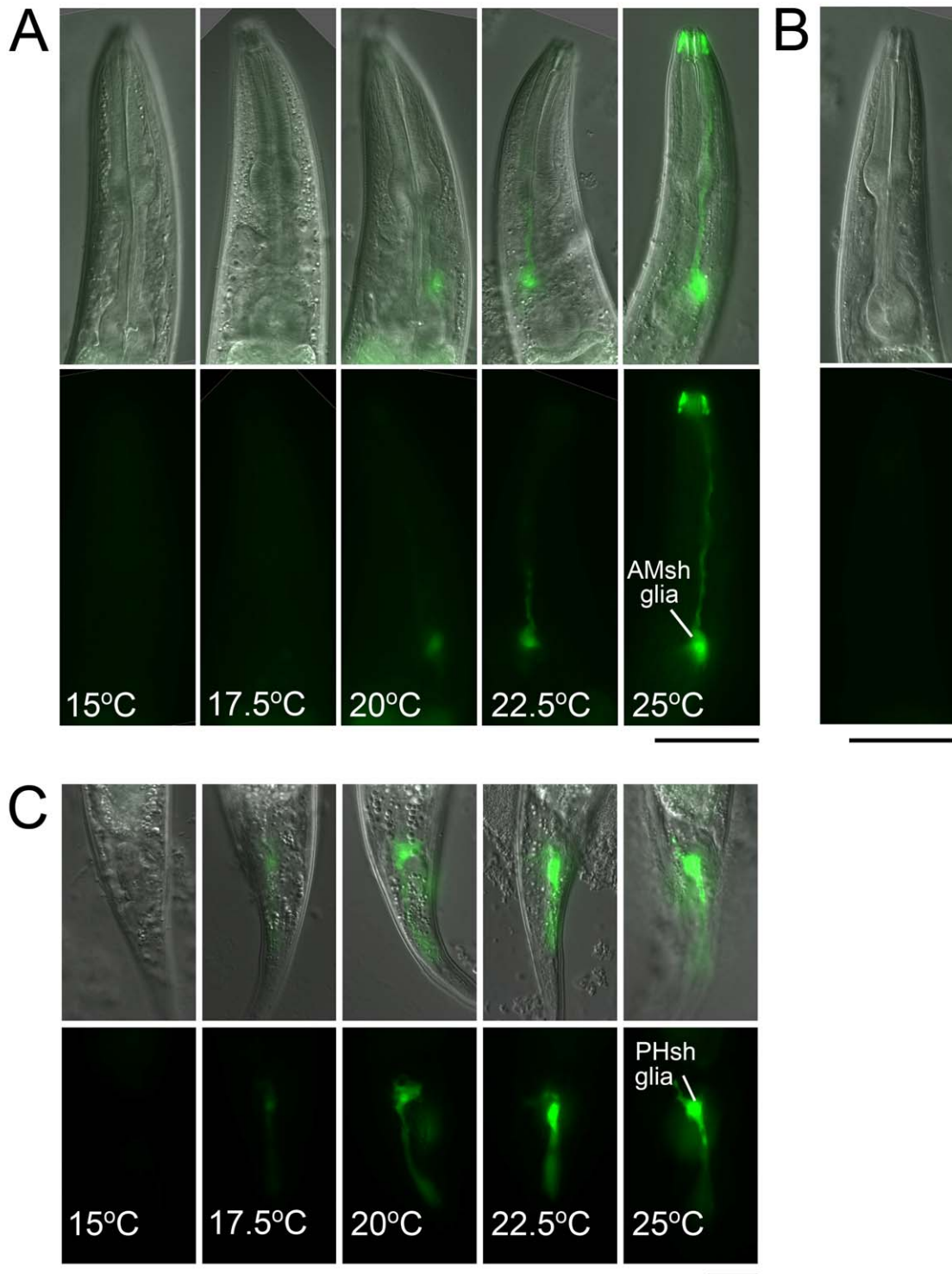
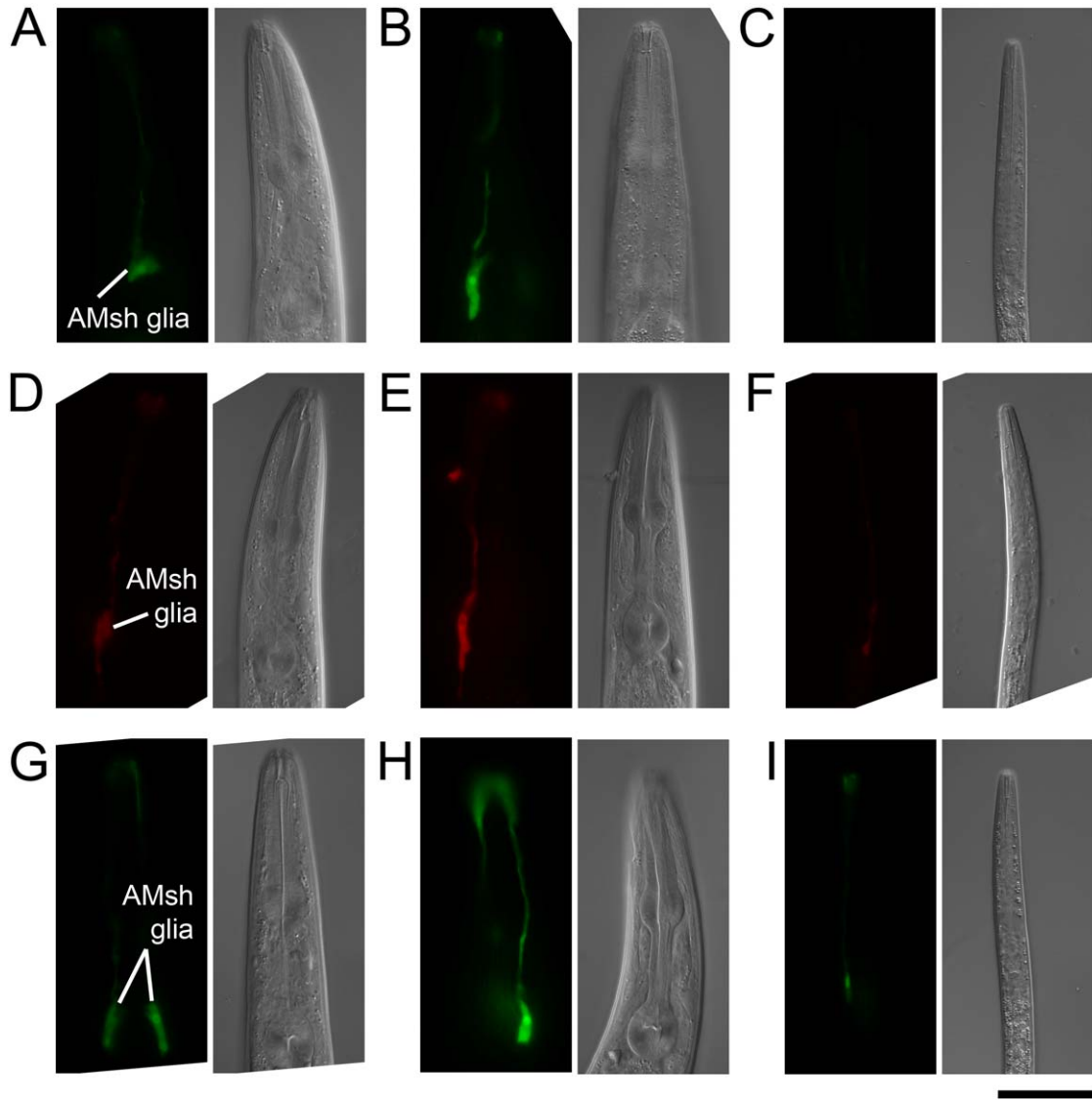


Figure 3.5. *ver-1* promoter::*gfp* has temperature-dependent expression in AMsh and PHsh glia.



**Figure 3.6. Effect of temperature and dauer on other AMsh glia reporters.** (A-C) Representative fluorescence (left) and DIC (right) images of animals carrying an *F16F9.3* promoter::*gfp* transgene: adults at 15°C (A), adults at 25°C (B), and dauer larvae at 15°C (C), exposure of 110 ms. (D-F) Same as (A-C) except using a *vap-1* promoter::*dsRed* transgene, exposure of 250 ms. (G-I) Same as (A-C) except using a *T02B11.3* promoter::*gfp* transgene, exposure of 150 ms. Scale bar, 50  $\mu$ m. Anterior is up.

**Table 3.2. Effects of mutations in genes controlling thermotaxis, neuronal morphology, dauer, and the heat-shock/UPR pathways on *ver-1* promoter::*gfp* expression.**

Genotype <sup>a</sup>	<i>ver-1</i> expression 15°C			<i>ver-1</i> expression 25°C		
	% PHsh on	% AMsh on	n	% PHsh on	% AMsh on	n
wild type	6	0	80	100	93	80
<b>AFD, AIY or AIZ neurons (thermotaxis circuit)</b>						
<i>ttx-1(p767)</i>	0	0	58	2	0	51
<i>ttx-1(oy26)</i>	0	0	47	0	0	44
<i>ceh-14(ch3)</i>	0	0	42	96	94	50
<i>dac-1(gk211)</i>	2	0	48	100	92	49
<i>tax-2(p691)</i>	0	0	41	100	88	50
<i>tax-4(p678)</i>	2	0	46	100	83	76
<i>pkc-1(nj1)</i>	5	0	40	100	88	40
<i>pkc-1(nj3)</i>	3	0	40	100	95	40
<i>pkc-1(nj4)</i>	5	0	40	100	95	40
<i>pkc-2(ok328)</i>	8	0	40	100	95	40
<i>ttx-3(ks5)</i>	5	0	39	100	80	51
<i>ttx-3(mg158)</i>	2	0	40	100	95	45
<i>lin-11(n389)</i>	5	0	41	100	98	54
<i>lin-11(n566)</i>	2	0	40	100	92	50
<i>unc-86(e1416)</i>	2	0	45	100	91	45
<i>unc-86(n846)</i>	2	0	43	100	94	54
<b>Otx/otd transcription factors</b>						
<i>ceh-37(ok642)</i>	10	0	40	100	85	40
<i>ceh-37(ok272)</i>	10	0	40	100	83	40
<i>ceh-36(ky646)</i>	20	3	40	100	98	40
<b>Neuronal cilia and dendritic morphology</b>						
<i>che-2(e1033)</i>	0	0	55	100	86	51
<i>che-13(e1805)</i>	0	0	49	100	94	52
<i>osm-6(p811)</i>	0	0	44	100	83	48
<i>dyf-7(ns89)</i>	0	0	44	88	98	50
<i>dyf-7(m537)</i>	0	0	43	88	98	50
<b>Dauer neuroendocrine pathways</b>						
<i>daf-7(e1372)</i>	5	0	42	100 <sup>b</sup>	100 <sup>b</sup>	53
<i>daf-12(m20)</i>	0	0	40	100	90	50
<i>daf-12(m25)</i>	0	0	54	100	90	50
<i>daf-2(m41)</i>	0	0	39	100 <sup>c</sup>	98 <sup>c</sup>	54
<i>daf-16(mu86)</i>	5	0	40	100	100	40
<b>Heat-shock and UPR pathways</b>						
wild type	8	0	40	93 <sup>d</sup>	43 <sup>d</sup>	80
<i>ire-1(zc14)</i>	8	0	40	98 <sup>d</sup>	45 <sup>d</sup>	40
<i>hsf-1(sy441)</i>	13	0	40	100 <sup>d</sup>	53 <sup>d</sup>	40

<sup>a</sup>All strains contained the *ver-1* promoter::*gfp* transgene (*nsIs22*).

Animals were scored as adults at the indicated temperature except for:

<sup>b</sup>Dauer-constitutive *daf-7* animals as dauer larvae at 25°C.

<sup>c</sup>Dauer-constitutive *daf-2* animals as dauer-recovered adults at 25°C.

<sup>d</sup>Due to increased lethality at high temperatures, *ire-1(zc14)*, *hsf-1(sy441)* and wild-type control animals were cultivated first at 15°C before shifting as L4 larvae to 25°C and scoring GFP intensity 24 h later.

(Table 3.3). In addition, the same promoter region and TTX-1/Otx2 binding site required for expression of *ver-1* in dauers were required for temperature-dependent expression of *ver-1* (Table 3.1).

*Otx2* is expressed in glia-like cells in vertebrate olfactory and vomeronasal organ epithelia (Mallamaci et al., 1996), as well as other neuronal tissues, suggesting that the functions of this family of proteins in sensory organs may be widely conserved. We found that expression of murine *Otx2*, but not *Otx1*, robustly rescued the defects in *ver-1* expression at 25°C of *ttx-1* mutants (Table 3.3). These results are consistent with the notion that both proteins may have similar functions in their natural settings.

Interestingly, restoring *ttx-1* to adult mutant animals using a heat-inducible promoter rescued *ver-1* expression at 25°C (Table 3.4). In addition, we found that the *ttx-1(oy26)* allele was temperature-sensitive (Figure 3.1E), and that shifting *ttx-1(oy26)* animals reared at 15°C (the permissive temperature) to 25°C (the restrictive temperature) at any larval stage abrogated *ver-1* promoter::*gfp* expression in glia (Figure 3.7), suggesting that *ttx-1* is continuously required for *ver-1* expression at 25°C, and consistent with our finding that TTX-1 can bind directly to the *ver-1* promoter. Strikingly, we also observed a continuous requirement for *ttx-1* in maintaining AFD sensory ending morphology: *ttx-1(oy26)* mutants shifted to the non-permissive temperature acquired an aberrant, single elongated cilium (Figure 3.8). Thus in both glia and neurons, *ttx-1* functions continuously to control specialized aspects of terminal differentiation.

To determine whether temperature control of *ver-1* expression was mediated by the sensory neurons associated with the AMsh glia, we genetically ablated both thermosensory AFD neurons and observed no defect in *ver-1* expression (Table 3.3).

**Table 3.3. TTX-1 acts in glia, and not AFD, to control temperature-dependent *ver-1* expression.**

Genotype <sup>a</sup>	<i>ver-1</i> expression 15°C			<i>ver-1</i> expression 25°C		
	% PHsh <sup>b</sup> on	% AMsh <sup>b</sup> on	n	% PHsh on	% AMsh on	n
wild type	6	0	80	100	93	80
<i>ttx-1(p767)</i>	0	0	70	0	0	70
<i>ttx-1(p767); AFD::ttx-1</i>	0	0	25	0	0	23
<i>ttx-1(p767); AMsh::ttx-1<sup>c</sup></i>	0	0	25	0	50	22
<i>ttx-1(p767); AM+PHsh::ttx-1</i>	30	7	30	87	97	30
<i>ttx-1(oy26)</i>	0	0	30	0	0	30
<i>ttx-1(oy26); AFD::ttx-1</i>	0	0	25	0	0	21
<i>ttx-1(oy26); AMsh::ttx-1<sup>c</sup></i>	0	4	25	0	48	23
<i>ttx-1(oy26); AM+PHsh::ttx-1</i>	57	7	30	83	93	25
<i>ttx-1(p767); glia::Otx1<sup>d</sup></i>	0	0	40	0	8	40
<i>ttx-1(p767); glia::Otx2</i>	0	0	40	45	100	40
AFD genetic ablation <sup>e</sup>	8	0	40	100	93	40
<i>tax-2(p691)</i>	0	0	41	100	88	50
<i>tax-4(p678)</i>	2	0	46	100	83	76
<i>osm-9(ky10)</i>	3	0	40	100	95	40
<i>tax-2(p691); osm-9(ky10)<sup>f</sup></i>	8	0	40	100	90	40

<sup>a</sup>All strains contained the *ver-1* promoter::*gfp* transgene (*nsIs22*).

<sup>b</sup>PHsh, PHsh glia. AMsh, AMsh glia.

<sup>c</sup>That *ttx-1* expression only in AMsh glia rescued *ver-1* expression only in AMsh glia supports a cell autonomous role for *ttx-1*.

<sup>d</sup>The glia promoter drives expression in both AMsh and PHsh glia.

<sup>e</sup>See Chapter 6.

<sup>f</sup>The *tax-2(p691); osm-9(ky10)* genotype also failed to affect *ver-1* expression in dauers. 100% of *tax-2(p691); osm-9(ky10)* starvation-induced dauers at 15°C expressed *ver-1* promoter::*gfp* in PHsh, and 82% in AMsh, compared to 100% of wild-type dauers in PHsh, and 88% in AMsh ( $n = 50$  both genotypes).

Two *ttx-1* cDNAs, *ttx-1a* and *ttx-1b*, were isolated, and gave equivalent rescue. TTX-1A and TTX-1B proteins are identical, except for an additional 53 amino acid residues in TTX-1A. Only *ttx-1a* rescue transgenes are shown. Transgenes were injected at 60 ng/μl of *ttx-1/Otx* plasmid, with 60 ng/μl of pRF4. Lines shown are *nsEx899*, *nsEx895*, *nsEx939*, *nsEx897*, *nsEx893*, *nsEx937*, *nsEx1661* and *nsEx1662*, and are representative of others.

**Table 3.4. Restoring *ttx-1* expression to *ttx-1(p767)* mutant adults using a heat-inducible promoter rescues *ver-1* expression.**

Genotype <sup>a</sup>	heat shock <sup>b</sup>	<i>ver-1</i> expression 15°C		<i>ver-1</i> expression 25°C	
		% PHsh on	% AMsh on	% PHsh on	% AMsh on
wild type	–	8	0	90	30
	+	10	0	95	40
<i>ttx-1(p767)</i>	–	0	0	0	0
	+	0	0	0	0
<i>ttx-1(p767)</i> ; heat shock:: <i>ttx-1a</i> <sup>c</sup>	–	0	0	0	0
	+	13	0	55	10
<i>ttx-1(p767)</i> ; heat shock:: <i>ttx-1b</i> <sup>c</sup>	–	0	0	0	0
	+	8	0	63	20

<sup>a</sup>All strains contained the *ver-1* promoter::*gfp* transgene (*nsIs22*).

<sup>b</sup>Animals carrying heat-shock promoter::*ttx-1* arrays were cultivated initially at 15°C. Adult animals were heat shocked at 34°C for 50 min, and then transferred either to 15°C or 25°C. *ver-1* promoter::*gfp* expression was scored 24 h later.

<sup>c</sup>heat-shock promoter::*ttx-1a* and heat-shock promoter::*ttx-1b* lines used were *nsEx1636* and *nsEx1680*, respectively. *ttx-1a* and *ttx-1b* are described in Table 3.3.  
*n* = 40 for all values.

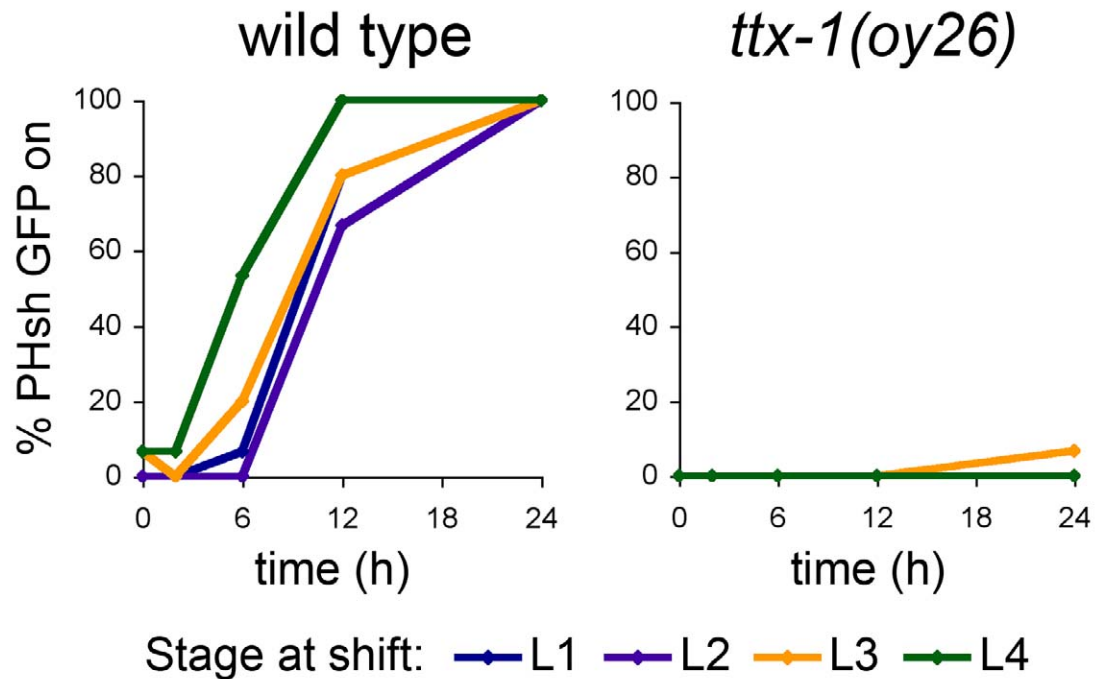


**Figure 3.7. TTX-1 is required continuously for temperature-dependent expression of *ver-1* in glia.** Percentage of wild-type and temperature-sensitive *ttx-1(oy26)* mutant larvae (L1-L4 stages) expressing *ver-1* promoter::*gfp* (*nsIs22*) in PHsh glia over time (h) following a temperature shift from 15°C to 25°C ( $n = 15$  for each data point). *ver-1* promoter::*gfp* expression in AMsh glia showed a similar trend; however, PHsh glial GFP fluorescence was greater (data not shown).

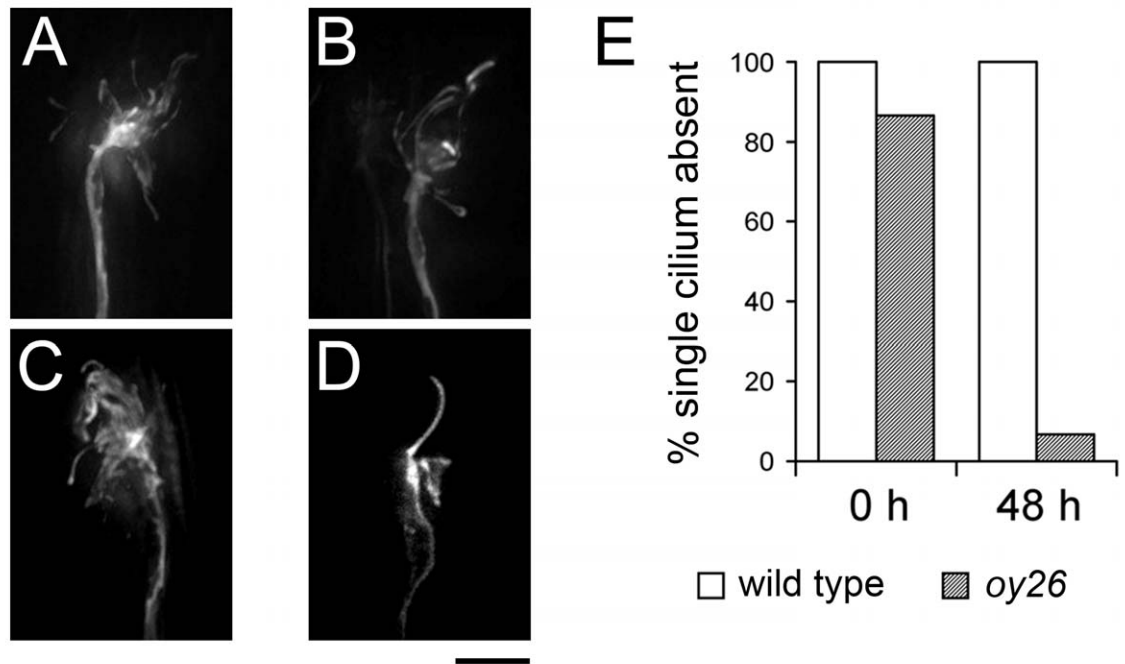


**Figure 3.8. TTX-1 is required continuously for AFD morphology.** (A-D) AFD microvillar morphology at the AFD dendrite endings of wild-type (A) and *ttx-1(oy26)* mutant (B) adult animals expressing a *gcy-8* promoter::*gfp* transgene (*oyIs17*) in the AFD neurons at 15°C; and wild-type (C) and *ttx-1(oy26)* (D) adults at 25°C. The microvillar morphology is more perturbed in *oy26* animals raised at 25°C (D) than at 15°C (B). Scale bar, 5  $\mu$ m. Anterior is up. The microvilli in (B) are more globular than (A). (E) The percentage of wild-type and *ttx-1(oy26)* L4 animals in which AFD dendrite endings do not exhibit an aberrant single cilium morphology at 0 and 48 h following a temperature shift from 15°C to 25°C. In some animals possessing a single aberrant cilium, some microvilli were still observable at the base of the cilium. Results are comparable with second- and third-stage larvae (data not shown).  $n = 15$  for both genotypes. A *gcy-8* promoter::*gfp* transgene (*oyIs17*) was used to visualize the AFD neurons.

Likewise, perturbation of all amphid and phasmid sensory neuron signaling activity by mutations in the *tax-2/tax-4* and *osm-9* sensory transduction ion channels (Coburn and Bargmann, 1996; Colbert et al., 1997; Komatsu et al., 1996) had little effect on the induction of *ver-1* expression at high temperature (Table 3.3). These mutations also had no effect on *ver-1* expression in dauer animals (Table 3.3; see footnote f). Finally, (1) mutations disrupting sensory neuron cilia morphology and/or circuitry, or (2) mutations in dauer-related TGF- $\beta$  (Ren et al., 1996) or insulin (Kimura et al., 1997) neuroendocrine signaling components, also had minor or no effects on *ver-1* expression at 25°C (Table 3.2). These observations suggest that AMsh and PHsh glia respond to temperature independently of sensory neuron input.

To assess whether increased *ver-1* expression was sufficient to drive AMsh glia remodeling, we examined non-dauer adults raised at 25°C for fusion of AMsh glia, a condition in which *ver-1* transcription is high. We found that fusion does not occur in these animals (see Chapter 2, Figure 2.5A), even though *ver-1* is highly expressed, suggesting that dauer entry provides additional necessary conditions for AMsh glia remodeling.

High ambient temperature is one of the environmental stressors that regulate dauer entry (Golden and Riddle, 1984a), raising the possibility that increased expression of *ver-1* at high temperatures may facilitate AMsh glia remodeling. However, robust expression of *ver-1* is still detected in dauers raised at 15°C, confounding a functional analysis of the effects of temperature on the remodeling of these glia. Nonetheless, we still observed a temperature dependence of *ver-1* expression in dauers raised at different temperatures (Table 3.1). Thus, although temperature and dauer signals both induce *ver-*

*I* expression, these signals must also converge independently on the *ver-1* promoter to induce expression in dauer animals. These results raise the speculative possibility that temperature, in addition to dauer cues, may play a modulatory role in remodeling of AMsh glia.

## **Discussion**

### **The VEGFR-related gene *ver-1* is required for glia remodeling**

Our studies demonstrate that neuronal remodeling must be tightly coordinated with glia remodeling in dauer animals, predicting the existence of proteins tasked with executing this coordination. That *ver-1* encodes a receptor tyrosine kinase is intriguing, suggesting the speculative possibility that it normally responds to as yet unidentified neuronal cues to promote coordinated glia-neuron remodeling. Expression of *ver-1* in non-dauer animals may serve to prime glia for remodeling, in preparation of pending dauer entry. Alternatively, *ver-1* expression may represent a neuroprotective or stress response of the glia. Supporting this possibility, the VER-1-related VEGF receptor Flk-1/VEGFR-2 is expressed in neurons and glia of the mammalian hippocampus following nerve injury stress (Wang et al., 2005), and VEGF signaling has neurotrophic and neuroprotective roles in some contexts (Sondell et al., 1999). In addition, the predicted *ver-1* kinase domain is similar to kinase domains encoded by the *C. elegans* genes *old-1* and *old-2* (~40% identity), and *old-1* has been implicated in longevity and resistance to environmental insults (Murakami and Johnson, 2001). Consistent with its organism-wide phenotype, a transcriptional reporter for *old-1* was expressed broadly in hypodermal

tissue and is induced by environmental stressors, including high temperature (Murakami and Johnson, 2001). The function of *old-2* is unknown; however, based on its homology to *old-1*, it may also have a role in stress responses. Surprisingly, we find that a transcriptional reporter for *old-2* is expressed in the AMsh and PHsh glia (Figure 3.9), further strengthening the idea that these cells respond to environmental stress. However, *old-2* expression was not affected by a mutation in *ttx-1* (data not shown), and we observed no defect in glial fusion as measured by cytoplasmic mixing in *daf-7(e1372)* dauer animals carrying a deletion in the *old-2* gene (46% of *old-2(ok1253); daf-7(e1372)* dauers had fused glia;  $n = 101$ ,  $P = 0.32$ ,  $\chi^2$  test), suggesting that the function of *ver-1* and *old-2* in glia may be different.

### ***ttx-1* regulates cell shape in thermoresponsive cells**

The temperature responses of AFD and AMsh glia may be mediated by either similar or different sensors. A sensor has not yet been identified in either cell; however, three guanylyl cyclases are important for temperature sensation in AFD (Inada et al., 2006). Reporter constructs for these guanylyl cyclases are not expressed in AMsh glia (Inada et al., 2006), suggesting that glia might employ a different upstream sensor. However, it is also possible that these cyclases function permissively in AFD. In collaboration with Erik Procko and Rachelle Gaudet (Department of Molecular and Cellular Biology, Harvard University, Cambridge MA), we found that the enzymatic activity of two of these guanyl cyclases in *in vitro* assays was constant at different temperatures, indicating that they are unlikely to be the thermosensors themselves (Appendix 2), suggesting instead a possible involvement of an upstream thermosensing

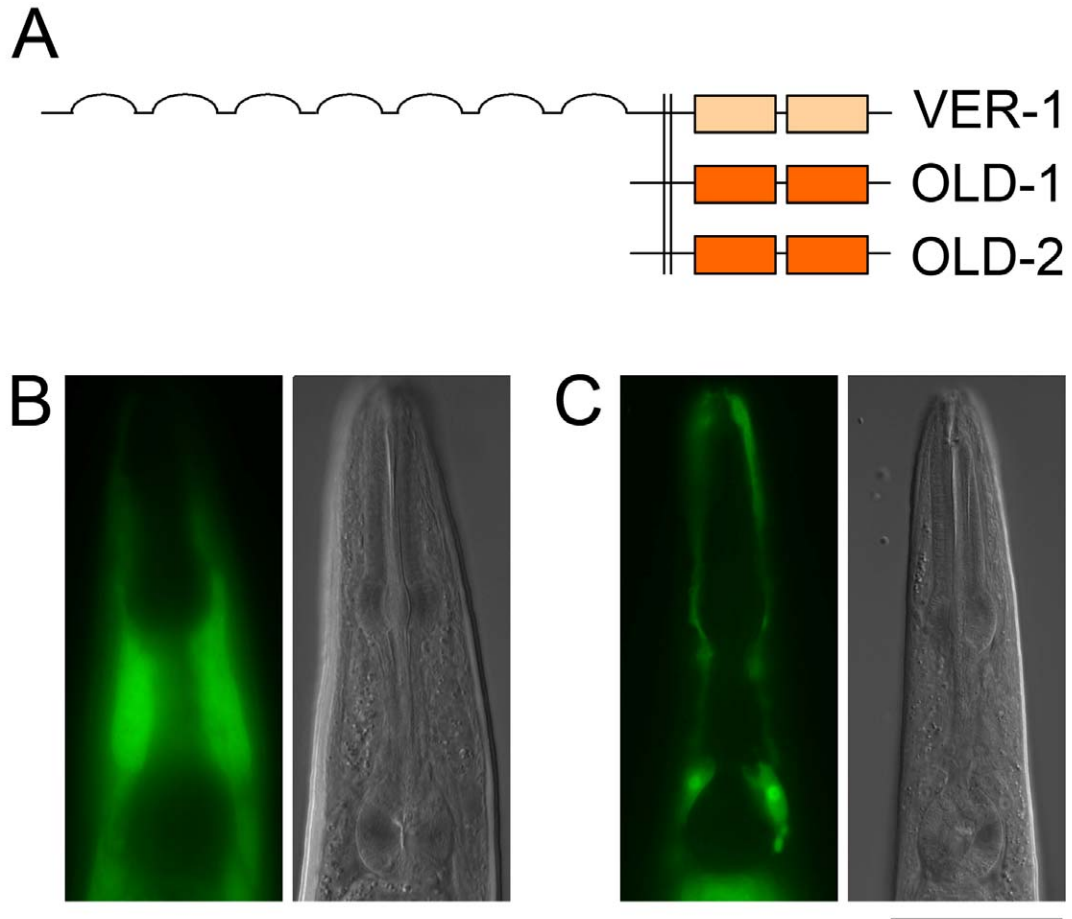


**Figure 3.9. *old-2*, a *ver-1*-related tyrosine kinase gene, is also expressed in AMsh glia.**

(A) A schematic representation of the VER-1, OLD-1 and OLD-2 proteins. Cell membrane is indicated by two vertical lines. VER-1 has a long extracellular region composed of immunoglobulin repeats (semi-circles) and an intracellular split-kinase domain (orange boxes) that most closely resembles the kinase domains of the *C. elegans*' proteins OLD-1 and OLD-2 (~40% identity). OLD-1 and OLD-2 share greater similarity to each other (indicated by level of shading). Not to scale. (B) Representative fluorescence image (left) and DIC image (right) of *old-1* promoter::*gfp* (*nsEx2299*) expression in the hypodermis. See also Murakami and Johnson, 2001. (C) Same as (B), except showing *old-2* promoter::*gfp* (*nsEx2317*) expression in the AMsh glia. All *old-2* promoter::*gfp* lines gave PHsh glia expression (12/12), while AMsh glia expression was rare (1/12; pictured). Scale bar (B,C), 50  $\mu$ m; anterior is up.

GPCR in AFD. In *Arabidopsis*, changes in ambient temperature cause fluctuations in the constituents of the nucleosomes on which the DNA is packaged (Kumar and Wigge, 2010). Thus, chromatin may act as a direct thermal sensor. Such a sensor is unlikely to be employed in AFD neurons, as it would not be compatible with the fast calcium transients observed in AFD neurons following temperature shifts (Kimura et al., 2004). A DNA-bound sensor would, however, be consistent with the kinetics of temperature-induced changes in *ver-1* expression we observe in glia. If such a sensor exists, TTX-1 would be unlikely to be its temperature-sensitive component, as constitutive expression of TTX-1 or its mammalian homolog, Otx2, in glia does not perturb temperature sensitivity of *ver-1* expression (Tables 3.3 and 3.4). However, some caution must be used when interpreting rescue data, as all glial promoters so far examined have some mild temperature response (Figure 3.6).

It is of note that *ttx-1* is required for determining the morphology of process endings of both glia (fusion/expansion) and neurons (AFD microvilli). Interestingly, ectopic expression of TTX-1 in non-AFD neurons induces protrusions in these cells (Satterlee et al., 2001). Thus, TTX-1 may have specific roles in regulating cell shape. Furthermore, the role of the protein as a terminal cell fate gene may be largely limited to thermoresponsive cells, as TTX-1 is required in two seemingly unrelated temperature-dependent processes in *C. elegans*: AFD neuron function and glial *ver-1* expression. Intriguingly, in the adult mouse brain, some hypothalamic neurons of the preoptic area, which senses body temperature (Boulant, 2000), express the TTX-1 related protein Otx2 (Kelley et al., 2000). Moreover, in the developing olfactory sensory epithelium Otx2 is expressed and largely restricted to the ensheathing glia (Mallamaci et al., 1996). Our

finding that murine *Otx2*, but not *Otx1*, robustly restored *ver-1* expression to *ttx-1* mutants in *C. elegans* may, therefore, indicate that *Otx2* has conserved roles in thermosensation and/or the function of glia in sensory organs, in addition to its other well-studied roles in development.

### ***ver-1* transcription can be used as a tool for finding genes required for glia remodeling**

Our studies have shown the involvement of a number of genes functioning in the glia to regulate dauer-induced remodeling, including *ttx-1*, *ver-1* and *aff-1*. However, using direct mutagenesis screens to find additional genes that regulate this process is challenging: neither EM nor the cytoplasmic mixing assay we have developed are high-throughput enough for screening large numbers of mutagenized animals. *ver-1* transcriptional reporters may represent a solution to this challenge. A *ver-1* promoter::*gfp* reporter is up-regulated by dauer entry, and mutations in *ver-1* and its transcriptional regulator *ttx-1* both affect glia remodeling. Therefore, mutant screens to find animals in which *ver-1* expression is mis-regulated may potentially uncover additional genes required for glia morphology. In the next chapter, I will describe ongoing work towards finding and characterizing these genes.

# Chapter 4

Transcriptional regulators of the receptor tyrosine kinase  
*ver-1* are required for AMsh glia remodeling

## Summary

Both neurons and glia display remarkable morphological plasticity. We have shown that changes in glial shape in the amphid sensory structures of *C. elegans* can in turn affect neuronal morphological plasticity when animals enter dauer development in response to environmental stressors. Glia remodeling is dependent on the receptor tyrosine kinase gene *ver-1*, its direct transcriptional activator *ttx-1*, and the *aff-1* cell fusogen, all acting within the glia. To identify other factors required for glia remodeling in dauer animals, we screened for mutants that failed to express the *ver-1* gene. We identified an additional transcriptional regulator, the C2H2 zinc finger factor *ztf-16*, as being required for both *ver-1* up-regulation in dauer animals and glia remodeling. Cell-specific rescue studies show that *ztf-16* is expressed and functions in the glia. Together, our results identify a transcriptional network in the glia that is required for morphological plasticity.

## Results

### **Mutants with reduced *ver-1* reporter expression generally fall into 3 complementation groups**

Glial morphology in vertebrate systems is dynamic (Lippman et al., 2008; Theodosis and Poulain, 1993); however, very little is known about what factors promote changes in glial shape. In response to environmental stressors, the nematode *C. elegans* becomes a developmentally-arrested dauer larva. Numerous morphological changes occur upon dauer entry, including the remodeling of the bilateral amphid sensory organs in the head of the animal. Our results have shown that changes in the AMsh glia in dauer animals are important for extension and overlap of the ensheathed AWC sensory neuron endings (see Chapters 2 and 3). Some of the signals regulating changes in AMsh glial shape may be mediated by sensory neurons or secondary signals as a result of dauer entry; for example, a mutation in the TGF- $\beta$ /DAF-7 neuroendocrine hormone causes both constitutive dauer entry (Ren et al., 1996) and glia remodeling (see Chapter 2). Other signals may be sensed by the glia directly. For example, mutations in the *ver-1* receptor tyrosine kinase gene cause a significant decrease in AMsh glia remodeling, and *ver-1* expression is dependent on both dauer entry and ambient temperature. Up-regulation of *ver-1* transcription in response to high temperature is likely independent of input from sensory neurons (see Chapter 3). In addition, both *ver-1* transcription and glia remodeling require the Otx-type transcription factor TTX-1, which directly regulates the *ver-1* gene.

Based on these observations, we sought to find other genes required for changes in glia morphology in dauer animals. However, screening directly for mutants with

defects in glia fusion would be a difficult undertaking: the assays available to us, EM and cytoplasmic mixing, are both problematic, limited by low *n* values and/or time-consuming protocols. Instead, we reasoned that mutations which affect expression of a *ver-1* promoter::*gfp* reporter in the AMsh glia might also affect glia fusion in dauers. This rationale is based on the observation that a *ver-1* promoter::*gfp* reporter is up-regulated in the AMsh and PHsh glia upon dauer entry, and that mutations in *ver-1* or its direct transcriptional activator *ttx-1* also affect dauer remodeling. Thus, we sought to find other genes that are required for *ver-1* expression.

Wild-type animals carrying a *ver-1* promoter::*gfp* transgene (*nsIs22*) were mutagenized with ethyl methanesulfonate (EMS) (see Chapter 6). To facilitate screening and animal recovery, we screened adult F2 animals grown at high temperature (25°C) rather than dauer animals directly. *ver-1* promoter::*gfp* expression is high at 25°C, as well as in dauers, and may be regulated by similar mechanisms in both conditions (see Chapter 3). More than 35,000 F2 animals were screened, and a total of 21 independent mutant alleles were isolated with reduced *gfp* expression in the AMsh glia (Table 4.1). Animals with reduced *gfp* expression in the PHsh glia only, and not in the AMsh glia, are not shown.

The mutant alleles generally fell into one of three complementation groups (Table 4.1). The first group failed to complement a *ttx-1*(*p767*) reference allele, which we have previously shown to affect *ver-1* expression (see Chapter 3). These 2 alleles, *ns235* and *ns252*, were found to have an identical nucleotide substitution in the *ttx-1* gene coding for a single amino acid change in a conserved residue of the TTX-1 DNA-binding homeodomain (Figure 4.1A,B). In addition, we isolated 4 mutant alleles with a dominant

**Table 4.1. Alleles that reduce *ver-1* promoter::*gfp* expression generally fall into one of three complementation groups.**

Allele <sup>a</sup>	<i>ver-1</i> expression 25°C <sup>a</sup>	
	% AMsh on	n
wild type	97	30
<b>Complementation group 1 (see also dominant alleles; below):</b>		
<i>ttx-1(p767)</i> (reference allele)	0	40
<i>ns235</i>	0	64
<i>ns252</i>	0	62
<b>Complementation group 2:</b>		
<i>tam-1(ns258)</i> (reference allele)	5	22
<i>ns167</i>	83	24
<i>ns170</i>	25	24
<i>ns174</i>	9	22
<i>ns234</i>	16	25
<i>ns237</i>	81	21
<i>ns238</i>	13	15
<i>ns241</i>	41	22
<i>ns249</i>	0	30
<i>ns268</i>	70	30
<b>Complementation group 3:</b>		
<i>ztf-16(ns171)</i> (reference allele)	4	25
<i>ns169</i>	29	21
<i>ns178</i>	5	22
<b>Alleles not falling into complementation groups 1-3:</b>		
<i>ns231</i>	32	22
<i>ns257</i>	90 <sup>b</sup>	20
<b>Dominant alleles<sup>c</sup>:</b>		
<i>ns255</i> <sup>d</sup>	0	42
<i>ns259</i> <sup>d</sup>	n.d.	n.d.
<i>ns260</i> <sup>d</sup>	n.d.	n.d.
<i>ns267</i>	0	40

<sup>a</sup>All strains contained the *ver-1* promoter::*gfp* transgene (*nsIs22*).

<sup>b</sup>Allele *ns257* had only a weak, qualitative effect on *ver-1* promoter::*gfp* expression.

<sup>c</sup>Dominant alleles were not scored for complementation. However, all dominant alleles were found to have a mutation in the *ttx-1* gene.

<sup>d</sup>Alleles *ns259* and *ns260* were homozygous sterile and lethal, respectively. Animals homozygous for allele *ns255* were slow growing and unhealthy, even after out-crossing.

Only alleles known to be isolated from independent mutagenized P0s are shown. The reference alleles were used in crosses to place other alleles into complementation groups.

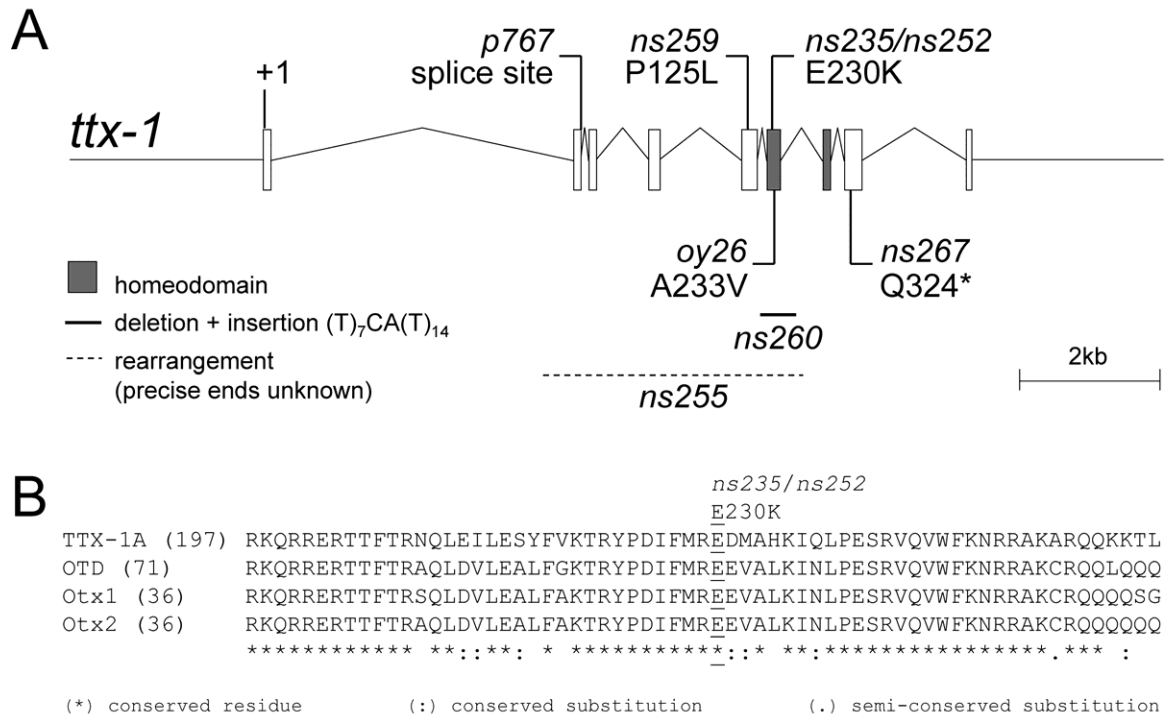


**Figure 4.1. Mutations in the *Otx*-type transcription factor *ttx-1* reduce *ver-1* promoter::*gfp* expression. (A)** A schematic of the *ttx-1* gene. Exons are represented by boxes; the start site (+1) is indicated; DNA-binding homeodomain, shaded. Mutant *ttx-1* alleles isolated in our screen are shown, and the corresponding amino acid change is indicated. (\*) indicates a premature stop mutation. The region of the *ns260* deletion and small insertion is shown. *ns255* likely represents a rearrangement of the gene, as PCR products using primers covering exons 2-6 are either absent, weak, or consist of multiple sized fragments (data not shown). In addition, *ns255* has the same base substitution as *ns235* and *ns252*, causing amino acid change E230K. Previously isolated *ttx-1* alleles *p767* and *oy26* are also shown (Hedgecock and Russell, 1975; Satterlee et al., 2001). **(B)** Alignment of the DNA-binding homeodomains of *Otx*-type factors TTX-1 (A isoform), *Drosophila* OTD, and murine Otx1 and Otx2. The amino acid position where each protein is being aligned is shown in brackets. *ns235* and *ns252* (and *ns255*) code for a glutamic acid to lysine change in a conserved residue.

effect on *ver-1* promoter::*gfp* (Table 4.1). In all 4 dominant mutant strains, we found sequence changes in the *ttx-1* coding region, suggesting that *ttx-1* dosage is important for *ver-1* expression (Figure 4.1A). Interestingly, one of these alleles, *ns259*, was homozygous sterile, while the allele with the strongest predicted effect on *ttx-1*, *ns260*, which codes for a deletion of the DNA-binding homeodomain, was homozygous lethal (Appendix 3). We were unable to rescue the *ns260* lethality phenotype by restoring *ttx-1* function to either the glia or AFD thermosensory neurons (Appendix 3), suggesting that *ttx-1* has functions in other cell types during early development that have yet to be elucidated.

The largest complementation group of mutant alleles causing a qualitative reduction in *ver-1* promoter::*gfp* expression was represented by 10 independently-isolated alleles (Table 4.1). Single nucleotide polymorphism (SNP) mapping techniques against the Hawaiian strain background (Wicks et al., 2001) were used to map one of these alleles, *ns268*. *ns268* was mapped to an interval of ~160 kb on chromosome V (Figure 4.2A). A cosmid within this interval, F26G5, was able to rescue high *ver-1* expression when injected into *ns268* mutants (Figure 4.2B). Sequencing of coding regions within this interval uncovered two base mutations in the *tam-1* gene, causing amino acid changes (Figure 4.2C). The other 9 alleles that failed to complement *ns258* were also found to have mutations in *tam-1* (Figure 4.2C), confirming the identity of the relevant gene.

*tam-1* codes for a predicted protein that includes a C3HC4 zinc finger (RING finger) and a B-box motif, which are found in proteins of diverse functions (Hsieh et al., 1999). Immunohistochemistry against TAM-1 in *C. elegans* suggested that the protein is

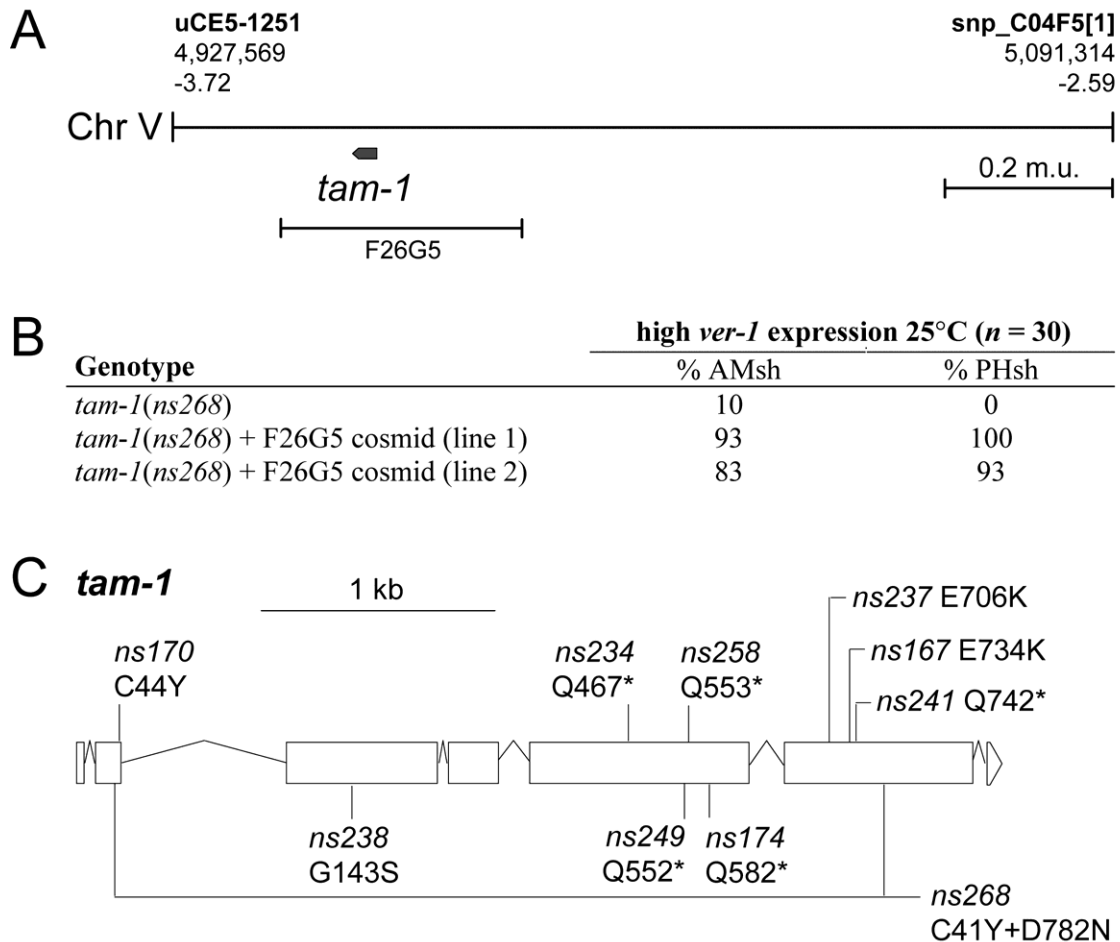


**Figure 4.2. Mutations in the RING finger and B-box domain factor *tam-1* reduce *ver-1* promoter::*gfp* expression.** (A) A schematic of the interval on chromosome V to which mutant allele *ns258* was mapped. Flanking single nucleotide polymorphism markers (uCE5-1251 and snp\_C04F5[1]) are shown, as are the physical base and map positions on the chromosome. The region spanned by the F26G5 cosmid and *tam-1* gene are also shown. (B) Rescue of qualitatively high *ver-1* promoter::*gfp* (*nsIs22*) expression of adult animals cultivated at 25°C in the amphid sheath (AMsh) and phasmid sheath (PHsh) glia of *ns258* mutants by 2 independent extrachromosomal arrays containing the F26G5 cosmid (*nsEx2169* and *nsEx2170*). (C) A schematic of the *tam-1* gene (WormBase release WS224). Exons are represented by boxes. Mutant *tam-1* alleles isolated in our screen are shown, and the corresponding amino acid change is indicated. (\*) indicates a premature stop mutation. *ns268* coded for two amino acid changes.

nuclear-localized and expressed in all somatic cells of the embryo (Hsieh et al., 1999). Furthermore, mutations in *tam-1* reduced the expression levels of many fluorescent reporter transgenes expressed in diverse cell-types. This reduction in reporter expression was context-dependent. Generally, transgenes injected into the animal are incorporated into simple arrays that consist of many tandem copies of the transgene (Mello et al., 1991). Mutations in *tam-1* affected the expression of transcriptional reporters from these simple arrays; however, complex arrays with a reduced repetitive structure generated by co-injection with *C. elegans* genomic DNA were unaffected (Hsieh et al., 1999). In addition, analysis of endogenous gene expression of the *myo-3* gene in *tam-1* mutants did not replicate the reduced expression of a simple array containing repetitive *myo-3* promoter::*gfp* elements (Hsieh et al., 1999). Thus, *tam-1* broadly regulates gene expression of transgenes from simple arrays; therefore, its effect on *ver-1* promoter::*gfp* expression may not reflect a true role in endogenous *ver-1* expression (although, it is intriguing that all previously isolated *tam-1* alleles were temperature sensitive; Hsieh et al., 1999). Thus, any involvement of the *tam-1* gene in glial function and morphology was not pursued further.

The third complementation group was defined by 3 independently isolated alleles, *ns169*, *ns171* and *ns178*, all with reduced *ver-1* promoter::*gfp* expression (Table 4.1). It was these mutants that we chose to characterize more fully.

### **The C2H2 zinc finger factor *ztf-16* is required for *ver-1* expression**

Mutations in *ns169*, *ns171* and *ns178* all caused a reduction in expression of a *ver-1* promoter::*gfp* transgene in the AMsh and PHsh glia of adult animals raised at high

temperature (Figure 4.3A,B; and data not shown). In addition, we found that these mutants failed to up-regulate *ver-1* expression in dauer animals induced by starvation at 15°C (Figure 4.3C; 100% of wild-type dauers expressed *ver-1* promoter::*gfp* [*nsIs22*] in the AMsh glia, whereas 0% of *ns169*, *ns171* and *ns178* dauer mutants at 15°C expressed the reporter, *n* = 50 all strains). By contrast, mutations in *ns169* and *ns171* had little or no effect on an AMsh glia reporter that is expressed constitutively and independent of dauer entry (Figure 4.3D; and data not shown); therefore, the glia are present in *ns169*, *ns171* and *ns178* mutants, and these mutants instead disrupt the expression of specific genes only.

Previously, we found that *ver-1* expression was dependent on the *Otx*-type transcription factor *ttx-1* (see Chapter 3 and above). Interestingly, mutations in *ttx-1* were first isolated in screens for aberrant morphology of the amphid AFD thermosensory neurons and AFD function in response to environmental temperature (Hedgecock and Russell, 1975; Satterlee et al., 2001). However, unlike *ttx-1*, we find no defects of *ns171* mutants in AFD function (thermotaxis behavior) or morphology (presence of microvillar protrusions at the anterior tip of the AFD sensory dendrite; *n* = 30) (Figure 4.4). This suggests that while *ns171* mutants and *ttx-1* mutants share some phenotypic similarities they are not completely identical.

SNP mapping (Wicks et al., 2001) was used to place the *ns171* mutation to an interval of ~370 kb on chromosome X, between polymorphisms on cosmid F55D10 (base 14867) and C42D8 (base 5707) (Figure 4.5A). Cosmids spanning the 5' region of this interval were injected into *ns171* mutants and scored for rescue of *ver-1* promoter::*gfp* expression in adults raised at 25°C. One of these cosmids, R08E3, gave rescue (Figure

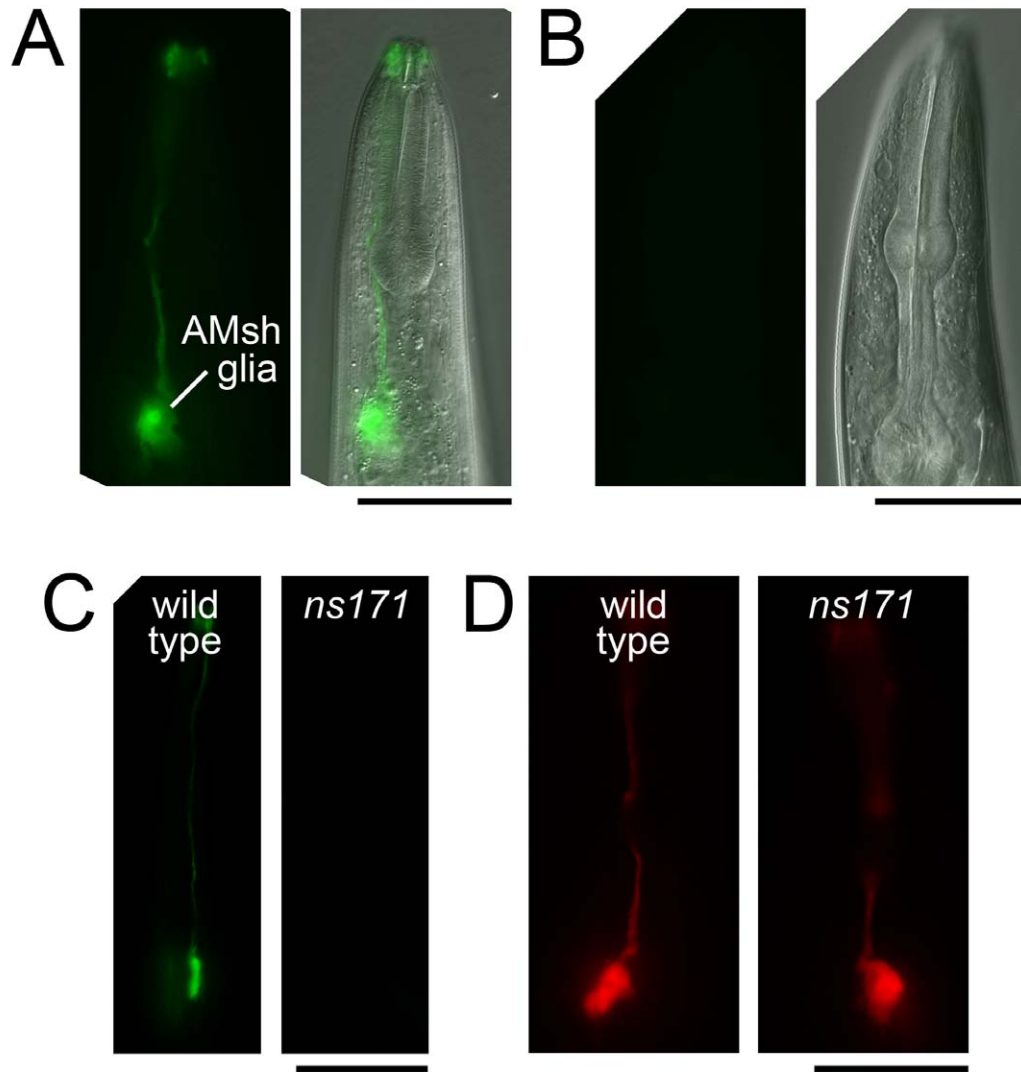


**Figure 4.3. Temperature- and dauer-induced expression of *ver-1* is reduced in *ns171* mutants.** (A,B) Representative fluorescence images (left), and DIC and fluorescence merged images (right) of *ver-1* promoter::*gfp* (*nsIs22*) expression in one of the two AMsh glial cells of a wild-type adult cultivated at 25°C (A) and in a *ns171* mutant animal (B). Exposure time for *gfp* was 800 ms. (C) Representative fluorescence images of *ver-1* promoter::*gfp* (*nsIs22*) expression in one of the two AMsh glial cells of a wild-type dauer induced by starvation at 15°C (left) and a *ns171* mutant dauer animal (right). Exposure time, 200 ms. (D) Representative fluorescence images of *vap-1* promoter::*dsRed* (*nsIs53*) expression in the AMsh glia of a wild-type adult (left) and a *ns171* mutant adult animal (right). Exposure time, 600 ms. In all images, scale bars, 50  $\mu$ m; anterior is up.

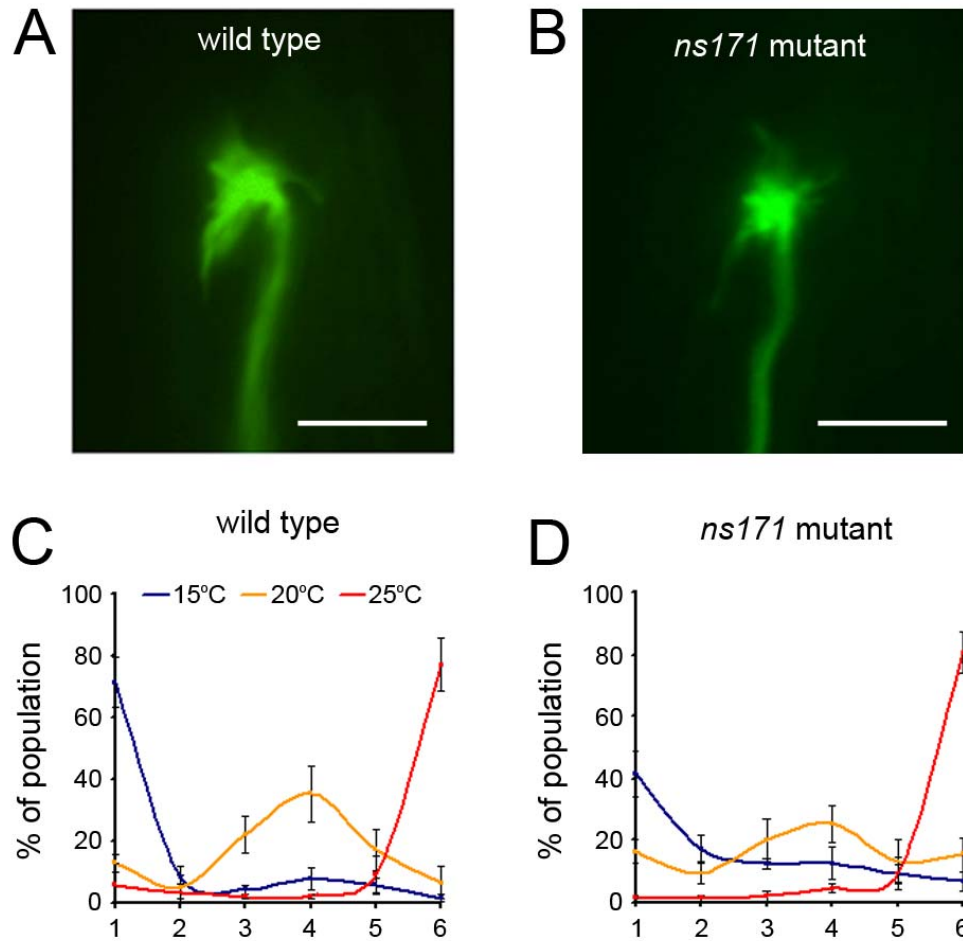


**Figure 4.4. *ns171* mutants have wild-type AFD sensory ending morphology and thermotaxis behavior.** (A,B) Representative fluorescence images of the AFD dendrite endings of adult wild-type (A) and *ns171* mutant (B) strains at 25°C. Scale bars, 5 μm. Anterior is up. (A) is reproduced from Chapter 2. A *gcy-8* promoter::*gfp* transgene (*oyIs17*) was used to visualize the AFD neurons. (C,D) Thermotaxis of wild-type (C) and *ns171* mutant (D) strains. Animals were cultivated at 15°C (blue), 20°C (yellow) or 25°C (red) prior to performing each assay (see Chapter 6). The linear temperature gradient is represented by bins 1-6 on the horizontal axis, from cold (~18°C) to hot (~26°C). All values are mean +/- s.d. All animals also carry the *ver-1* promoter::*gfp* transgene (*nsIs22*).

**Figure 4.5. The C2H2 zinc finger gene *ztf-16* is required for *ver-1* expression.** (A) A schematic of the interval on chromosome X to which mutant allele *ns171* was mapped. The flanking single nucleotide polymorphisms (SNPs) are on cosmid F55D10 (base 14867) and C42D8 (base 5707). The regions spanned by the cosmids used for the rescue experiments shown in (B) are indicated, as is the position of the *ztf-16* gene. (B) The number of lines carrying extrachromosomal arrays of the indicated cosmid that rescued the reduced *ver-1* promoter::*gfp* (*nsIs22*) expression phenotype of *ns171* mutant adult animals cultivated at 25°C. (C) A schematic of the *ztf-16* gene; exons are boxed; C2H2 zinc finger domains are shaded. We isolated 2 splice forms of *ztf-16* based on EST data available from WormBase (release WS224), and have named these gene models as *ztf-16a* and *ztf-16b* consistent with the EST nomenclature. The mutant *ztf-16* alleles isolated in our screen are shown, and the corresponding amino acid change is indicated. (\*) indicates a premature stop mutation.

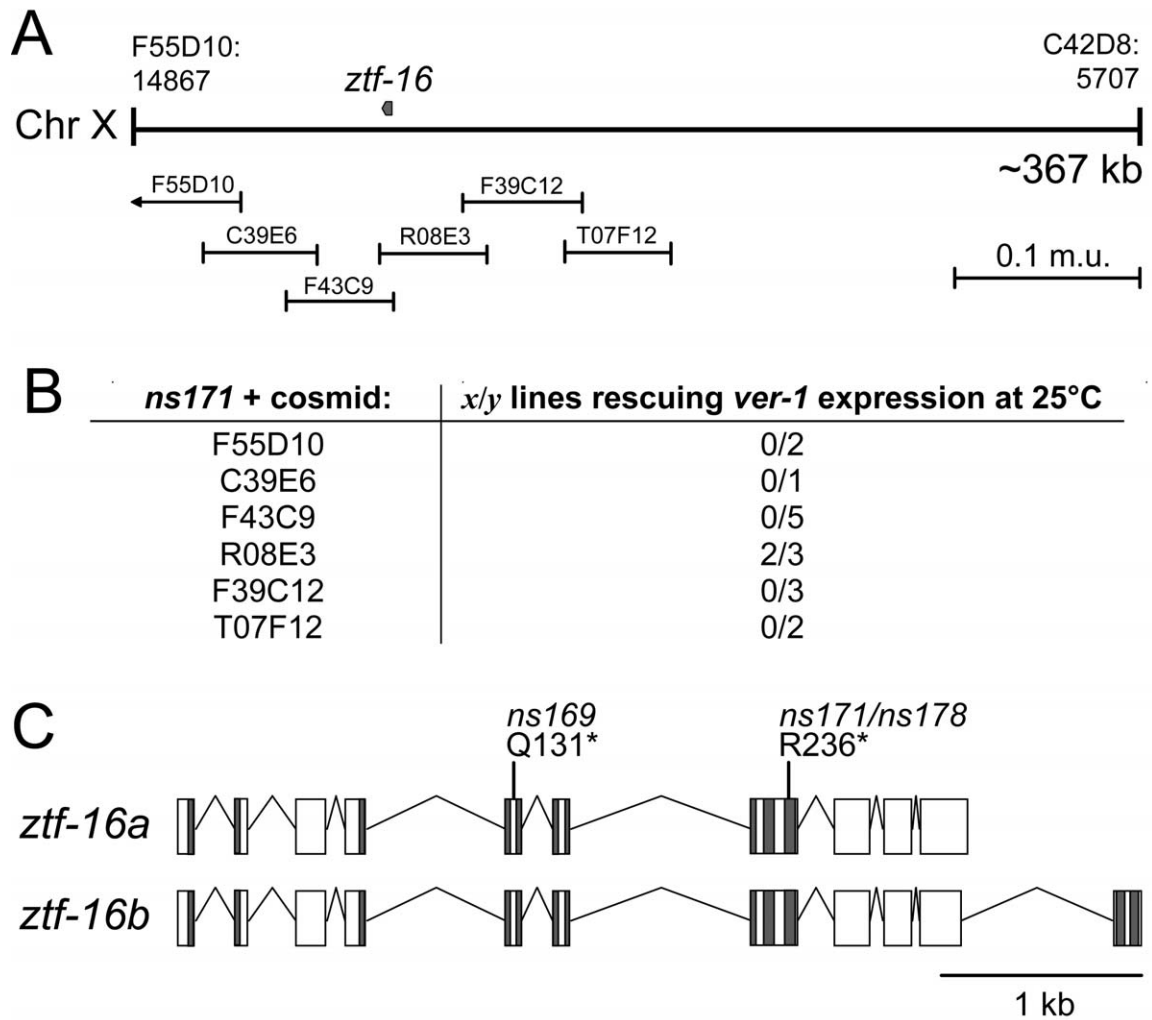


Figure 4.5. The C2H2 zinc finger gene *ztf-16* is required for *ver-1* expression.

4.5B). Candidate coding regions were sequenced within this interval, and a single base substitution causing a premature stop mutation in the *ztf-16* gene of the *ns171* strain was found (Figure 4.5C).

*ztf-16*, for *z*inc *f*inger *putative t*ranscription *f*actor *f*amily-16, codes for a predicted protein containing up to eight C2H2 zinc finger domains. C2H2 zinc finger proteins are abundant transcriptional regulators in mammals, with over 130 expressed in the brain alone (Iuchi, 2001). Based on the pattern of C2H2 zinc fingers, the *C. elegans ztf-16* gene has been described as a *hunchback*- and *Ikaros*-like transcription factor (Large and Mathies, 2010). In vertebrates, the *Ikaros* family of C2H2 zinc finger transcription factors have broad roles in the development of the hematopoietic system (Smale and Dorshkind, 2006), while *hunchback* was identified as a transcription factor regulating *Drosophila* embryo patterning (Tautz et al., 1987). *hunchback*- and *Ikaros*-like transcription factors have a unique arrangement of C2H2 zinc fingers: four amino-terminal or middle C2H2 zinc fingers bind DNA (Molnar and Georgopoulos, 1994), while two carboxy-terminal C2H2 zinc fingers mediate dimerization (McCarty et al., 2003). In *ztf-16*, it is likely that zinc fingers 3-6 form the putative DNA-binding domain (Large and Mathies, 2010).

Based on EST data available from WormBase (release WS224), we isolated two alternatively spliced cDNAs of the *ztf-16* gene. In accord with the EST nomenclature, we have defined these transcripts as *ztf-16a* and *ztf-16b* (as opposed to the alternative promoter hypothesis and nomenclature described by Large and Mathies, 2010). *ztf-16a* and *ztf-16b* differ in the presence of the two carboxy-terminal zinc finger domains (zinc fingers 7-8) and a short extension of exon 10 in *ztf-16a* (Figure 4.5C).

When we sequenced the other two independently-isolated alleles that failed to complement *ns171*, we also found mutations in the *ztf-16* gene. *ns178* had the same base mutation as *ns171* (a C to T substitution at position 706 of the cDNA), coding for a truncated protein with loss of zinc fingers 6-8, while *ns169* coded for another nonsense mutation (a C to T substitution at position 391 of the cDNA) with a loss of zinc fingers 3-8 (Figure 4.5C). These findings identify these mutants as probable loss of function alleles of the *ztf-16* gene, and show that *ztf-16* is required for *ver-1* expression in glia.

### ***ztf-16* functions within glia to regulate *ver-1***

A previous report has indicated that *ztf-16* has minor functions in the somatic gonad. Specifically, mutations in *ztf-16* interacted synergistically with mutations in a related transcription factor, *ehn-3*, to regulate early somatic gonad development (Large and Mathies, 2010). In the *C. elegans* hermaphrodite, the two somatic gonadal precursor cells (SGPs) divide asymmetrically to form daughter cells that will generate the distal tip cells (DTCs). The DTCs each migrate to form the two gonad arms (Kimble and Hirsh, 1979). *ztf-16* single mutants had little or no defect on gonad arm development, while *ztf-16; ehn-3* double mutants had increased penetrance of *ehn-3* single mutant defects, including absence of gonadal arms and ectopic germ line proliferation near the center of the gonad (Large and Mathies, 2010). These defects correlated with abnormal position and morphology of the SGPs. Consistent with the mutant phenotypes, a *ztf-16* promoter::*gfp* reporter was expressed in the somatic gonad, hypodermis, and other undescribed tissues (Large and Mathies, 2010).

Our findings here that *ztf-16* affects *ver-1* expression in the AMsh glia suggested to us that *ztf-16* might have roles in glial cell types in addition to the somatic gonad. To determine if endogenous *ztf-16* was expressed in the glia, we fused upstream enhancer regions from the *ztf-16* promoter to a *gfp* fluorescent reporter. Short regions immediately adjacent to the *ztf-16* start site generated reporter expression in hypodermal and other cell types, but not in glia (data not shown). This is consistent with the fact that cosmid F43C9, which includes all *ztf-16* coding fragments but only ~300 bp of upstream promoter, failed to rescue the reduced *ver-1 promoter::gfp* expression of *ztf-16(ns171)* mutants (Figure 4.5A,B). By contrast, a region from the *ztf-16* promoter that was further upstream and ~2 kb in length (Figure 4.6A) gave strong, specific reporter expression in the AMsh and PHsh glia, as well as the amphid and phasmid socket glia and an unidentified pair of neurons in the head (Figure 4.6B; and data not shown). In addition, we found that a ZTF-16::GFP fusion protein, expressed specifically in the AMsh and PHsh glia, localized tightly to the nucleus (Figure 4.6C; *n* = 50). This suggests that *ztf-16* may function as a cell-autonomous transcriptional regulator in the glia.

Consistent with this hypothesis, we found that we could rescue the low *ver-1 promoter::gfp* defect of *ztf-16(ns169)* and *ztf-16(ns171)* mutants by driving *ztf-16* cDNA under a continuous glia promoter (Table 4.2). That we observed rescue of *ver-1* expression with both *ztf-16a* and *ztf-16b* splice forms suggests that the two carboxy-terminal C2H2 zinc fingers are dispensable for *ztf-16* function in regulating *ver-1*. By contrast, we were unable to rescue *ver-1 promoter::gfp* expression by driving *ztf-16* cDNA under an embryonic glia promoter that is not expressed in later larval and adult stages (Table 4.2). This embryonic promoter is able to rescue other early AMsh glia

**Figure 4.6. ZTF-16 is expressed in glia and localizes to the nucleus.** (A) A schematic of the *ztf-16* promoter. The start site (+1) is shown, as well as ~4.6 kb of upstream sequence (solid, horizontal line). The promoter region/glia enhancer element used in (B) is between -4637 and -2536 relative to the +1 start site. (B) Fluorescence image (left) and fluorescence and DIC merged image (right) of an adult animal carrying a transgene containing the *ztf-16* promoter region shown in (A) driving *gfp* expression (*nsEx3001*). Fluorescence is seen in the two AMsh glia (arrows), the amphid socket glia (arrow heads), and a pair of unidentified neurons anterior of the AMsh cell bodies. Expression is also observed in the PHsh and phasmid socket glia in the tail (data not shown). (C) Localization of a ZTF-16::GFP fusion protein to the nucleus of the AMsh glia when expressed under a glia-specific promoter (*nsEx1347*). AMsh glia nucleus, arrow. In (B,C), scale bar, 50  $\mu$ m; anterior is up.

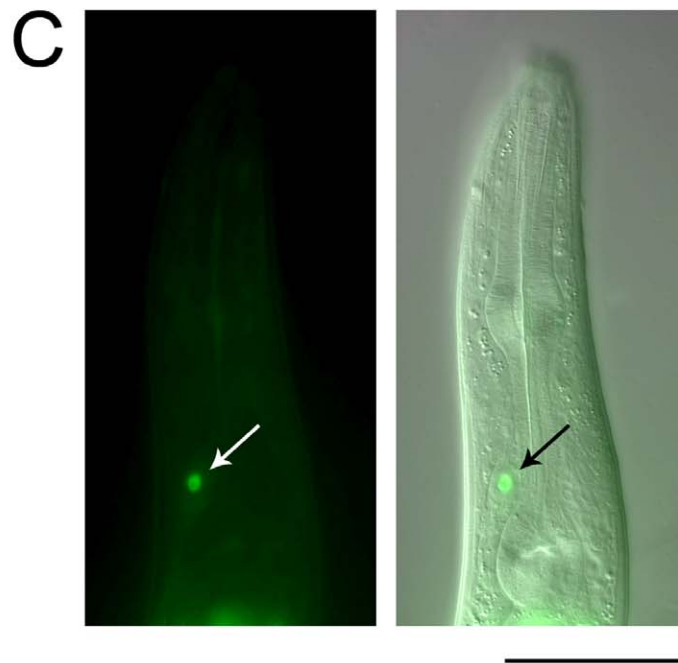
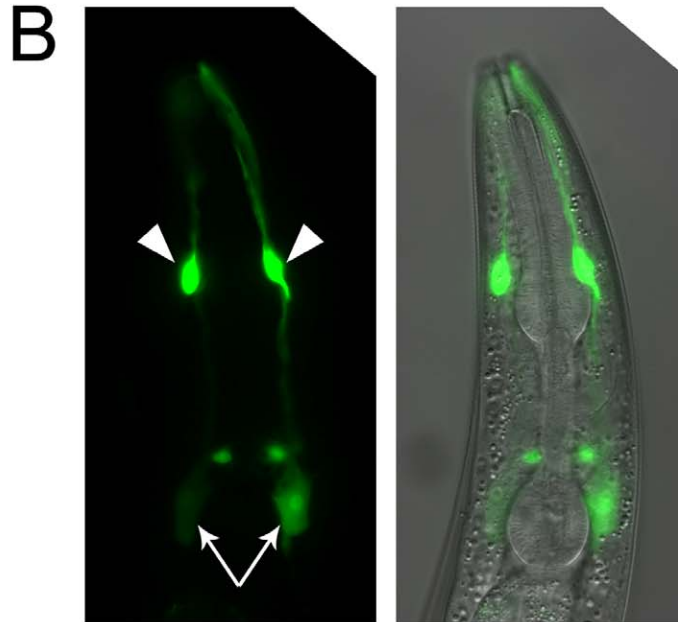
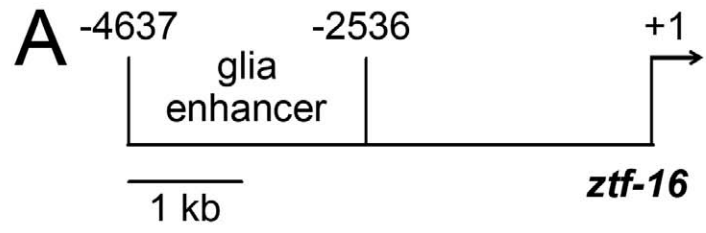


**Figure 4.6. ZTF-16 is expressed in glia and localizes to the nucleus.**

**Table 4.2. *ztf-16* acts in glia to control *ver-1* expression.**

Genotype <sup>a</sup>	% adult animals expressing <i>ver-1</i> in AMsh glia at:	
	15°C	25°C
wild type	0	93
<i>ztf-16(ns171)</i>	0	16
<i>ztf-16(ns171); glia::ztf-16a</i> <sup>b</sup>	0	64 ( $P < 0.001$ ) <sup>c</sup>
<i>ztf-16(ns171); glia::ztf-16b</i>	0	80 ( $P < 0.001$ )
<i>ztf-16(ns171); embryonic glia::ztf-16b</i> <sup>d</sup>	n.d.	10 ( $P = 0.47$ )
<i>ztf-16(ns169)</i>	0	4
<i>ztf-16(ns169); glia::ztf-16a</i>	0	44 ( $P < 0.01$ )
<i>ztf-16(ns169); glia::ztf-16b</i>	0	60 ( $P < 0.001$ )

<sup>a</sup>All strains contained the *ver-1* promoter::*gfp* transgene (*nsIs22*).

<sup>b</sup>The glia promoter (*F16F9.3*) drives expression in the AMsh and PHsh glia (Bacaj et al., 2008). However, rescue of *ver-1* promoter::*gfp* expression in the PHsh glia was not observed, perhaps due to low expression levels (data not shown).

<sup>c</sup> $P$  values were determined using the  $\chi^2$  test. Rescue lines were compared against the corresponding mutant alone at 25°C.

<sup>d</sup>The glial enhancer element from the *lin-26* promoter (Landmann et al., 2004) was used to drive expression in embryonic glial cells.

Transgenes were injected at 60 ng/ $\mu$ l of the rescuing plasmid, with 60 ng/ $\mu$ l of pRF4. Lines shown are *nsEx1389*, *nsEx1410*, *nsEx3266*, *nsEx1382* and *nsEx1405*, and are representative of others.  $n > 25$  all strains.

defects (Perens and Shaham, 2005). Together, these results show a continual, cell-autonomous requirement of *ztf-16* for *ver-1* expression in glia.

### **ZTF-16 regulates the *ver-1* promoter through a site distinct from that bound by TTX-1**

Previously, we showed that full *ver-1* promoter::*gfp* reporter expression required residues +1 to +263 of the *ver-1* gene (relative to the ATG start site) fused to *gfp* (see Chapter 3). Using *ver-1* promoter deletion studies, we identified a smaller ~90 bp interval that was sufficient for weak glia-specific and dauer-dependent reporter expression. Within this interval, we identified a direct TTX-1 binding site based on the homology of TTX-1 to its mammalian ortholog, Otx2 (Kelley et al., 2000). The core residues of this binding site were located at position +176 to +179 of the *ver-1* gene. By contrast, we find that a mutation in *ztf-16* only reduces *ver-1* reporter expression if residues +220 to +263 of the *ver-1* gene are present (Figure 4.7). This suggests that *ztf-16* acts either directly or indirectly through a site/s somewhere in this interval, distinct from the TTX-1 binding site. Consistent with this, a *ver-1* fluorescent reporter with the *ztf-16*-regulated region removed (residues +1 to +220 of the *ver-1* gene fused to *gfp*) had reduced expression compared to the full-length reporter, similar to the effect of a *ztf-16* mutation (Figure 4.7).

Within the region of the *ver-1* promoter regulated by *ztf-16* we found a potential ZTF-16 direct binding site based on the homology of ZTF-16 to *Drosophila* Hunchback. Hunchback binds the consensus sequence (G/C)(C/A)TAAAAA (Stanojevic et al., 1989). In the *ver-1* regulatory region, a similar sequence of CATGAAAAC is found at

<b><i>ver-1</i> promoter fragment fused to <i>gfp</i>:</b>	<b>% animals with AMsh glia GFP expression (<i>n</i> &gt; 25):</b>					
	<b>wild type</b>				<b><i>ztf-16</i> mutants</b>	
	adult 15°C	adult 25°C	dauer 15°C	dauer 25°C	adult 25°C	dauer 25°C
	0	93	100	100	16	60 ( <i>P</i> <0.001)
	0	100	100	100	n.d.	n.d.
	0	0	0	63	0	0 ( <i>P</i> <0.001)
	0	0	0	63	18	76 ( <i>P</i> =0.26)
	n.d.	18	n.d.	n.d.	n.d.	n.d.

**Figure 4.7. ZTF-16 regulates expression from the *ver-1* promoter through a site independent of the TTX-1 binding site.** The indicated *ver-1* promoter fragments (left column, boxes) were fused to a *gfp* fluorescent reporter and tested for expression in the AMsh glia in adults raised at 15°C and 25°C, and dauers induced by starvation at 15°C and 25°C. The *ver-1* gene fragments used are indicated relative to the +1 start site. The *ver-1* promoter::*gfp* transgene used for the mutant screen (*nsIs22*) is shown at top (~2 kb of upstream promoter sequence through +263 of the *ver-1* gene). The positions of the TTX-1 binding site (see Chapter 3) and the potential Hunchback (Hb)-related binding site are shown. (\*) indicates that the site is mutated (see Results). To test if *ztf-16* mutants affect a particular reporter, the reporter was crossed to *ztf-16(ns171)*. *P* values of reporter expression in the *ztf-16* mutant dauers at 25°C were determined by comparing the mutant strain against wild type;  $\chi^2$  test. The integrated transgenes and extrachromosomal arrays used were, from top to bottom, *nsIs22*, *nsEx1136*, *nsEx2174*, *nsEx1269*, and *nsEx3022*. To generate arrays, the *ver-1* reporter construct was injected at 60 ng/ $\mu$ l with 60 ng/ $\mu$ l pRF4. Arrays are representative of others. n.d., not determined.

position +217 to +225 relative to the *ver-1* start site. Mutating these residues to GGGCCCCAAC resulted in a loss of *ver-1* promoter::*gfp* expression, not unlike the effect of a *ztf-16* mutation on the wild-type reporter (Figure 4.7). This finding is consistent with the hypothesis that ZTF-16 binds directly to the *ver-1* gene to regulate its expression at a site distinct from that bound by TTX-1. However, we were unable to verify conclusively that a purified GST::ZTF-16 fusion protein could recognize this site in an *in vitro* gel shift assay. We could not purify soluble full-length GST::ZTF-16B under a variety of conditions when induced in *E. coli*. By contrast, zinc fingers 2-6 fused to GST [GST::ZTF-16(znf2-6)] were in part soluble when the fusion protein was induced at 20°C (Figure 4.8A). However, GST::ZTF-16(znf2-6) showed only weak, non-specific binding to a 40 bp biotin-labeled probe from the *ver-1* gene. In some assays, weak binding was consistent with ZTF-16 directly associating with the wild-type *ver-1* sequence and not to a probe where the predicted binding site was mutated (Figure 4.8B); however, due to the non-reproducibility of these results we cannot be conclusive.

### ***ztf-16* function is required in glia for AMsh glia fision in dauer animals**

Our rationale for screening for mutants with defective *ver-1* expression was that these same animals would have defects in AMsh glia remodeling upon dauer entry. Previously, we designed an assay to score fusion of the two AMsh glia by taking advantage of instability of an extrachromosomal array expressing an AMsh glia::*gfp* reporter (*nsEx1391*). Mosaic first- and second-stage larvae expressing the reporter in just one of the two AMsh glia were selected and cultivated for a further 48 h at 25°C. Dauer entry was induced by the presence of a temperature-sensitive dauer constitutive mutation,

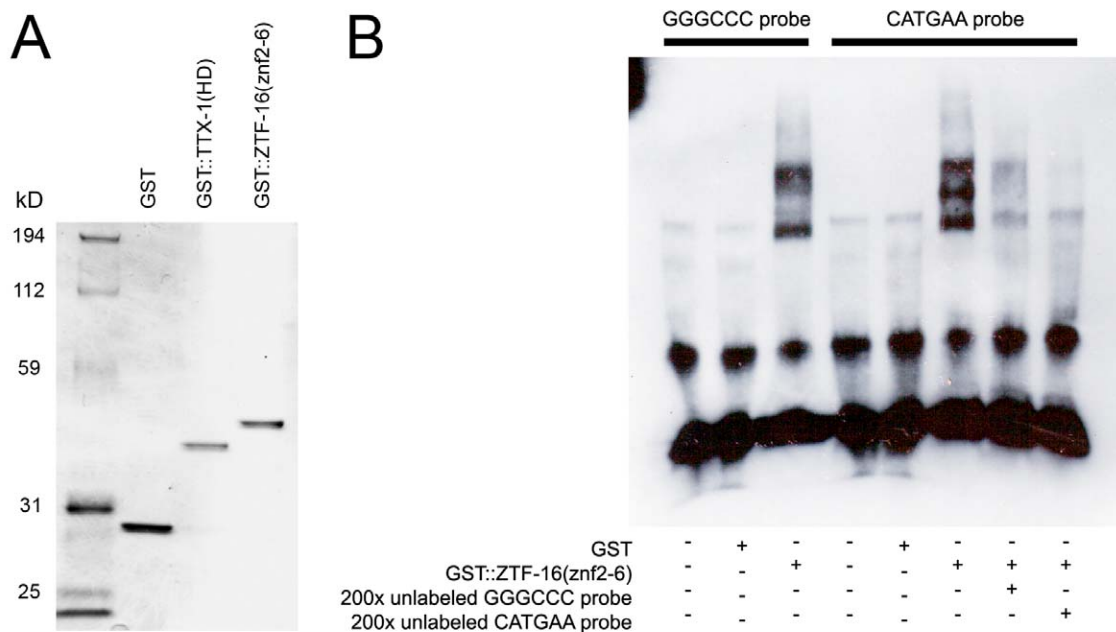


**Figure 4.8. ZTF-16 may bind directly to the *ver-1* promoter.** (A) SDS-PAGE analysis of purified GST::ZTF-16 zinc fingers 2-6 (znf2-6) protein. Marker size in kD is shown, as are comparisons against GST and GST::TTX-1 homeodomain (HD) purified proteins. ~1  $\mu$ g of each purified protein is loaded. (B) Example of an electrophoretic mobility-shift assay suggestive of ZTF-16 binding to the *ver-1* promoter. Either a GST control or a purified GST::ZTF-16(znf2-6) fusion protein was bound to a wild-type (CATGAA) or mutant (GGGCCC) 40 bp biotin-labeled probe from the *ver-1* promoter. Competitor, unlabeled wild-type or mutant probes were added in 200-fold excess. Binding of GST::ZTF-16(znf2-6) to both DNA probes was generally weak, and a difference between the shifts of the mutant and wild-type probes was not always observed (data not shown).

*daf-7(e1372)* (see Chapter 2, Figure 2.2). Cytoplasmic mixing between the two glia occurs in dauer animals where the glia fuse at the anterior tip of their cellular processes. In these animals, GFP is free to diffuse into the other cell, and both glia now fluoresce.

Using our cytoplasmic mixing assay, we found that *ztf-16(ns169)* and *ztf-16(ns171); daf-7(e1372)* dauers had significantly reduced AMsh glia fusion compared to *daf-7(e1372)* dauers (Figure 4.9A). Furthermore, we could rescue the fusion defect by restoring *ztf-16* function specifically to the glia (Figure 4.9A). These findings suggest that *ztf-16* function in glia is required for dauer-induced glia remodeling, and, like *ttx-1*, that *ztf-16* acts in part to affect fusion by regulating the *ver-1* gene. Previously, we also showed a requirement of the *aff-1* fusogen in glia fusion. However, it is unlikely that *ztf-16* transcriptionally regulates *aff-1*: 95% of wild-type dauer animals carrying an *aff-1* promoter::*gfp* reporter (*hyEx167*) expressed GFP in the AMsh glia, while 87% of *ztf-16(ns171)* mutants expressed GFP in the AMsh glia; *n* = 44 and 38, respectively.

In addition to our cytoplasmic mixing assay, we found that 3 out of 3 *ztf-16(ns171); daf-7(e1372)* mutant dauer animals failed to exhibit AMsh glia extension and fusion at the anterior tip of the cells by EM analysis (Figure 4.9B,C). In these same animals, the AWC sensory neuron wing-like cilia that are ensheathed by the glia do not exhibit the large expansion characteristic of wild-type dauers. These findings are consistent with our observation that changes in the glia are important for concomitant changes in the AWC neurons.

Together, our results show that the *ztf-16* gene is required for expression of the AMsh glia gene *ver-1* in response to dauer entry, and that *ztf-16* function is required for AMsh glia morphological remodeling during dauer development.

**Figure 4.9. *ztf-16* function is required for AMsh glial remodeling in dauer animals.**

(A) Percentage of *daf-7(e1372)* dauer animals of the indicated genotype with fused AMsh glia as scored by cytoplasmic mixing. Number of animals (*n*) is shown above each column. (\*) indicates  $P = 0.001$  (Fisher's exact test), (\*\*) indicates  $P < 0.001$  ( $\chi^2$  test). The *glia::ztf-16* transgene is *nsIs245 (T02B11.3 promoter::ztf-16b)*. (B,C) Electron micrograph (EM) (left) and schematic outline (right) of the amphid sensory organs of a *daf-7(e1372)* dauer (B) and a *ztf-16(ns171); daf-7(e1372)* dauer (C). Left and right AWC neuron sensory cilia (AWCL/R; dark shading) and AMsh glia (AMshL/R; light shading) are indicated. In (C), a section close to the anterior tip of the glial processes is shown where maximum AWC expansion occurs. Due to the reduced morphology of AWCL, we were unable to conclusively identify this neuron from the other ensheathed wing-ciliated neurons (indicated by ?). Scale bar, 5  $\mu\text{m}$ ; dorsal is up. Wild-type data and images used in (A,B) are reproduced from Chapter 2.

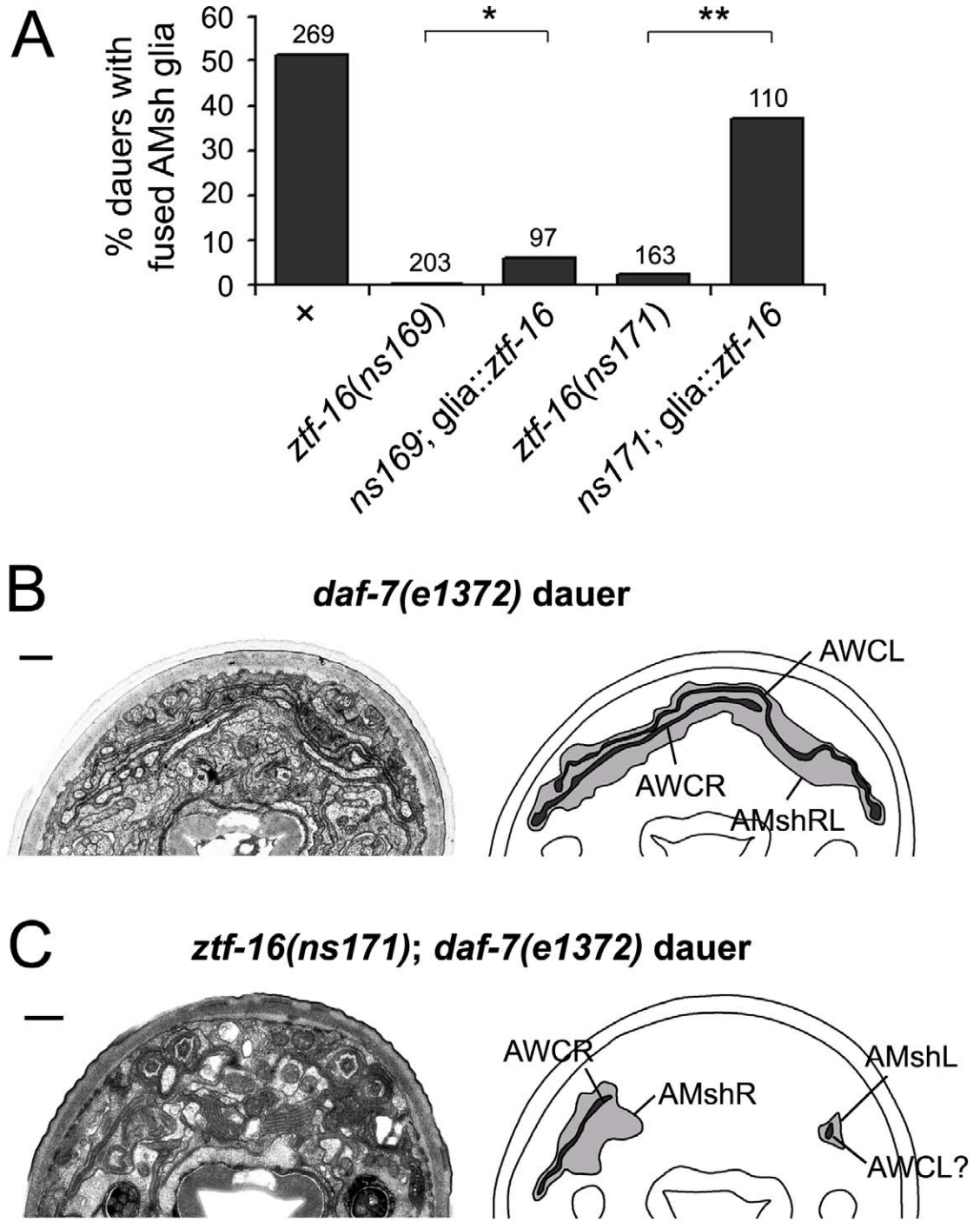


Figure 4.9. *ztf-16* function is required for AMsh glial remodeling in dauer animals.

## Discussion

Previously, we demonstrated that morphological remodeling and fusion of the two AMsh glial cells in dauer animals was dependent on the gene *ttx-1* and its direct downstream target, the receptor tyrosine kinase *ver-1*. Transcriptional reporters for *ver-1* indicate that the gene is upregulated by dauer entry and also by an environmental stimulus that induces dauer, high temperature (see Chapter 3). Based on these observations, we hypothesized that other mutations that affect expression of a *ver-1* transcriptional reporter would also affect AMsh glia remodeling. To this end, we have performed a mutant screen for loss of *ver-1* promoter::*gfp* expression, and identified the transcription factor *ztf-16* as being required for both *ver-1* expression and dauer-induced AMsh glia fusion. Our results are consistent with a model whereby the transcriptional regulators TTX-1 and ZTF-16 act through distinct binding sites to regulate both *ver-1* and other genes required for AMsh glia fusion.

Our EM analysis of dauer animals suggests that the AWC wing-like cilia fail to take on their expanded morphology in *ztf-16* mutants. It remains to be tested if AWC wing morphology is also reduced in non-dauer *ztf-16* mutant animals, perhaps due to reduced size of the AMsh glia at the anterior tip of the glial processes. Such a possibility can be explored by either EM or fluorescence-based studies; however, preliminary analysis suggests that AWC-mediated chemotaxis towards benzaldehyde in adult animals is unaffected by mutations in *ztf-16* (data not shown).

Interestingly, *ztf-16* was also identified as a possible effector of AMsh glial channel morphology in an unrelated screen performed within our lab (Oikonomou et al., in press). While some amphid sensory neurons like AWC and the thermosensory neuron

AFD are completely ensheathed by the AMsh glia, others project simple cilia through a channel in the glia that is open to the outside environment. One factor that regulates embryonic channel formation is the Nemo-like kinase LIT-1, that localizes to the channel and there interacts with actin regulators to increase channel size (Oikonomou et al., in press). Surprisingly, ZTF-16 was identified as a protein that potentially interacts with LIT-1 in a yeast two hybrid (Y2H) assay. Intriguingly, *lit-1* expression is strongly regulated by the DAF-12 nuclear hormone receptor, which integrates dauer neuroendocrine signals to induce dauer entry (Shostak et al., 2004). That LIT-1/Nemo-like kinase may also transmit signals between the nucleus and cytoplasm (Ishitani et al., 2011) may support an interaction with ZTF-16 in the nucleus in dauer animals to regulate AMsh glia morphology. However, while we find defects in dauer-induced glia fusion by our cytoplasmic mixing assay in *lit-1(ns132)* mutants (6% fusion,  $n = 133$ ), these same mutants had no defect in *ver-1* promoter::*gfp* expression in dauer animals or at high temperature (data not shown). Likewise, more severe *lit-1(t1512ts)* mutants had no defect in *ver-1* expression in adults shifted to high temperature (data not shown). These findings suggest that if LIT-1 does regulate AMsh glia fusion it is unlikely through an interaction with ZTF-16, and rather may be a secondary defect of early developmental abnormalities of the glia in *lit-1* mutants. It is possible that ZTF-16 interacts with LIT-1 in early glia development to have some effect on channel morphology, or alternatively the two proteins may interact in other cell types (for example, both are expressed in hypodermal cells) or not at all.

If ZTF-16 does interact with other factors, it is possible that these interactions occur via the two amino-terminal or two carboxy-terminal C2H2 zinc finger domains,

which are unlikely to be required for DNA binding (Large and Mathies, 2010). For example, the carboxy-terminal zinc fingers of the related Ikaros transcription factor enable dimerization of the protein (Sun et al., 1996). However, in our rescue studies we find that these two zinc fingers are dispensable for *ztf-16* function in regulating *ver-1* expression (Table 4.2; both splice forms *ztf-16a* to *ztf-16b* rescue *ver-1* promoter::*gfp* expression). Therefore, it is unclear what role these domains play in the ZTF-16 protein. One possibility is the creation of ZTF-16 isoforms that are able to or prohibited from complexing with other factors. For example, Ikaros activity can be controlled by dimerization with non-functional isoforms of the protein (Sun et al., 1996). Such a system may enable finer control over ZTF-16 activity.

That most of the mutations we isolated in our screen for reduced *ver-1* promoter::*gfp* expression in adults raised at 25°C were alleles of one of three different genes, *ztf-16*, *ttx-1* or *tam-1*, suggests that the screen has been performed close to saturation. Although our analysis has identified *ztf-16* and *ttx-1* as glial factors required for *ver-1* expression, it remains unclear how dauer signals that induce *ver-1* transcription are perceived by the AMsh glia. These signals may be direct neuroendocrine signals from amphid sensory neurons (for example, the TGF- $\beta$  ligand DAF-7), secondary signals as a result of dauer entry (for example, radial shrinkage of the body circumference, pushing the glia into closer proximity), or in part environmental signals perceived directly by the glia (for example, temperature; see Chapter 3). It is possible that mutant screens assessing *ver-1* expression specifically in dauer animals rather than non-dauer adults may uncover what these signals are.

Although glial shapes are known to be plastic, very little is known about the genes required for glial shape changes in any system. Here, we have shown that AMsh glia remodeling in *C. elegans* dauer larvae is a tractable system for genetic screens to uncover a molecular pathway regulating changes in glia shape.

# **Chapter 5**

Conclusions and future directions

## **Glia are required for dendrite morphological plasticity**

Neurons display a myriad of shapes, from complex dendritic arbors to the receptive endings on dendrites that receive sensory and synaptic information. These shapes are plastic, and can be remodeled by developmental, hormonal, and environmental signals. For example, changes in somatosensory input increases the turnover of pyramidal neuron dendritic spines in the mouse barrel cortex (Trachtenberg et al., 2002), while estrogen levels affect the number and density of hippocampal neuron dendritic spines in rats (Woolley et al., 1990). These changes in receptive-ending shape reflect changes in synaptic connections and the strength of those connections (Holtmaat and Svoboda, 2009).

Glia, which are intimately associated with neurons, also display vast morphological specializations. Changes in glial shape can correlate with neuronal remodeling; for example, the retraction of astrocytic glia in the hypothalamus of lactating rats correlates with synaptic changes in associated neurons (Theodosis and Poulain, 1993), while perturbation of the glial ephrin-A3 cell-surface molecule affects the shape of dendritic spines in the mouse hippocampus (Carmona et al., 2009). These observations, coupled with the close proximity of glia to neurons and the ability of glia to regulate and perceive their extracellular environment (Meyer-Franke et al., 1995; Porter and McCarthy, 1996), suggests that glia are well-positioned to facilitate or, more speculatively, to direct changes in dendritic shapes.

In response to environmental stressors, including starvation, crowding, and high temperature, the nematode *C. elegans* becomes a developmentally-arrested dauer larva. Various morphological changes occur in dauer animals, including the remodeling of the

amphid sensory organs (Albert and Riddle, 1983). Here, we find that remodeling of the AMsh glia is required for correct morphological remodeling of the ensheathed AWC neuron dendrite endings. Although it is unclear in mammalian systems if glia are instructive or permissive for neuronal plasticity, our results in *C. elegans* are consistent with a predominantly permissive role of the glia in affecting AWC shape. The observation that some AWC sensory endings continue to expand in mutant animals where glial remodeling is blocked (Figure 2.12), suggests that expansion and fusion of the glial cells defines a new compartment in which the two AWC sensory endings can expand and significantly overlap with one another. However, our finding that the glia remodel and fuse even in the absence of AWC expansion (Figure 2.7) is suggestive that glial remodeling is not simply a passive outcome of changes in the associated neurons and that the glia and AWC neurons may receive remodeling cues independently of each other.

In addition to AWC, other amphid neurons also remodel during dauer development. The single ciliated dendritic endings of the ASI and ASG neurons are repositioned more posteriorly in the AMsh channel, while the AFD thermosensory neuron may have an increase in the number of microvillar protrusions ensheathed by the AMsh glia (Albert and Riddle, 1983). Although our studies have not addressed the role of AMsh glial remodeling in facilitating these other neuronal shape changes, a careful study of the glial remodeling mutants isolated here may determine if changes in the AMsh glia are generally required for sensory neuron plasticity.

## **Glia can respond to environmental and developmental cues**

Glia, like neurons, can sense changes in their extracellular environment. Glia can directly sense stimuli such as Na<sup>+</sup> levels (Shimizu et al., 2007), neurotransmitters (Porter and McCarthy, 1996), and protons (Wang et al., 2008). Furthermore, glial sensory activity can regulate behavior. For example, astrocytic glia of the ventral brainstem surface are proposed to sense CO<sub>2</sub>-evoked acidosis of cerebrospinal fluid, in turn causing adenosine 5'-triphosphate (ATP) release and activation of neurons that control inspiratory breathing movements (Ballanyi et al., 2010; Gourine et al., 2010). In *C. elegans*, the AMsh glia express the acid-sensitive Na<sup>+</sup> channel ACD-1 (for *acid sensitive channel, degenerin-like-1*), the activity of which is inhibited by protons (Wang et al., 2008). In combination with a mutation in a neuronal degenerin Na<sup>+</sup> channel, *deg-1*, *acd-1* mutants have defects in avoidance responses to acid (Wang et al., 2008). This suggests that glial sensory function may affect behavior in diverse organisms.

Our studies demonstrate that the AMsh glia can respond to dauer entry and temperature, both exogenous stimuli. Furthermore, at least one gene, *ver-1*, is dynamically regulated by both cues. What are the molecular dauer signals perceived by the glia, and how do these regulate *ver-1* transcription? These signals could be derived from neuroendocrine pathways that regulate dauer entry. For example, mutations in the neuron-secreted TGF- $\beta$ /DAF-7 ligand can affect both dauer entry (Ren et al., 1996) and glia remodeling. The TGF- $\beta$ /DAF-7 and insulin receptor/DAF-2 neuroendocrine pathways that regulate dauer entry converge onto the nuclear hormone receptor (NHR) DAF-12 (Antebi et al., 2000). Intriguingly, at least two potential DAF-12 binding sites are found within the minimal interval of the *ver-1* promoter that is required for dauer

responses. Mutating either of these sites causes a loss of *ver-1* reporter expression in the glia of adult animals raised at 25°C (data not shown). This is consistent with a model whereby factors such as TTX-1 and ZTF-16 confer glial specificity to *ver-1* expression, while DAF-12 activity confers dauer- and temperature-dependence. It is unlikely that *ttx-1* and *ztf-16* are dauer-regulated themselves: another direct *ttx-1* target gene in the glia was not induced by dauer entry (see Chapter 3) and *ztf-16* does not regulate *ver-1* transcription through the minimal interval of the *ver-1* promoter required for dauer-dependence (see Chapter 4). However, we were unable to detect specific binding of a GST::DAF-12 (DNA-binding domain) fusion protein to these potential DAF-12-binding sites in *in vitro* gel shift assays (data not shown), and *daf-12* loss of function mutations do not result in a loss of *ver-1* promoter::*gfp* expression in animals raised at 25°C (see Chapter 3). It is possible that DAF-12-related NHR factors may bind these sites, or other factors altogether. Our screen for loss of *ver-1* promoter::*gfp* expression may not have uncovered these factors as we did not screen animals in the dauer state. An alternative approach to finding transcriptional regulators that bind to the *ver-1* promoter would be a yeast-1-hybrid (Y1H) screen, which may circumnavigate these difficulties.

Alternatively, the dauer signals perceived by glia may be secondary signals as a result of dauer entry. Many morphological changes occur in dauer animals, including the radial shrinkage of the body circumference. This may physically push the glia and AWC neurons into closer proximity with one another, leading to amphid remodeling (Albert and Riddle, 1983). Consistent with this idea, mutations in factors that make up part of the neuroendocrine dauer pathways, TGF- $\beta$ /*daf-7* and insulin receptor/*daf-2*, only affect *ver-1* promoter::*gfp* expression if the mutant animals enter the dauer state and not in

response to temperature (see Chapter 3; by contrast, *daf-2* mutants have alterations in longevity regardless if the animal enters dauer or not; Kimura et al., 1997).

A third possibility, not exclusive of the others, is that the glia directly sense some environmental stressors that induce dauer entry. Our findings that *ver-1* transcription in the glia is highly dependent on ambient temperature, and that this is independent of the AFD thermosensory neurons, is consistent with the notion that the glia can respond directly to temperature. That the glia express the transcription factor *ttx-1*, also required by the AFD thermosensory neuron for morphology and function, is intriguing. The slow induction of *ver-1* expression is consistent with a transcriptional mechanism of *ver-1* temperature-dependence. For example, in the model plant *Arabidopsis thaliana*, chromatin components may be directly affected by temperature (Kumar and Wigge, 2010). However, we have been unable to determine from our studies the relevance of *ver-1* up-regulation in response to temperature. It may reflect a shared stress response of dauer animals with animals raised at high temperature. Another possibility is that the temperature response primes the glia for subsequent signals to be received when the animal enters the dauer state. If this were true, then dauer animals raised at different temperatures might be expected to have different incidences of amphid remodeling. Although our cytoplasmic mixing assay is unsuitable for such an analysis due to the use of a dauer-constitutive *daf-7* mutant allele that has a temperature-sensitive phenotype, alternative assays using dauer pheromone to induce dauer entry or extensive EM analysis may address this question.

## Identifying glial factors required for morphological plasticity

Our finding that remodeling of the AMsh glia is important for changes in the associated sensory neurons suggests that factors that affect glial shape changes may also be important for neuronal shape and function. To this end, we have shown the transmembrane receptor tyrosine kinase *ver-1*, its transcriptional regulators *ttx-1* and *ztf-16*, and the cell fusogen *aff-1* are all glial factors required for glia remodeling and fusion in dauer animals. The involvement of *ver-1* is intriguing, suggesting that a kinase signaling pathway may regulate the process of fusion. However, our inability to rescue the *ver-1* mutant phenotype (Appendix 1) has hindered further studies of the VER-1 protein.

Our data posits that *ttx-1* and *ztf-16* function in part to regulate glia fusion by transcribing the *ver-1* gene. Transcriptional profiling of the AMsh glia from wild-type and *ttx-1* and *ztf-16* mutant strains may be a fruitful approach to find other targets also required for glia remodeling. In addition, AMsh glia-specific mRNA microarray analysis comparing dauer to non-dauer animals may find additional factors involved in the process. One successful method to generate cell-specific transcript information in *C. elegans* has been the dissociation of embryonic cells carrying a terminal differentiated cell marker, and subsequent fluorescence-activated cell sorting (FACS) of these cells following differentiation in culture (Bacaj et al., 2008; Colosimo et al., 2004). However, such an approach does not permit the identification of developmental stage-specific or environmentally-regulated transcripts. Alternative techniques, including co-immunoprecipitation of poly(A) RNA with a cell-specific tagged poly(A)-binding protein

(Kunitomo et al., 2005; Takayama et al., 2009) or the generation of cell-specific biotin-labeled RNA (Miller et al., 2009) are in the process of being developed in our laboratory.

It is unclear from our studies if the transcriptional network regulating *ver-1* also affects *aff-1* function. Expression of an *aff-1* promoter::*gfp* reporter in the AMsh glia was unaffected in either *ztf-16* or *ttx-1* mutants; however, this does not preclude the possibility that the regulation of *aff-1* is post-transcriptional. The tight and easily-observed localization of an AFF-1::GFP fusion protein to the apical region of the glial processes where fusion occurs suggests that screening for factors that regulate AFF-1 polarity is feasible. It is not known in *C. elegans* if factors that regulate glial polarity are identical to polarity genes identified in other cell types. In addition, it is possible that some of the signals determining AFF-1 localization are given by the placement of the sensory neuron cilia, as has been suggested for factors required for glial channel morphogenesis (Perens and Shaham, 2005).

Our studies have shown that screening for factors that regulate *ver-1* promoter::*gfp* expression is a useful method for finding new genes that affect glia remodeling in dauer animals. However, such an approach may be limited to finding transcriptional regulators. In addition, the fact that mutations reducing *ver-1* promoter::*gfp* in adults raised at 25°C fell largely into three complementation groups suggests that this screen may be close to saturation. Our method of screening adults at high temperature may also fail to find signals that are only present in dauer animals. One alternative is to screen instead for mutations that increase *ver-1* promoter::*gfp* expression, rather than reducing it. A screen for suppression of the *ttx-1(p767)* phenotype in non-dauer adult animals at 25°C generated only one allele with wild-type *gfp* levels (from >

15,000 EMS-mutagenized F2 animals). This mutant allele, *ns228*, was found to be an intragenic suppressor (having the *p767* G to A substitution at position +4502 of the *ttx-1* gene, and an additional G to A substitution at +4506). This suggests that suppression of a *ttx-1* mutation by loss of function mutations in other genes may be biologically difficult. In addition, mutations in a gene identified to have inappropriately high *ver-1* promoter::*gfp* expression in a wild-type background did not affect AMsh glia fusion in dauer animals (Appendix 4). These results place into doubt the physiological significance of high *ver-1* promoter::*gfp* expressing mutants.

## **What is the physiological purpose of amphid remodeling?**

The functional outcome of AWC receptive-ending remodeling in dauers is unclear; however, previous studies have correlated AWC sensory ending shape with function (Perkins et al., 1986). Therefore, it is possible that the morphological changes in AWC promote a change in the behavior of the animal. It is not unreasonable to speculate that dauer animals may wish to perceive their environment differently so that they may quickly locate favorable conditions, exit dauer and become reproductive adults. Alternatively, the remodeling of AWC and the AMsh glia may be a result of radial shrinkage of body circumference and serve no physiological purpose (Albert and Riddle, 1983). To date, no AWC-mediated behaviors have been described for dauers. Indeed, in dauer animals the expression of at least one AWC odorant receptor is repressed (Peckol et al., 2001), and the classical AWC-sensed attractants benzaldehyde and isoamylalcohol act instead as repulsive cues (Appendix 5; and data not shown), either as a result of changes in AWC neuronal circuitry or AWC odorant receptor repertoire. These

observations suggest that assessing the functional consequences of dauer remodeling will require a more thorough description of sensory neuron function and molecular biology in dauers than is presently available. Future work may address this issue by carefully characterizing the behavior of dauers, and comparing wild-type and mutant animals with and without fusion of the AMsh glia.

It is possible that changes in the amphid sensory structures are required to directly modulate the perception of dauer exit signals. Consistent with this idea, *ttx-1(p767); daf-7(e1372)* mutants have been reported to exit dauer prematurely compared to *daf-7(e1372)* single mutants (Satterlee et al., 2001). However, cell-specific studies suggest that this effect can be rescued by restoring *ttx-1* function to the AFD thermosensory neurons and not the glia, although we cannot rule out different growth rates in the transgenic lines used for the analysis (Appendix 6).

Our observation that some aspects of amphid remodeling may be retained in post-dauer adults (Figure 2.5) may suggest that post-dauer animals have some memory of past experiences. It has previously been shown that the expression profiles of post-dauer animals differ from animals that did not pass through dauer, and that post-dauers live marginally longer and have increased brood sizes (Hall et al., 2010). However, it is unclear if the permanent changes in amphid structure observed here have physiological relevance. Further behavioral and other studies may be revealing.

## **Amphid sensory organ remodeling as a model of nervous system plasticity**

Although vertebrate glial and dendritic shapes are known to be plastic, the relevance of glial plasticity in guiding neuron shape has not been well explored. In addition, very little is known about the factors required for glial shape changes. Here, we have described a system in the nematode *C. elegans* where glia and neurons are remodeled by an inducible developmental state of the animal. Studies of *C. elegans* may prove particularly useful in understanding glia-neuron interactions. *C. elegans* has a small, invariant number of neurons and glia, which have stereotyped shapes and connections. In contrast to other systems, *C. elegans* glia are not essential for neuronal survival (Bacaj et al., 2008; Yoshimura et al., 2008). Furthermore, we have shown here that the facile genetics of *C. elegans* provides a powerful setting for gene discovery, which may prove useful for uncovering the molecular basis of glial actions on facilitating nervous system plasticity. The conserved functional, morphological, and molecular features of mammalian and *C. elegans* glia (Bacaj et al., 2008; Yoshimura et al., 2008) suggest that this ‘simple’ nematode may be able to teach us something about the role of glia in the development and function of the most complex of organs: the human brain.

# **Chapter 6**

## Experimental Procedures

## Strains

*C. elegans* were cultivated using standard methods (Brenner, 1974). All animals cultivated at 20°C unless otherwise mentioned. The wild-type strain used was Bristol (N2).

Mutant alleles used: LGI: *tax-2(p691)*, *lin-11(n389, n566)*, *che-13(e1805)*, *daf-16(mu86)*, *hsf-1(sy441)*; LGII: *ire-1(zc14)*, *old-2(ok1253)*; LGIII: *dac-1(gk211)*, *tax-4(p678)*, *unc-86(e1416, n846)*, *daf-7(e1372)*, *daf-2(m41)*, *ver-1(ok1738, tm1348)*, *lit-1(ns132, t1512)*; LGIV: *osm-9(ky10)*; LGV: *ttx-1(p767, oy26)*, *pkc-1(nj1, nj3, nj4)*, *osm-6(p811)*; LGX: *ceh-14(ch3)*, *pkc-2(ok328)*, *ttx-3(ks5, mg158)*, *ceh-37(ok642, ok272)*, *ceh-36(ky646)*, *che-2(e1033)*, *dyf-7(ns89, m537)*, *daf-12(m20, m25)*, *lin-15(n765)*.

Mutant alleles isolated in this study were: LGV: *tam-1(ns167, ns170, ns174, ns234, ns237, ns238, ns241, ns249, ns258, ns268)*, *ttx-1(ns235, ns252, ns255, ns259, ns260, ns267)*; LGX: *ztf-16(ns169, ns171, ns178)*, *fkh-9(ns168, ns177, ns181, ns182, ns198, ns242, ns243, ns261)*, *his-24(ns183)*. Alleles not mapped to a chromosome include *ns231, ns257*.

Integrated transgenes used: LGIV: *nsIs22[P<sub>ver-1</sub>gfp; lin-15(+)]*, *nsIs53[P<sub>vap-1</sub>dsRed; unc-119(+)]*, *nsIs142[P<sub>F16F9.3</sub>dsRed; lin-15(+)]*; LGV: *oyIs17[P<sub>gcy-8</sub>gfp; lin-15(+)]*, *oyIs45[P<sub>odr-1</sub>yfp; lin-15(+)]*; LGX: *nsIs143[P<sub>F16F9.3</sub>dsRed; lin-15(+)]*. The sheath glia-specific integrated *ttx-1* rescuing transgene (glia::*ttx-1*) was LGI: *nsIs101[P<sub>F16F9.3</sub>ttx-1a; P<sub>gcy-7</sub>dsRed; lin-15(+)]* and LGV: *nsIs219[P<sub>T02B11.3</sub>ttx-1a; P<sub>unc-122</sub>dsRed; pSL1180]*. The sheath glia-specific integrated *ztf-16* rescuing transgene (glia::*ztf-16*) was LGV: *nsIs245[P<sub>T02B11.3</sub>ztf-16b; P<sub>unc-122</sub>dsRed; pSL1180]*. The integrated AFD-specific rescuing transgene (AFD::*ttx-1*) was LGX: *nsIs99[P<sub>gcy-8</sub>ttx-1a; P<sub>gcy-7</sub>gfp; lin-15(+)]*. Strains carrying *nsIs99* may also contain the linked *lin-15* allele *n765*. The integrated *ver-1* promoter::*ver-1* transgenes [*P<sub>ver-1</sub>ver-1*; *P<sub>unc-122</sub>dsRed*; pSL1180] used in Appendix 1 were: LGI: *nsIs204*; LGIII: *nsIs205*; LGIV: *nsIs208*; LGX: *nsIs211, nsIs213*.

Extrachromosomal arrays used: *nsEx755[P<sub>gcy-8</sub>egl-1[x2]; rol-6(su1006)]*, *nsEx1320[P<sub>ttx-1(AFD)</sub>dsRed; rol-6(su1006)]*, *nsEx1942[P<sub>ttx-1(glia)</sub>gfp; rol-6(su1006)]*, *nsEx2436[P<sub>T02B11.3</sub>gfp; rol-6(su1006)]*, *nsEx2703[P<sub>F16F9.3</sub>eff-1a::gfp; rol-6(su1006)]*, *nsEx2727[P<sub>F16F9.3</sub>aff-1::gfp; rol-6(su1006)]*, *nsEx1685/nsEx1391[P<sub>F16F9.3</sub>gfp; rol-6(su1006)]*, *nsEx2284[P<sub>F58F9.10</sub>gfp; rol-6(su1006)]*, *nsEx2330[P<sub>F58F9.6</sub>gfp; rol-6(su1006)]*, *nsEx2317[P<sub>old-2</sub>gfp; rol-6(su1006)]*, *nsEx2299[P<sub>old-1</sub>gfp; rol-6(su1006)]*, *nsEx1347[P<sub>F16F9.3</sub>ztf-16b::gfp; rol-6(su1006)]*, *nsEx3022[P<sub>ver-1(Hb site\*)</sub>gfp; rol-6(su1006)]*, *nsEx3162/nsEx3171[ver-1 gDNA (fosmid WRM0636cD01); rol-6(su1006)]*, *nsEx962[P<sub>F16F9.3</sub>ver-1::gfp; rol-6(su1006)]*, *nsEx1517[P<sub>F16F9.3</sub>fkh-9a::gfp; rol-6(su1006)]*, *nsEx1526[P<sub>fkh-9</sub>gfp; rol-6(su1006)]*, *nsEx1590[P<sub>F16F9.3</sub>his-24::gfp; rol-6(su1006)]*. *ver-1*

promoter deletion::*gfp* arrays included *nsEx1136* (+1 to +263), *nsEx2174* (+1 to +220), *nsEx1269* (+130 to +263) and others. *hyEx167* ( $P_{\text{eff-1gfp}}$ ) and *zzEx26* ( $P_{\text{eff-1gfp}}$ ) were gifts from Benjamin Podbilewicz and William Mohler.

*ttx-1* rescuing arrays included: *nsEx875/nsEx897/nsEx899/nsEx1913/nsEx1914*[ $P_{\text{gcy-8ttx-1a}}$ ; *rol-6(su1006)*], *nsEx877/nsEx893/nsEx895*[ $P_{\text{vap-1ttx-1a}}$ ; *rol-6(su1006)*], *nsEx930/nsEx937/nsEx939/nsEx1923/nsEx1924*[ $P_{\text{F16F9.3ttx-1a}}$ ; *rol-6(su1006)*], *nsEx1636*[ $P_{\text{heat shockttx-1a}}$ ; *rol-6(su1006)*], *nsEx1680*[ $P_{\text{heat shockttx-1b}}$ ; *rol-6(su1006)*], *nsEx1915/nsEx1916*[ $P_{\text{lin-26ttx-1a}}$ ; *rol-6(su1006)*], *nsEx1948/nsEx1953*[ $P_{\text{ttx-1(AFD)ttx-1a}}$ ; *rol-6(su1006)*]. *glia::Otx* rescuing arrays included: *nsEx1661*[ $P_{\text{F16F9.3Otx1}}$ ; *rol-6(su1006)*], *nsEx1662*[ $P_{\text{F16F9.3Otx2}}$ ; *rol-6(su1006)*]. *ztf-16* rescuing arrays included: *nsEx3001*[ $P_{\text{ztf-16(glia)gfp}}$ ; *rol-6(su1006)*], *nsEx1382/nsEx1389*[ $P_{\text{F16F9.3ztf-16a}}$ ; *rol-6(su1006)*], *nsEx1405/nsEx1410*[ $P_{\text{F16F9.3ztf-16b}}$ ; *rol-6(su1006)*], *nsEx3266*[ $P_{\text{lin-26ztf-16b}}$ ; *rol-6(su1006)*]. *fkh-9* rescuing arrays included: *nsEx1505/nsEx1508*[ $P_{\text{F16F9.3fkh-9a}}$ ; *rol-6(su1006)*], *nsEx1569*[ $P_{\text{F16F9.3fkh-9(31aa)}}$ ; *rol-6(su1006)*], *nsEx1711*[ $P_{\text{F16F9.3Foxg1}}$ ; *rol-6(su1006)*].

## Germline transformation and transgene integration

Germline transformations were carried out using standard protocols (Mello and Fire, 1995). Co-injection markers used were either plasmid pRF4 containing the dominant marker *rol-6(su1006)* (Mello et al., 1991), plasmid pJM23 containing wild-type *lin-15* (Huang et al., 1994), or plasmids as otherwise noted. pSL1180 is an empty cloning vector used to increase the DNA concentration of injection mixtures. *ver-1* promoter::GFP and *ttx-1* rescue transgenes were integrated by treating animals carrying extrachromosomal arrays with UV/psoralen. The generated strains were backcrossed to N2 more than three times.

## Microscopy

*ver-1* promoter::*gfp* (*nsIs22*) expression was assayed using a fluorescence dissecting microscope (Leica). Adult hermaphrodites were scored, except as noted. Compound

microscope images were taken on an Axioplan II microscope using an AxioCam CCD camera (Zeiss) and analyzed using the Axiovision software (Zeiss). Additional images were taken on a Deltavision Image Restoration Microscope (Applied Precision/Olympus) and analyzed using SoftWoRx software (Applied Precision). Dauer animals for electron microscopy were grown at 25°C. These were prepared and sectioned using standard methods (Lundquist et al., 2001). Imaging was performed with an FEI Tecnai G2 Spirit BioTwin transmission electron microscope equipped with a Gatan 4K x 4K digital camera.

### **Mutagenesis and mapping**

L4 animals carrying the *ver-1* promoter::*gfp* transgene (*nsIs22*) in the N2 strain background were mutagenized with 30 mM ethyl methanesulfonate (EMS) for 4 h. Individual P0s were picked to separate 9 cm NGM agar plates with OP50 and cultivated at the relevant temperature. F2 animals were screened. Mapping was performed by crossing to the Hawaiian strain (CB4856), picking mutant F2 progeny and observing linkage to single nucleotide polymorphisms (SNPs) (Wicks et al., 2001).

### **Dauer selection**

Animals were starved and dauers selected by treatment with 1% SDS in M9 solution for 20 min. Alternatively, animals carrying the *daf-7(e1372)* mutation were induced to form dauers by incubation at 25°C.

### **Cytoplasmic mixing assay to score AMsh glia fusion**

Adult animals carrying an *nsEx1391* (AMsh glia::*gfp*) array were picked to plates seeded with OP50 bacteria or bacteria expressing dsRNA, and cultivated at 25°C. From these plates, L1 and L2 progeny carrying the *nsEx1391* array in one of the two AMsh glia were picked 24 h later to fresh seeded plates. Mosaic animals were incubated for 48 h at 25°C before scoring GFP presence in either one or both AMsh glia. Animals carrying a *daf-7(e1372)* mutation were only scored if they were dauer larvae by morphology at the end of the assay period. See Figure 2.2.

### **Thermotaxis assays**

A linear thermal gradient from 18°C to 26°C was established across an aluminium surface using two Peltier feedback devices (Ryu and Samuel, 2002). Staged adult animals cultivated on OP50 bacteria at either 15°C, 20°C, or 25°C were washed in S-basal medium and transferred to the center of a 10-cm square petri dish containing 12 ml of NGM agar. This dish was placed onto the aluminium surface, with a thin layer of glycerol between the dish and aluminium slab to ensure adequate heat conductance. Animals were allowed to disperse for a period of 45 min, fixed with chloroform, and counted across 6 bins, from cold to hot. The center third of the assay plate, including equal areas across all parts of the temperature gradient, was removed from the analysis as some animals did not disperse. 50 to a few hundred worms participated in each assay. Results shown are averages of four independent trials.

## **Chemotaxis assays**

Chemotaxis of adult animals was performed as previously described (Bargmann et al., 1993). A modified protocol was used for chemotaxis of dauer animals (see Appendix 5).

## **Electrophoretic mobility-shift assays (EMSAs)**

For the GST::TTX-1(HD) EMSA, double-stranded probes covering 40 bp of the *ver-1* gene, with the predicted TTX-1 wild type ATTA core binding sequence at the center, were generated by annealing single-stranded, 5' biotin end-labeled oligonucleotides. GST::TTX-1(homeodomain) and GST control protein (from the pGEX-5X-1 empty vector) were induced and purified from BL21(DE3) cells using the Bulk GST Purification Module (GE Healthcare). Binding reactions were performed using the LightShift Chemiluminescent EMSA kit (Pierce). Reaction conditions included 400 ng of TTX-1 homeodomain::GST fusion protein, 1x binding buffer, 2.5% glycerol, 5 mM MgCl<sub>2</sub>, 1 ug poly (dI-dC), 0.05% NP-40, and 20 fmol of biotin-labeled DNA probe. GST control protein was added in excess of 400 ng. In competition reactions, a 200-fold molar excess of unlabeled probe was added (4 pmol). Reactions were performed at 20°C for 20 min, then run on a 6% polyacrylamide DNA retardation gel (Invitrogen) in 0.5x TBE buffer. The reactions were transferred to a positively charged nylon membrane, and the biotin-labeled DNA imaged. EMSAs of GST::ZTF-16(znf2-6) were performed in the same manner, except 800 ng of purified fusion protein and GST control were added to each binding reaction. GST::ZTF-16(znf2-6) was insoluble in *E. coli* when induced at 37°C; therefore, inductions were performed at 20°C.

### **RNAi of *aff-1* and *eff-1***

Plasmids expressing double-stranded RNA (dsRNA) were obtained from the Ahringer library (Fraser et al., 2000). An empty vector was used as the control. RNAi was performed by plating adult *daf-7(e1372); nsEx1391* animals onto bacteria expressing the dsRNA and allowing them to feed (Timmons and Fire, 1998). Early-laid L1 larvae mosaic for the *nsEx1391* array were re-plated onto fresh RNAi plates and scored 48 h later. Both *eff-1* and *aff-1* RNAi treated animals had grossly normal morphology, suggesting that the animals initially develop normally before knockdown of the two genes occurs, or that knockdown is weak.

### **Cell ablations**

AFD was genetically ablated by expressing the *egl-1/BH3*-only cell death gene (Conradt and Horvitz, 1998) using an AFD-specific promoter (*nsEx755*). AFD ablation was determined by loss of expression of an AFD::*gfp* reporter (*oyIs17*). 33% of amphids expressed AFD::*gfp* when carrying *nsEx755*, whereas in a *ced-3(n717)* caspase mutant background, 100% of amphids expressed AFD::*gfp* (both  $n = 100$ ), demonstrating that EGL-1 kills AFD neurons. Laser ablations of AWC were performed as described (Bargmann and Avery, 1995) in L1 larvae expressing YFP in AWC (*oyIs45*). Ablation was confirmed by loss of YFP expression in AWC.

## Statistics

To calculate the significance of *ttx-1* mutant animals showing defects in AWC remodeling by EM, we proceeded as follows. AMsh glia fusion could occur on either the dorsal or ventral side of the animal or both. By cytoplasmic mixing, 50% of *daf-7* mutant dauers fail to exhibit either dorsal or ventral fusion. Thus, if  $Q$  is the frequency of fusion dorsally or ventrally in a dauer population, then  $(1-Q)^2=0.5$ , and  $Q=0.293$ . For any 6 animals without AWC overlap, therefore, the probability,  $P$ , of not having fusion at all is  $P=(1-Q)^{12}=0.707^{12}=0.0156$ . The same values of  $P$  are obtained even if  $Q$  is different between dorsal and ventral sides. Other  $P$  values were obtained using the indicated statistical tests.

## Plasmid construction and isolation of cDNAs

The initial *ver-1* promoter::*gfp* construct (~2 kb upstream promoter through +263 of the *ver-1* gene fused to *gfp*) was a gift of R. Roubin and C. Popovici. Most vector backbones are derived from the pPD vectors (gift of A. Fire). cDNA template was prepared by washing animals from mixed-stage plates and extracting total RNA using TRIzol Reagent (Invitrogen). Poly(A) RNA was purified using the Poly(A) Purist kit (Ambion) and cDNA was generated using SuperScript II Reverse Transcriptase (Invitrogen). For a list of plasmids generated in this work, see Table 6.1.

**Table 6.1. List of plasmids generated in this work (pages 143 to 145)**

Name in text	Plasmid	Promoter	cDNA	Notes
AMsh:: <i>ttx-1b</i>	pCP.1	<i>vap-1</i>	<i>ttx-1b</i>	5 kb <i>vap-1</i> promoter into pPD49.78 at PstI/BamHI, <i>ttx-1b</i> cDNA at BamHI/NcoI.
AMsh:: <i>ttx-1a</i>	pCP.2	<i>vap-1</i>	<i>ttx-1a</i>	5 kb <i>vap-1</i> promoter into pPD49.78 at PstI/BamHI, <i>ttx-1a</i> cDNA at BamHI/NcoI.
AFD:: <i>ttx-1b</i>	pCP.5	<i>gcy-8</i>	<i>ttx-1b</i>	2 kb <i>gcy-8</i> promoter into pPD49.78 at PstI/BamHI, <i>ttx-1b</i> cDNA at BamHI/NcoI.
AFD:: <i>ttx-1a</i>	pCP.6	<i>gcy-8</i>	<i>ttx-1a</i>	2 kb <i>gcy-8</i> promoter into pPD49.78 at PstI/BamHI, <i>ttx-1a</i> cDNA at BamHI/NcoI.
AFD:: <i>egl-1(x2)</i>	pCP.9	<i>gcy-8</i>	<i>egl-1(x2)</i>	2 kb <i>gcy-8</i> promoter into pPD49.78 at PstI/BamHI, <i>egl-1</i> cDNA at BamHI/NcoI. A double insertion of <i>egl-1</i> occurred, both 5' to 3'. <i>egl-1</i> cDNA not as in WormBase, starts at position 46.
	pCP.17	<i>ver-1</i> (-2110 to -1)	<i>nls-gfp</i>	<i>ver-1</i> gene fragment into pPD95.69 at SphI/BamHI
AMsh+PHsh:: <i>ttx-1a</i>	pCP.19	<i>F16F9.3</i>	<i>ttx-1a</i>	2 kb <i>F16F9.3</i> promoter into pPD49.78 at PstI/BamHI, <i>ttx-1a</i> cDNA at BamHI/NcoI.
AMsh+PHsh:: <i>ttx-1b</i>	pCP.20	<i>F16F9.3</i>	<i>ttx-1b</i>	2 kb <i>F16F9.3</i> promoter into pPD49.78 at PstI/BamHI, <i>ttx-1b</i> cDNA at BamHI/NcoI.
glia promoter:: <i>ver-1::gfp</i>	pCP.21	<i>F16F9.3</i>	<i>ver-1::gfp</i>	<i>ver-1</i> cDNA (including first intron) into pPD95.75 at PstI/BamHI. 2 kb <i>F16F9.3</i> promoter into single PstI site.
	pCP.23	<i>F16F9.3</i>		2 kb <i>F16F9.3</i> promoter into pPD49.78 at PstI/BamHI
<i>ttx-1pro1::dsRed</i>	pCP.26	<i>ttx-1</i> (-7482 to +23)	<i>dsRed</i>	Indicated <i>ttx-1</i> promoter fragment into pEP9 (Elliot Perens) at NotI/KpnI.
	pCP.33	<i>ver-1</i> (-2110 to +262; -1 frame)	<i>gfp</i>	<i>ver-1</i> gene fragment into pPD95.75 at PstI/BamHI, -1 frame relative to <i>gfp</i> .
	pCP.34	<i>ver-1</i> (-2110 to +261, -2 frame)	<i>gfp</i>	<i>ver-1</i> gene fragment into pPD95.75 at PstI/BamHI, -2 frame relative to <i>gfp</i> .
	pCP.36	<i>ver-1</i> (+1 to +263)	<i>gfp</i>	<i>ver-1</i> gene fragment into pPD95.75 at PstI/BamHI.
<i>F16F9.3</i> promoter:: <i>gfp</i>	pCP.41	<i>F16F9.3</i>	<i>gfp</i>	2 kb <i>F16F9.3</i> promoter into pPD95.75 at PstI/BamHI.
	pCP.43	<i>ver-1</i> (+130 to +263)	<i>gfp</i>	<i>ver-1</i> gene fragment into pPD95.75 at PstI/BamHI.
glia:: <i>ztf-16b</i>	pCP.50	<i>F16F9.3</i>	<i>ztf-16b</i>	<i>ztf-16b</i> cDNA into pCP.23 at XmaI/NcoI
<i>ttx-1pro2::dsRed</i>	pCP.58	<i>ttx-1</i> (-10965 to -7451) + <i>myo-2</i>	<i>dsRed</i>	Indicated <i>ttx-1</i> promoter fragment into PEP9 (Elliot Perens) at NheI/NotI. To facilitate expression, 160 bp <i>myo-2</i> minimal promoter added at XbaI/KpnI (Okkema et al., 1993). To create <i>ttx-1pro2::gfp</i> , <i>dsRed</i> was replaced by <i>gfp</i> from pPD95.75 at KpnI/ApaI (pMH.28; Max Heiman). When injected, all lines expressed GFP in amphid and phamid socket cells, some also in AMsh and PHsh. Occasionally weak GFP observed other cell types.

glia promoter:: <i>ztf-16b::gfp</i>	pCP.61	<i>F16F9.3</i>	<i>ztf-16b::gfp</i>	<i>F16F9.3</i> promoter inserted into single PstI site of pPD95.75. <i>ztf-16b</i> cDNA inserted XmaI/KpnI in frame with <i>gfp</i> .
glia:: <i>ztf-16a</i>	pCP.62	<i>F16F9.3</i>	<i>ztf-16a</i>	<i>ztf-16a</i> cDNA into pCP.23 at XmaI/NcoI
glia:: <i>fkh-9</i>	pCP.70	<i>F16F9.3</i>	<i>fkh-9a</i>	<i>fkh-9a</i> cDNA into pCP.23 at BamHI/NcoI.
glia promoter:: <i>fkh-9::gfp</i>	pCP.71	<i>F16F9.3</i>	<i>fkh-9a::gfp</i>	<i>fkh-9a</i> cDNA into pCP.41 at BamHI/KpnI.
<i>fkh-9</i> promoter:: <i>gfp</i>	pCP.73	<i>fkh-9</i>	<i>gfp</i>	300 bp upstream plus exon 1 and 6kb intron 1 of the <i>fkh-9</i> gene inserted into pPD95.75 at SalI/SalI. SalI/BamHI and BamHI/AgeI.
glia:: <i>fkh-9(31aa)</i>	pCP.79	<i>F16F9.3</i>	<i>fkh-9(31aa)</i>	A cDNA coding for the first 31 amino acids of FKH-9A into pCP.23 at BamHI/NcoI.
<i>F16F9.3</i> promoter:: <i>dsRed</i>	pCP.81	<i>F16F9.3</i>	<i>dsRed</i>	2 kb <i>F16F9.3</i> promoter into pEP9 (Elliot Perens) at NheI/AgeI.
glia:: <i>his-24</i>	pCP.83	<i>F16F9.3</i>	<i>his-24</i>	<i>his-24</i> cDNA into pCP.23 at XmaI/NheI.
heat shock:: <i>ttx-1a</i>	pCP.94	<i>hsp16.2</i>	<i>ttx-1a</i>	<i>ttx-1a</i> CDNA into pPD49.78 at BamHI/NcoI.
heat shock:: <i>ttx-1b</i>	pCP.95	<i>hsp16.2</i>	<i>ttx-1b</i>	<i>ttx-1b</i> CDNA into pPD49.78 at BamHI/NcoI.
	pCP.98	<i>ver-1 (+57 to +263)</i>	<i>gfp</i>	<i>ver-1</i> gene fragment into pPD95.75 at PstI/BamHI.
	pCP.99	<i>ver-1 (+112 to +263)</i>	<i>gfp</i>	<i>ver-1</i> gene fragment into pPD95.75 at PstI/BamHI.
glia:: <i>Otx1</i>	pCP.100	<i>F16F9.3</i>	<i>Otx1</i>	Mouse <i>Otx1</i> cDNA from Marathon-Ready mouse cDNA (Clontech) into pCP.23 at XmaI/NheI.
glia:: <i>Otx2</i>	pCP.101	<i>F16F9.3</i>	<i>Otx2</i>	Mouse <i>Otx2</i> cDNA from Marathon-Ready mouse cDNA (Clontech) into pCP.23 at XmaI/NheI.
glia:: <i>Foxg1</i>	pCP.106	<i>F16F9.3</i>	<i>Foxg1</i>	Mouse <i>Foxg1</i> cDNA inserted as AfeI/KpnI fragment from MGC 6314329 (I.M.A.G.E. Consortium) into SmaI/KpnI of pCP.23. 3' end of cDNA amplified from mouse cDNA library and inserted at KpnI/SacI.
	pCP.109	<i>ver-1 (+170 to +263)</i>	<i>gfp</i>	<i>ver-1</i> gene fragment into pPD95.75 at PstI/BamHI.
	pCP.110	<i>ver-1 (+201 to +263)</i>	<i>gfp</i>	<i>ver-1</i> gene fragment into pPD95.75 at PstI/BamHI.
embryonic glia:: <i>ttx-1</i>	pCP.111	<i>lin-26 + myo-2</i>	<i>ttx-1a</i>	<i>ttx-1a</i> cDNA inserted into pPD9575lin-26myo-2pro-GFP (gift of Max Heiman) at XmaI/EcoRI
<i>ttx-1</i> (AFD) promoter:: <i>ttx-1</i>	pCP.113	<i>ttx-1</i> (AFD)	<i>ttx-1a</i>	<i>ttx-1a</i> cDNA into pEP9 dsRed vector (Elliot Perens) at KpnI/EcoRI. From this, a KpnI/PvuI fragment was inserted into pCP.26.
	pCP.128		<i>gcy-8</i>	<i>gcy-8</i> cdna into pSL1180 at AflIII/XmaI. This was inserted into pFB-flag to generate GCY-8(FLAG) (Erik Procko).
	pCP.131	<i>ver-1 (+1 to +263; TTX-1 site*)</i>	<i>gfp</i>	Site-directed mutagenesis on pCP.36 to mutate the TTX-1/Otx2 binding site at position +176 from ATTA to GGGG.
	pCP.132	<i>ver-1 (+1 to +132)</i>	<i>gfp</i>	<i>ver-1</i> gene fragment into pPD95.75 at PstI/BamHI.

	pCP.133	<i>ver-1</i> (+1 to +220)	<i>gfp</i>	<i>ver-1</i> gene fragment into pPD95.75 at PstI/BamHI.
	pCP.134	<i>ver-1</i> (+1 to +201)	<i>gfp</i>	<i>ver-1</i> gene fragment into pPD95.75 at PstI/BamHI.
GCY-23(FLAG)	pCP.136		<i>gcy-23(flag)</i>	<i>gcy-23</i> cDNA into pFB-flag (from Erik Procko) as NdeI/NdeI and NdeI/NotI fragments.
GCY-28A(FLAG)	pCP.141		<i>gcy-28a(flag)</i>	<i>gcy-28a</i> cDNA into pFB-flag as NdeI/NdeI and NdeI/NotI fragments. A single codon difference is observed compared to the predicted WormBase sequence (removal of Q464).
GST::TTX-1(HD)	pCP.142		<i>GST::ttx-1(hd)</i>	The <i>ttx-1</i> homeodomain was inserted into pGEX 5X-1 at BamHI/XhoI. This construct removes the first 154 and last 95 amino acids of the TTX-1A protein.
<i>F58F9.10</i> promoter:: <i>gfp</i>	pCP.145	<i>F58F9.10</i>	<i>gfp</i>	2 kb <i>F58F9.10</i> promoter into pPD95.75 at SphI/BamHI.
<i>old-2</i> promoter:: <i>gfp</i>	pCP.149	<i>old-2</i>	<i>gfp</i>	2 kb <i>old-2</i> promoter into pPD95.75 at SphI/XmaI
<i>old-1</i> promoter:: <i>gfp</i>	pCP.151	<i>old-1</i>	<i>gfp</i>	2 kb <i>old-1</i> promoter into pPD95.75 at BamHI/KpnI
<i>F58F9.6</i> promoter:: <i>gfp</i>	pCP.154	<i>F58F9.6</i>	<i>gfp</i>	4 kb <i>F58f9.6</i> promoter inserted into pPD95.75 at BamHI/AgeI as a BamHI/XmaI fragment
	pCP.158	<i>T02B11.3</i>		2.5 kb <i>T02B11.3</i> promoter into pPD49.78 at PstI/BamHI.
<i>glia::ttx-1</i>	pCP.161	<i>T02B11.3</i>	<i>ttx-1a</i>	2.5 kb <i>T02B11.3</i> promoter into pPD49.78 at PstI/BamHI, <i>ttx-1a</i> cDNA from pCP.2 at BamHI/SpeI.
<i>ver-1</i> promoter:: <i>ver-1</i>	pCP.167	<i>ver-1</i>	<i>ver-1</i>	<i>ver-1</i> cDNA, including intron 1 (remainder fully spliced), into pPD49.78 at BamHI/NcoI; a silent A to G mutation at position 924 of the fragment exists. 2.1 kb <i>ver-1</i> upstream promoter inserted at SphI/BamHI.
<i>T02B11.3</i> promoter:: <i>gfp</i>	pCP.169	<i>T02B11.3</i>	<i>gfp</i>	2.5 kb <i>T02B11.3</i> promoter into pPD95.75 at SphI/BamHI.
<i>glia</i> promoter:: <i>eff-1::gfp</i>	pCP.179	<i>F16F9.3</i>	<i>eff-1a::gfp</i>	<i>eff-1a</i> cDNA into pCP.41 at XmaI/KpnI
<i>glia</i> promoter:: <i>aff-1::gfp</i>	pCP.186	<i>F16F9.3</i>	<i>aff-1::gfp</i>	<i>aff-1</i> cDNA into pCP.41 at XmaI/KpnI.
<i>glia::ztf-16</i>	pCP.191	<i>T02B11.3</i>	<i>ztf-16b</i>	<i>ztf-16b</i> cDNA into pCP.158 at XmaI/SacI
<i>ztf-16</i> promoter:: <i>gfp</i>	pCP.192	<i>ztf-16</i> (-4637 to -2536)	<i>gfp</i>	<i>ztf-16</i> promoter region into pPD95.75 at SphI/KpnI
	pCP.36	<i>ver-1</i> (+1 to +263; Hb site*)	<i>gfp</i>	Site-directed mutagenesis on pCP.36 to mutate the Hunchback-like site at position +217 from CATGAAAC to ggcccAAC.
GST::ZTF-16(znf2-6)	pCP.198		<i>GST::ztf-16(znf2-6)</i>	<i>ztf-16</i> cDNA fragment coding for C2H2 zinc fingers 2-6 inserted into pGEX 5X-1 at XmaI/XhoI.
embryonic <i>glia::ztf-16b</i>	pCP.204	<i>lin-26</i> + <i>myo-2</i>	<i>ztf-16b</i>	<i>lin-26</i> + <i>myo-2</i> promoter from pPD9575lin-26myo-2pro-GFP (gift of Max Heiman) was inserted into pCP.50 at SphI/XmaI.

# Appendices

## **Appendix 1: Attempted rescue of the AMsh glia fusion defect of *ver-1* mutants**

Attempts were made to rescue the AMsh glia fusion defect of *ver-1(tm1348)* mutant dauers. The predicted *ver-1* cDNA was isolated (WormBase release WS224), and integrated transgenes expressing the *ver-1* cDNA from its own promoter (2 kb upstream and intron 1; see Table 3.1) were generated. These transgenes failed to rescue the fusion defect of *ver-1(tm1348); daf-7(e1372)* dauer animals as assayed by cytoplasmic mixing (Table A1.1). Indeed, the percentage of dauers with fused AMsh glia appeared even smaller than the *ver-1* mutant alone. As such, the transgenes may be inhibiting fusion, perhaps by expressing inappropriate levels of *ver-1* or an incorrect or misfolded *ver-1* protein. Furthermore, it is possible that the *ver-1* promoter::*ver-1* transgene acts to inhibit AMsh glia fusion by sequestering factors such as TTX-1 away from other genes that are also required for fusion. In support of such possibilities, these same *ver-1* promoter::*ver-1* transgenes significantly reduced AMsh glia fusion in *daf-7(e1372)* dauers wild-type for *ver-1* (Table A1.1).

In addition, we have not been able to ascertain if the *ver-1* cDNA we have isolated is fully functional. For example, a VER-1::GFP translational fusion protein generated from this cDNA and expressed specifically in the glia localized to puncta throughout the cell body and glial process (Figure A1.1). This could represent activated and internalized VER-1 signaling complexes (Rosette and Karin, 1996), or may indicate that the protein is misfolded.

**Table A1.1. Attempted rescue of the AMsh glia fusion defect of *ver-1(tm1348)* mutant dauer animals.**

<b>Genotype<sup>a</sup></b>	<b>% dauers with fused AMsh glia<sup>b</sup></b>
<i>ver-1(tm1348)</i>	10% ( <i>n</i> = 154)
+ <i>nsIs204</i> ( <i>ver-1</i> promoter:: <i>ver-1</i> )	1% ( <i>n</i> = 135)
+ <i>nsIs205</i> ( <i>ver-1</i> promoter:: <i>ver-1</i> )	0% ( <i>n</i> = 115)
+ <i>nsIs208</i> ( <i>ver-1</i> promoter:: <i>ver-1</i> )	1% ( <i>n</i> = 72)
+ <i>nsIs211</i> ( <i>ver-1</i> promoter:: <i>ver-1</i> )	6% ( <i>n</i> = 80)
+ <i>nsIs213</i> ( <i>ver-1</i> promoter:: <i>ver-1</i> )	3% ( <i>n</i> = 128)
+ <i>nsEx3162</i> ( <i>ver-1</i> gDNA) <sup>c</sup>	2% ( <i>n</i> = 65)
+ <i>nsEx3171</i> ( <i>ver-1</i> gDNA) <sup>c</sup>	6% ( <i>n</i> = 82)
wild type	51% ( <i>n</i> = 269)
+ <i>nsIs205</i> ( <i>ver-1</i> promoter:: <i>ver-1</i> )	3% ( <i>n</i> = 109)
+ <i>nsIs211</i> ( <i>ver-1</i> promoter:: <i>ver-1</i> )	4% ( <i>n</i> = 156)
+ <i>nsIs213</i> ( <i>ver-1</i> promoter:: <i>ver-1</i> )	6% ( <i>n</i> = 101)

<sup>a</sup>All strains also include *daf-7(e1372)*, and are selected for larval mosaic expression of an AMsh glia::*gfp* reporter (*nsEx1391*) in one of the two glial cells.

<sup>b</sup>AMsh glia fusion was determined by cytoplasmic mixing assay.

<sup>c</sup>Fosmid WRM0636cD01 was used for *ver-1* gDNA.

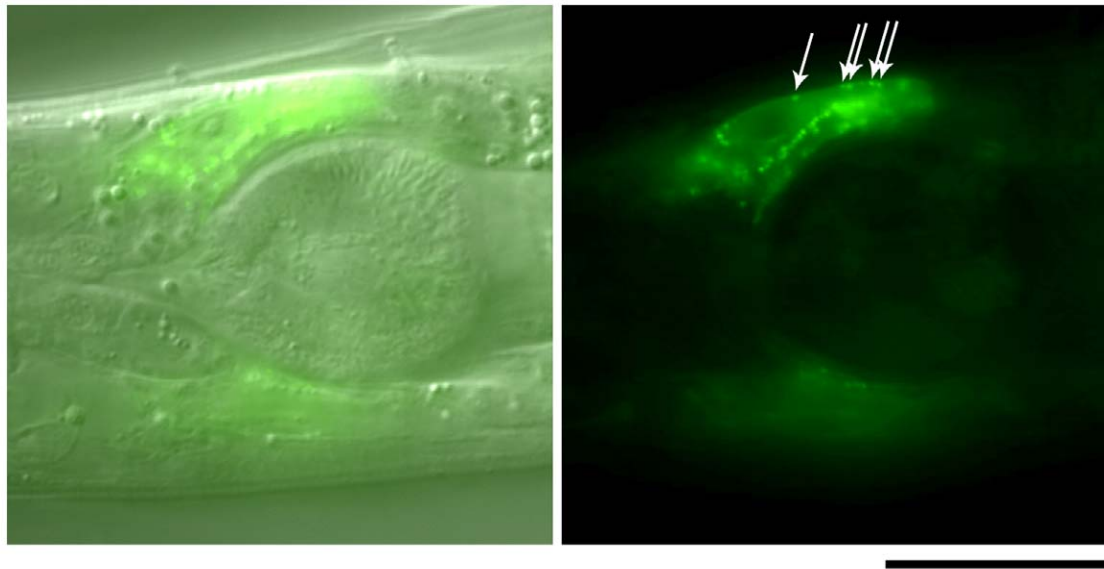


**Figure A1.1. VER-1::GFP localizes as puncta.** Representative DIC and fluorescence merged image (left) and fluorescence only image (right) of an animal expressing a VER-1::GFP fusion protein specifically in the AMsh glia (*nsEx962*). Arrows indicate examples of punctal localization of the fusion protein. Scale bar, 20  $\mu$ m. Anterior is left.

In an additional experiment to rescue the fusion defect of *ver-1(tm1348)* mutants, we generated lines carrying wild-type *ver-1* genomic DNA (gDNA; fosmid WRM0636cD01). We predict that these lines have no bias towards any particular *ver-1* splice form. Two lines were generated carrying the gDNA as an extrachromosomal array and were scored for AMsh glia fusion by cytoplasmic mixing. Specifically, mosaic first- and second-stage *daf-7(e1372); ver-1(tm1348)* larvae carrying an AMsh::*gfp* array in just one of the two AMsh glia (*nsEx1391*), in addition to carrying the *ver-1* gDNA rescuing array, were picked and induced to form dauers at 25°C. This method assumes that the two extrachromosomal arrays (*nsEx1391* and the *ver-1* rescue array) segregate independently from one another, such that *nsEx1391* mosaic animals are unlikely to also be mosaic for the *ver-1* gDNA-containing array. In this experiment, we again observed no rescue of AMsh glia fusion (Table A1.1), either due to incorrect copy number of the *ver-1* gene, sequestration of TTX-1 and other transcriptional regulators away from other genes, or non-independent segregation of the two arrays in the AMsh glia. Therefore, although the *ver-1* expression pattern and the mutant analysis of *ver-1* and its transcriptional regulators *ttx-1* and *ztf-16* are highly suggestive that *ver-1* is required for AMsh glia fusion in dauer animals, we have been unable to ascertain this with complete certainty.

## **Appendix 2: The guanylyl cyclases GCY-8 and GCY-23 are not directly activated by temperature**

cDNAs for the AFD-expressed guanylyl cyclases (GCYs) *gcy-8* and *gcy-23* (Inada et al., 2006) were PCR amplified and ligated into expression vectors (see Chapter 6). The expression constructs included a carboxy-terminal FLAG tag. An attempt was made to clone another AFD-expressed GCY protein, *gcy-18*; however, all *gcy-18* clones isolated contained PCR-induced mutations, and attempts to piece together wild-type sequences were unsuccessful, suggesting the cDNA may be lethal in *E. coli*.

In collaboration with Erik Procko and Rachele Gaudet (Department of Molecular and Cellular Biology, Harvard University, Cambridge MA), Sf21 insect cells were infected with baculoviruses encoding the FLAG-tagged GCY proteins and measured directly for cGMP levels by immunoassay. Briefly, Sf21 cells were infected at a density of  $1 \times 10^6$  cells/ml and harvested 48 h later (Figure A2.1A). The cells were resuspended in fresh media (Supplemented Grace's Medium with 10% fetal bovine serum, 0.1% pluronic F-68 polyol and 10 ug/ml gentamicin sulfate) to a density of  $2 \times 10^6$  cells/ml and incubated on ice for 30 min. Pentoxifylline (1.5 mM) and MnCl<sub>2</sub> (4 mM) were added, and the cells were incubated at the indicated temperatures for 30 min (Figure A2.1B). The reactions were stopped by addition of HCl to 0.1 M, and the cells lysed by addition of Triton X-100 to 0.67% and freeze-thawing. Cell debris was removed by centrifugation and the supernatant analyzed by an enzyme immunoassay for cGMP according to the manufacturer's directions (Assay Designs). The GCY-8 and GCY-23 proteins had no activity over a temperature range of 12-33°C, while a non-AFD expressed control GCY, GCY-28A, had relatively constant activity over the temperature range at which *C.*

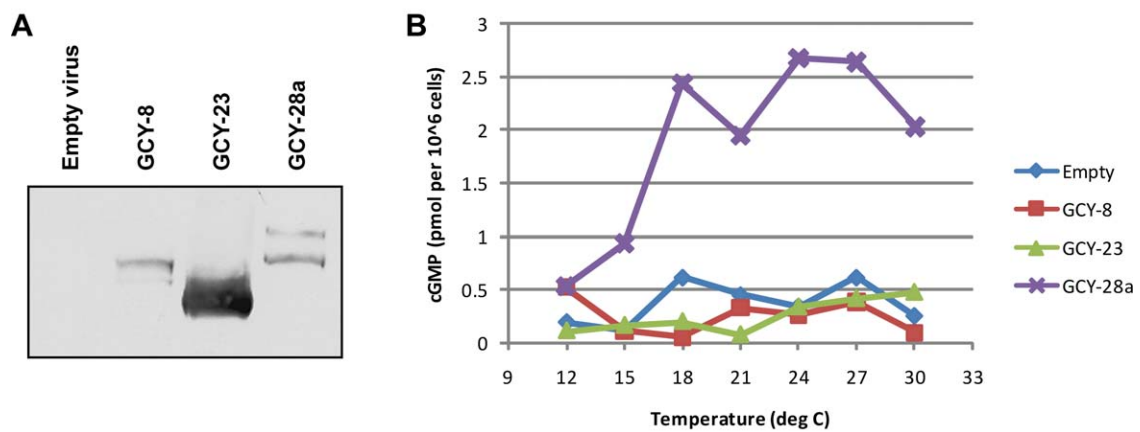


**Figure A2.1. GCY-8 and GCY-23 are not directly activated by temperature. (A)** Anti-FLAG Western blot of Sf21 insect cells infected with baculoviruses encoding the indicated GCY proteins with carboxy-terminal FLAG tags. **(B)** cGMP levels of GCY-8, GCY-23 and GCY-28A infected cells when cultivated at 12-30°C.

*elegans* are cultivated (18-27°C) (Figure A2.1B). Co-infection with both *gcy-8* and *gcy-23* expression constructs also had no effect (data not shown).

### Appendix 3: Null alleles of *ttx-1* may be lethal

The allele predicted to have the strongest mutation in the *ttx-1* gene isolated in our mutant screens was *ns260*, which codes for a deletion of exon 6, removing the DNA-binding domain. Animals heterozygous for the *ns260* allele had low *ver-1 promoter::gfp* expression (Figure A3.1). By contrast, *ns260* homozygosity was lethal. A significant number of eggs laid by *ns260* heterozygous parents (also carrying a *ver-1 promoter::gfp* transgene; *nsIs22*) failed to hatch (data not shown). All viable progeny were either homozygous for the wild-type *ttx-1* allele and expressed wild-type levels of *ver-1 promoter::gfp*, or were *ns260/+* heterozygous and expressed low *gfp* (Figure A3.2A). There was no difference between animals grown at 15°C or 25°C, indicating that the phenotype is not temperature-dependent (Figure A3.2A).

We were unable to rescue *ttx-1(ns260)* lethality using either glial or AFD-specific promoters (Figures A3.2B,C), suggesting that *ttx-1* may be acting in additional cells early in development. Alternatively, the lethality phenotype may result from a linked mutation in an unrelated gene. *ttx-1(ns260)/ttx-1(oy26ts)* transheterozygous animals were viable, although the percentage of transheterozygous progeny derived from a *ns260/oy26ts* parent grown at 25°C (the *oy26* non-permissive temperature) was slightly reduced compared to animals grown at 15°C (at 15°C 59% of progeny are *oy26/ns260*,  $n = 29$ ; whereas at 25°C 40% of progeny are *oy26/ns260*,  $n = 94$ ;  $P = 0.0927$ ,  $\chi^2$  test).

In addition, we noticed that animals homozygous for the *ttx-1* allele *ns259* (and carrying the *nsIs22* transgene) were viable but sterile. This allele, like *ns260*, had a dominant effect on *ver-1 promoter::gfp* expression (data not shown). Individual animals were genotyped by sequencing reactions. 7 out of 68 progeny from an *ns259/+*

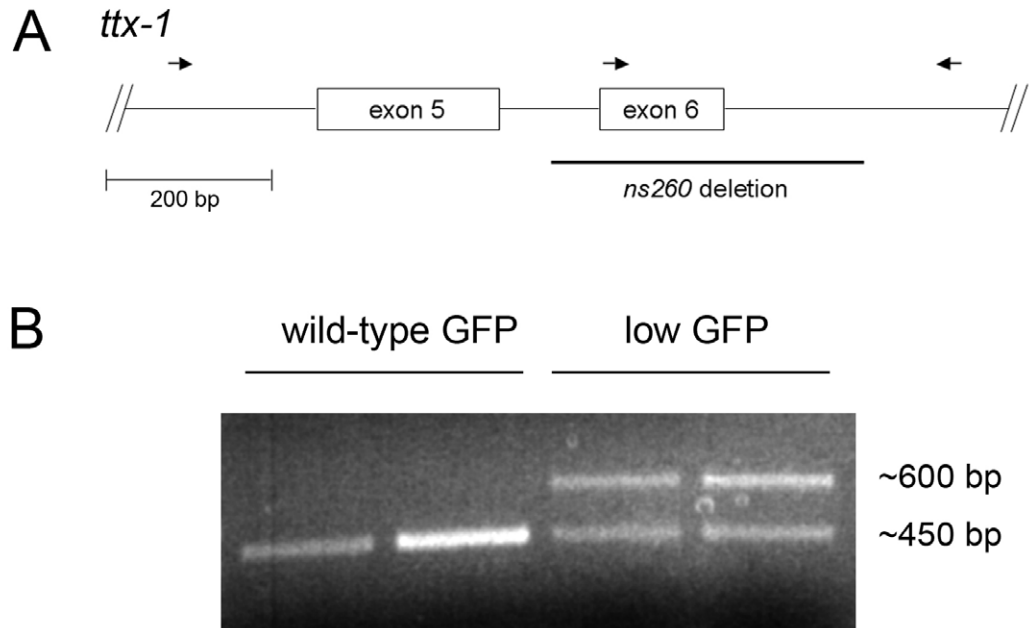


**Figure A3.1. *ttx-1(ns260)* heterozygous animals express low *ver-1* promoter::*gfp*.** (A) Schematic of the *ttx-1* gene, showing only exons 5 and 6 (boxes). The *ns260* deletion is marked. The location of the three oligonucleotide primers used to genotype individual animals (see part B) are indicated by arrows (5' to 3'). (B) Genotyping of four individual progeny from an *ns260/+* heterozygous parent grown at 25°C and carrying a *ver-1* promoter::*gfp* transgene (*nsIs22*). Two of these animals had wild-type levels of *gfp* expression (left), while the other two had low levels (right). Primers used in the PCR assay are shown in (A). Wild-type animals exhibit a single amplified DNA fragment of ~450 bp (a faint ~1 kb-sized band is sometimes also observed) (data not shown). *ns260* homozygous animals are predicted to produce only a single DNA band of size ~600 bp.

**Figure A3.2. Glial and AFD-specific expression of *ttx-1* cDNA fail to rescue *ns260* lethality.** (A) Genotyping of viable progeny from *ns260/+* heterozygous parents grown at either 15°C or 25°C. Wild type, +/+; *ns260* heterozygous, +/-; and *ns260* homozygous, -/-. All animals also carry a *ver-1* promoter::*gfp* transgene (*nsIs22*), and levels of *gfp* expression in the sheath glia in each individual animal were scored as either high, low, or not determined. The number of progeny examined (*n*) is indicated. (B) Same as (A), except the progeny also carry extrachromosomal arrays restoring *ttx-1* expression in the AMsh glia. Cell-specific promoters driving *ttx-1* cDNA include the *F16F9.3* promoter (late embryo to adult expression) and the *lin-26* promoter (embryonic expression only). Two different rescuing arrays using each promoter were scored, and are indicated. (C) Same as (B), except using AFD-specific *gcy-8* and *ttx-1* promoters. In (B,C), the *ttx-1a* splice form was used. In all lines shown in (A,B,C), viable *ns260* homozygous animals (-/-) were never observed.

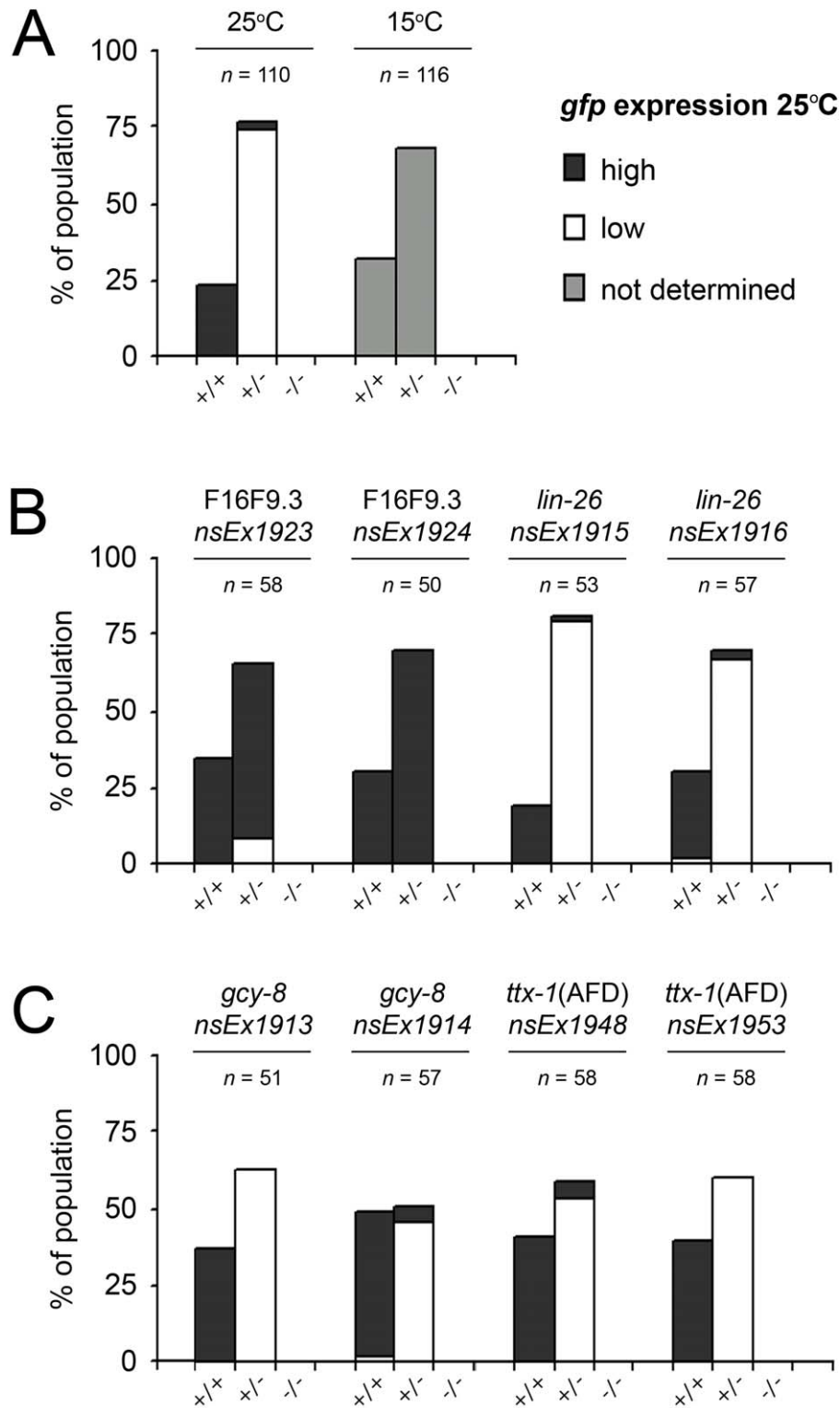


**Figure A3.2. Glial and AFD-specific expression of *ttx-1* cDNA fail to rescue *ns260* lethality.**

heterozygous parent grown at 25°C were *ns259* homozygous, of which all 7 were sterile (no eggs laid). At 15°C, 6 out of 65 progeny were *ns259* homozygous and sterile. In a separate experiment, sterile *ns259* homozygous animals were selected and observed to express a *F16F9.3* promoter::*dsRed* transgene in the AMsh glia ( $n = 16$ ; data not shown), indicating that the sterility phenotype is not due to a loss of the glia. In all experiments, a *ver-1* promoter::*gfp* transgene (*nsIs22*) was included in the strain background to facilitate following of the allele. These results further support a role for *ttx-1* in other developmental processes.

## **Appendix 4: *fkh-9* may set a baseline for glial *ver-1* promoter::*gfp* expression**

To find other molecules required for *ver-1* expression, we screened for mutants with inappropriately high *ver-1* promoter::*gfp* activity in the AMsh and PHsh glia. 4th-stage larvae carrying the reporter (*nsIs22*) were treated for 4 h with ethyl methanesulfonate (EMS). Single mutagenized P0s were picked to individual plates, and from these > 50,000 non-dauer F2 progeny were screened for increased GFP expression at either 15°C or 25°C. A total of 23 alleles were isolated.

One of these alleles, *ns198*, had increased *ver-1* promoter::*gfp* expression in both AMsh and PHsh glia at both 15°C and 25°C; however, strong temperature-dependence of the reporter was still observed (Figure A4.1). *ns198* had a dominant effect on *ver-1* expression (Table A4.1; compare *ns198/+* to wild type), indicating that either dosage of the gene is important or that the mutation may be a gain of function. The effect of *ns198* on AMsh glia transcription may have some specificity, as another sheath cell reporter (*vap-1* promoter::*dsRed*) did not appear dramatically different in *ns198* mutants than wild-type animals (Figure A4.2). Unlike *ttx-1* mutants, *ns198* mutants had wild-type thermotaxis behavior (Figure A4.3) and AFD sensory ending morphology ( $n = 50$ ; data not shown), suggesting that *fkh-9* does not affect AFD function.

Single nucleotide polymorphism (SNP) mapping techniques against the Hawaiian strain background (Wicks et al., 2001) were used to map the *ns198* mutation to an interval ~200 kb in length on chromosome X, between polymorphisms on cosmid C01C4 (base 322) and F47F2 (base 21021), a map distance of 0.57 m.u. 31 genes were

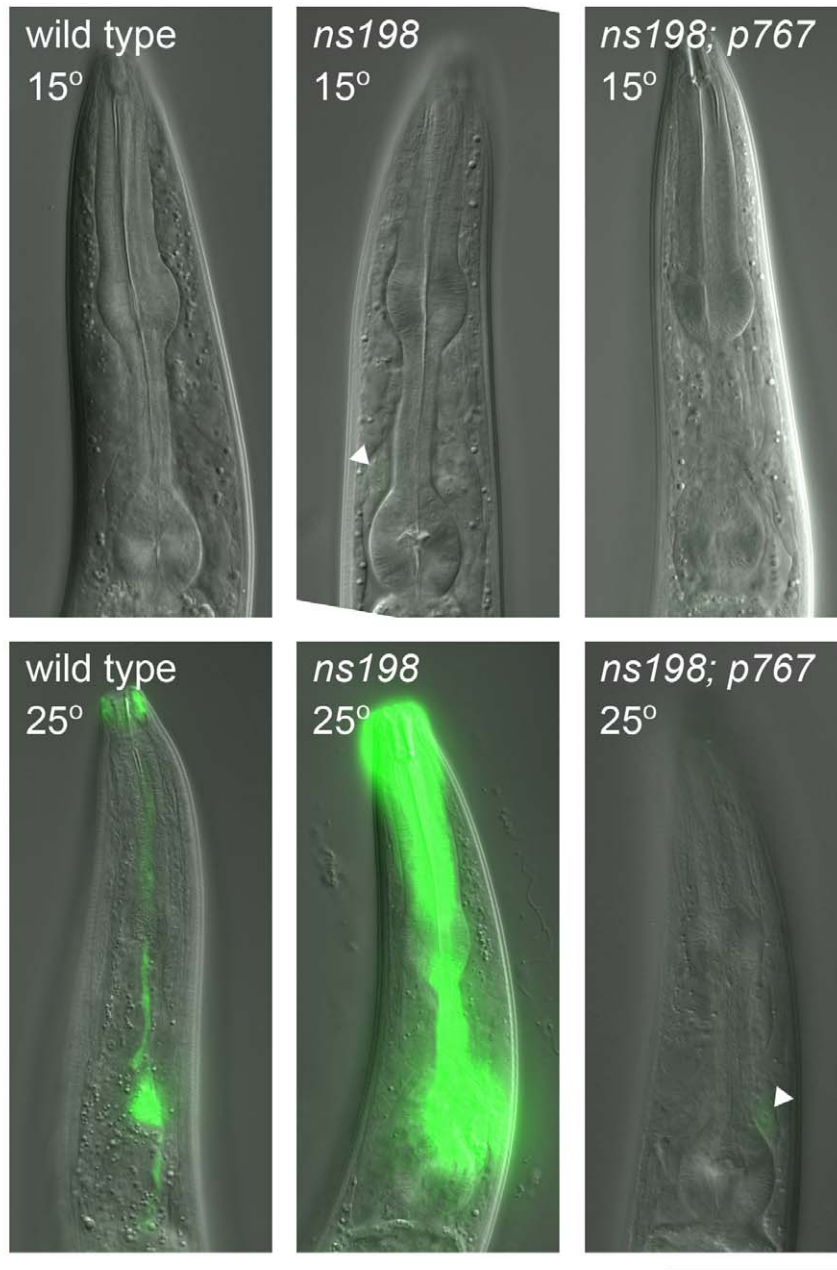


**Figure A4.1.** *ns198* mutants have increased *ver-1* promoter::*gfp* reporter intensity. Representative DIC and fluorescence merged images of wild type (left), *ns198* mutant (center), and *ns198; ttx-1(p767)* double mutant (right) adult animals carrying a *ver-1* promoter::*gfp* transgene (*nsIs22*) at 15°C (top) and 25°C (below). Arrowheads, weak GFP. In all images, anterior is up. GFP exposure, 400 ms. Scale bar, 50  $\mu$ m.

**Table A4.1. Mutations in the *fkh-9* gene increase *ver-1* promoter::*gfp* expression.**

Genotype <sup>a</sup>	<i>ver-1</i> expression adults 15°C			<i>ver-1</i> expression adults 25°C		
	% PHsh on	% AMsh on	n	% PHsh on	% AMsh on	n
wild type	8	0	40	100	95	40
<i>fkh-9(ns198)</i>	98	73	40	100	100 (high) <sup>b</sup>	40
<i>fkh-9(ns198)/+<sup>c</sup></i>	88	n.d.	40	100	100 (high) <sup>b</sup>	40
wild type; glia:: <i>fkh-9(31aa)</i> <sup>d</sup>	0	0	40	100	88	40
<i>fkh-9(ns168)</i>	20	0	40	100	100 (high) <sup>b</sup>	40
<i>fkh-9(ns177)</i>	100	85	40	100	100 (high) <sup>b</sup>	40
<i>fkh-9(ns181)</i>	98	70	40	100	100 (high) <sup>b</sup>	40
<i>fkh-9(ns182)</i>	98	55	40	100	100 (high) <sup>b</sup>	40
<i>fkh-9(ns242)</i>	98	65	40	100	100 (high) <sup>b</sup>	40
<i>fkh-9(ns243)</i>	90	45	40	100	100 (high) <sup>b</sup>	40
<i>fkh-9(ns261)</i>	100	70	40	100	100 (high) <sup>b</sup>	40
wild type; glia:: <i>fkh-9a</i>	0	0	40	85	18	40
<i>fkh-9(ns198)</i> ; glia:: <i>fkh-9a</i>	75	40	40	88	20	40
<i>fkh-9(ns198)</i> ; glia:: <i>Foxg1</i>	88	75	40	100	100 (high) <sup>b</sup>	40
<i>ttx-1(p767)</i>	0	0	40	0	0	40
<i>ttx-1(oy26)</i>	0	0	40	0	3	40
<i>ttx-1(p767)</i> ; <i>fkh-9(ns198)</i>	5	0	40	23 (low) <sup>e</sup>	80 (low) <sup>e</sup>	40
<i>ttx-1(oy26)</i> ; <i>fkh-9(ns198)</i>	98	75	40	48	100	40

<sup>a</sup>All strains contained the *ver-1* promoter::*gfp* transgene (*ns1s22*).

<sup>b</sup>All *fkh-9* mutants had increased intensity of GFP fluorescence at 25°C compared to wild type (noted as “high”). This difference in intensity was most dramatic in the AMsh glia. See Figure A4.1.

<sup>c</sup>The heterozygous genotype was confirmed by crossing *ns198* mutant hermaphrodites to males carrying a neuronal *gfp* reporter (*oy1s17*), and scoring only the progeny that carried the reporter. This reporter obscured the AMsh glia at 15°C (n.d., not determined). This result shows that *ns198* has a dominant effect on *ver-1* promoter::*gfp* expression.

<sup>d</sup>The glia promoter used to drive rescue constructs was *F16F9.3* (Bacaj et al., 2008). The 31aa form of *fkh-9* represents a truncated form of the *fkh-9a* splice form that codes for only the first 31 amino acids of the protein, representing the *ns198* mutation. The fact that this fails to increase *ver-1* promoter::*gfp* expression suggests that *ns198* is a loss of function allele, and that gene dosage of *fkh-9* is therefore important.

<sup>e</sup>*fkh-9(ns198)*; *ttx-1(p767)* double mutants had a greatly reduced intensity of GFP compared to either wild type or *fkh-9(ns198)* single mutants at 25°C (noted as “low”). See Figure A4.1.

Transgenes were injected at 60 ng/μl of rescuing plasmid, with 60 ng/μl of pRF4. Lines shown are *nsEx1569*, *nsEx1508*, *nsEx1505* and *nsEx1711*, and are representative of others.

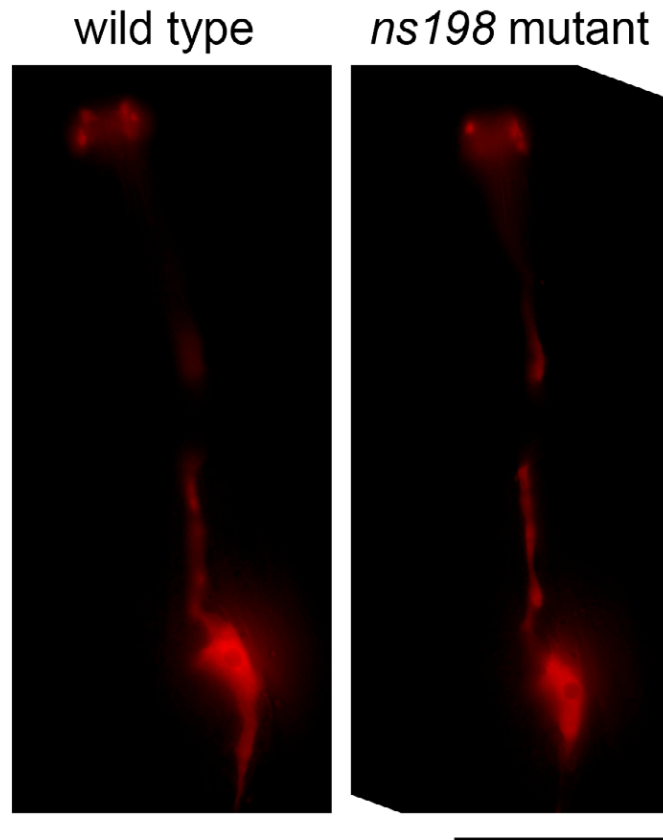


**Figure A4.2. *ns198* does not affect *vap-1* promoter::*dsRed* expression in AMsh glia.** Representative fluorescence images of *vap-1* promoter::*dsRed* (*nsIs53*) expression within an AMsh glial cell at 20°C in wild-type and *ns198* mutant adults. Exposure time, 250 ms; scale bar, 50  $\mu$ m; anterior is up.

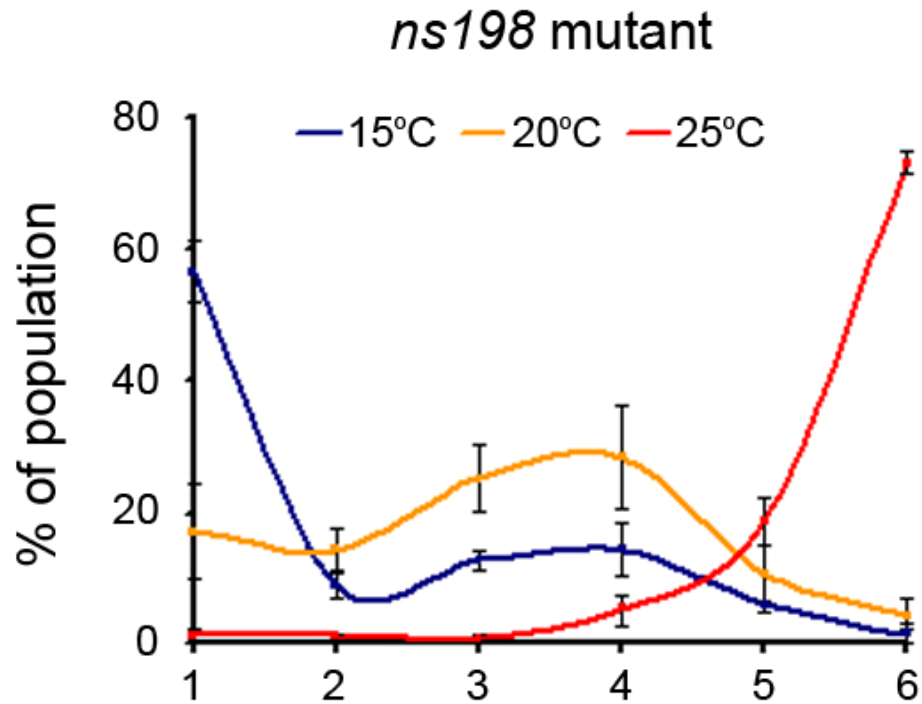


**Figure A4.3. *ns198* mutants have wild-type thermotaxis behavior.** Thermotaxis of *ns198* mutants. Animals were cultivated at 15°C (blue), 20°C (yellow) or 25°C (red) prior to performing each assay (see Chapters 1 and 6). The linear temperature gradient is represented by bins 1-6 on the horizontal axis, from cold (~18°C) to hot (~26°C). All values are mean +/- s.d. Animals also carry the *ver-1* promoter::*gfp* transgene (*nsIs22*).

annotated in this region (WormBase release WS224), and the coding regions of candidate genes were sequenced. We identified a point mutation causing a premature stop mutation in the coding sequence of the putative transcription factor *fkh-9*. The other mutant alleles isolated with increased *ver-1* promoter::*gfp* expression were also sequenced, and an additional 7 alleles of *fkh-9* were found (Figure A4.4). Each of these alleles caused an increase of *gfp* expression at low and high temperatures (Table A4.1), suggesting that *fkh-9* likely sets a baseline for *ver-1* promoter::*gfp* expression.

*fkh-9* codes for a putative winged helix/forkhead domain transcription factor of unknown function. Interestingly, the closest-related mammalian protein to FKH-9, Foxg1 (46% identity over the winged helix DNA-binding domain), has roles in anterior brain development (Xuan et al., 1995), similar to orthologues of TTX-1 (Acampora et al., 1996; Rhinn et al., 1998). However, murine *Foxg1* was unable to rescue *fkh-9* mutants [I.M.A.G.E. Consortium clone ID 6314329 (Lennon et al., 1996)], suggesting some divergence of function between these proteins (Table A4.1).

Five of the *fkh-9* alleles code for premature stop mutations, suggesting they are loss of function alleles (Figure A4.4). Alternatively, the truncated proteins could be gain of function alleles, which may explain the dominant phenotype of *fkh-9* mutations on *ver-1* promoter::*gfp* expression. However, over-expressing a truncated form of the *fkh-9* cDNA coding for only the first 31 amino acids, equivalent to the *ns198* allele, did not reproduce the mutant phenotype (Table A4.1). This suggests that the mutations are loss of function and that dosage of the *fkh-9* gene is important.

The other *fkh-9* alleles isolated, *ns168*, *ns182* and *ns243*, are missense mutations within the putative winged helix DNA-binding domain (Figure A4.4). This suggests that

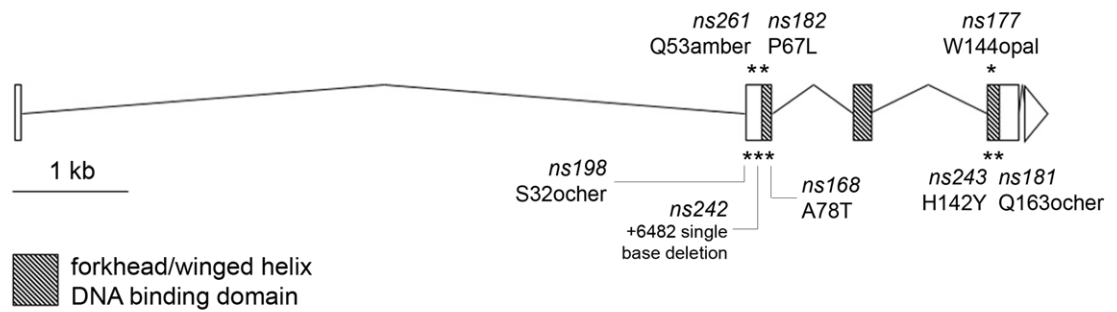


**Figure A4.4. Mutations in *fkh-9* increase *ver-1* promoter::*gfp* expression.** A schematic of the predicted *fkh-9* gene; exons are indicated by boxes, introns as connecting lines. The forkhead/winged helix domain is shown. The location of the genetic lesion in alleles *ns177*, *ns181*, *ns182*, *ns198*, *ns242*, *ns243*, *ns261*, and *ns168* are marked (\*), as is the corresponding amino acid change in the FKH-9A protein. Premature stop mutations are indicated by amber, ocher or opal. Allele *ns242* codes for a single base deletion, causing a frame-shift and premature stop.

FKH-9 acts as a transcription factor. Consistent with this, a cDNA coding for the longest-length splice form of the gene predicted by WormBase (release WS224), the *a* form, was isolated, and a FKH-9A::GFP fusion protein expressed specifically in the AMsh glia was nuclear localized (Figure A4.5A). In addition, the cDNA of a predicted splice form of *fkh-9* which lacks the DNA binding domain, *fkh-9c* (WormBase release WS224), failed to rescue the mutant phenotype (data not shown).

To test in which cell types *fkh-9* may be expressed, we generated a *fkh-9* promoter::*gfp* reporter, including 300 bp of *fkh-9* upstream promoter followed by ~6.2 kb through to the end of intron 1. This construct gave GFP expression in many cell types as previously reported (Hope et al., 2003), including the AMsh and PHsh glia (Figure A4.5B; and data not shown). This implies that *fkh-9* likely functions cell autonomously within the glia to regulate *ver-1* expression. We verified this by expressing wild type *fkh-9a* cDNA under a sheath cell promoter. This construct rescued the *fkh-9* mutant phenotype and caused a decrease of *ver-1* promoter::*gfp* expression in wild-type animals (Table A4.1), consistent with dosage of the gene being important.

Furthermore, we found that mutations in *fkh-9* affected the minimal interval of the *ver-1* promoter required for glia-specific and temperature- and dauer-dependent expression identified in Chapter 2 (data not shown). This was the same interval acted upon by *ttx-1*. In addition, the increased expression of *ver-1* promoter::*gfp* observed in *fkh-9* mutants required functional *ttx-1*. Specifically, in *fkh-9(ns198); ttx-1(p767)* double mutants, *ver-1* promoter::*gfp* expression in adults was almost completely absent (Figure A4.1; Table A4.1). The *fkh-9(ns198); ttx-1(oy26)* double mutant had reduced *gfp* expression in adults raised at 25°C but not at 15°C, further evidence that *oy26* is a

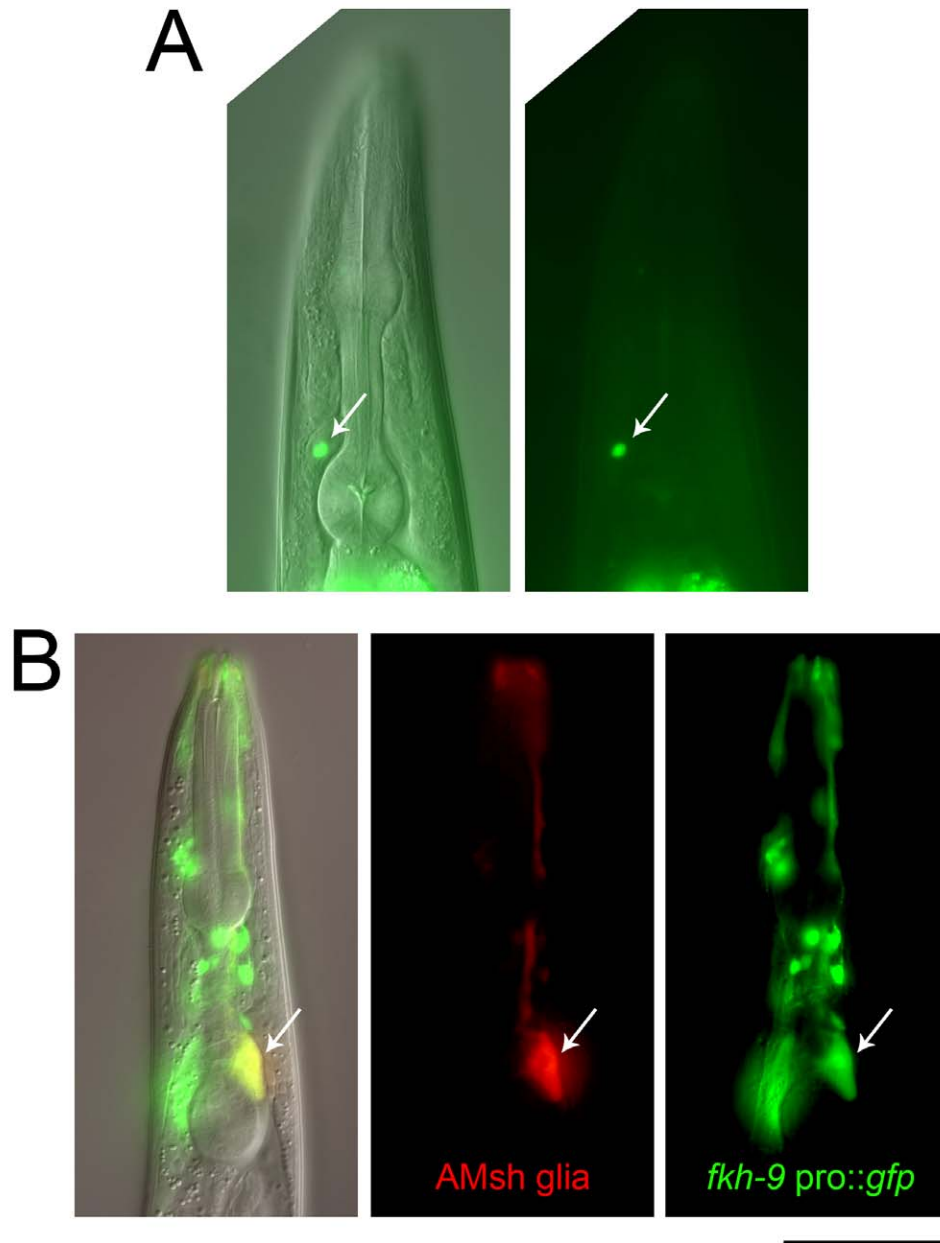


**Figure A4.5. *fkh-9* is a glia-expressed nuclear factor.** (A) DIC and fluorescence merged (left) and fluorescence (right) image of a wild-type adult animal expressing a FKH-9A::GFP fusion protein specifically in the AMsh glia (*nsEx1517*). Note nuclear localization (arrow). (B) DIC and fluorescence merged (left), DsRed fluorescence (center) and GFP fluorescence (right) image of an adult wild-type animal carrying a *fkh-9* promoter::*gfp* reporter (*nsEx1526*) and AMsh glia::*dsRed* marker (*nsIs53*). Note AMsh glia expression (arrow). In all images, anterior is up; scale bar, 50  $\mu$ m.

temperature sensitive allele (Table A4.1; see Chapter 3). Similarly, a mutation in *fkh-9* failed to suppress the loss of *ver-1* promoter::*gfp* expression in *ztf-16* mutant dauers (*ztf-16(ns171)* mutants never expressed GFP in the AMsh glia in dauers induced by starvation at 15°C,  $n = 50$ ; while *ztf-16(ns171); fkh-9(ns261)* expressed weak GFP in only 5% of animals,  $n = 40$ ;  $P = 0.19$ , Fisher's exact test).

Based on the potential role of *fkh-9* in regulating *ver-1* expression, we hypothesized that *fkh-9* mutants may also have a role in dauer-induced AMsh glia fusion, perhaps by increasing the percentage of animals with fused glia. Alternatively, glia fusion may already be maximized in a wild-type background, and increasing *ver-1* levels above this by using a mutation in *fkh-9* may have no additional effect. Consistent with this second notion, we find that mutations in four different alleles of *fkh-9* have no effect on glia fusion in dauer animals as assessed by cytoplasmic mixing (Figure A4.6). In addition, and consistent with the failure of *fkh-9* mutations to strongly suppress the loss of *ver-1* promoter::*gfp* expression in *ttx-1* and *ztf-16* mutants, we found no suppression of the fusion defects of *ttx-1* and *ztf-16* mutants when combined with a mutation in *fkh-9* (Figure A4.6). Thus, it is unlikely that *fkh-9* affects glial fusion, and these results raise doubt as to whether screening for mutants that increase *ver-1* promoter::*gfp* expression in non-dauer animals is a useful method for finding glia remodeling genes.

Interestingly, a mutation in a second gene found to cause increased *ver-1* promoter::*gfp* expression also codes for a protein with a winged helix-like DNA-binding domain. Mutant allele *ns183* had weakly elevated levels of *ver-1* promoter::*gfp* in the PHsh glia (Figure A4.7A). *ns183* was mapped to chromosome X using SNP methods (Wicks et al., 2001) between polymorphisms on cosmid M163 at position 3785 to cosmid

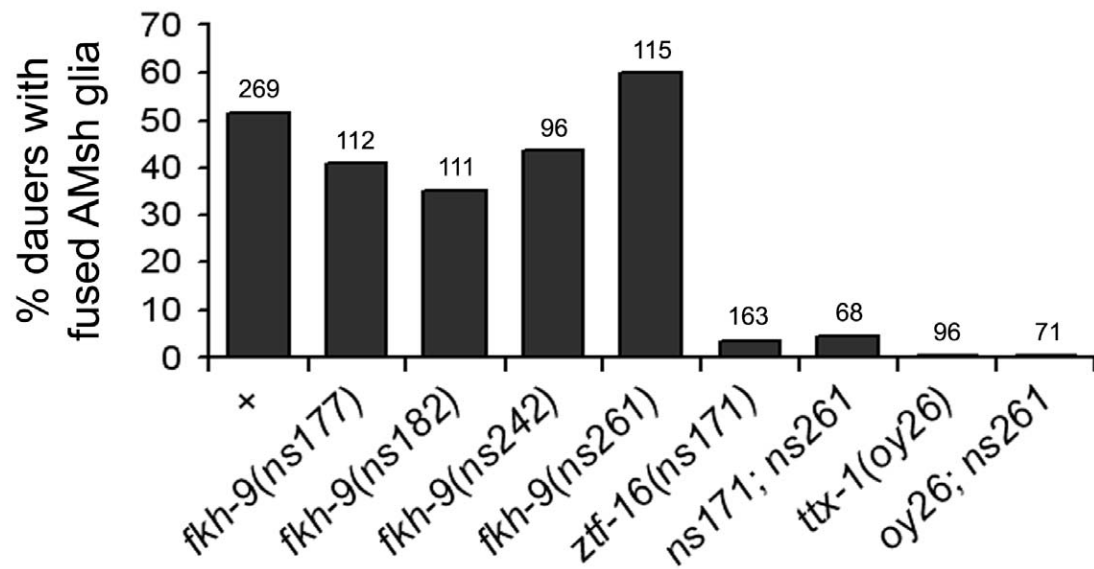


**Figure A4.6. Mutations in *fkh-9* do not affect dauer-induced glia remodeling.** Percentage of *daf-7(e1372)* dauer animals of the indicated genotype with fused AMsh glia as assayed by cytoplasmic mixing. Number of animals examined (*n*) is above each column.

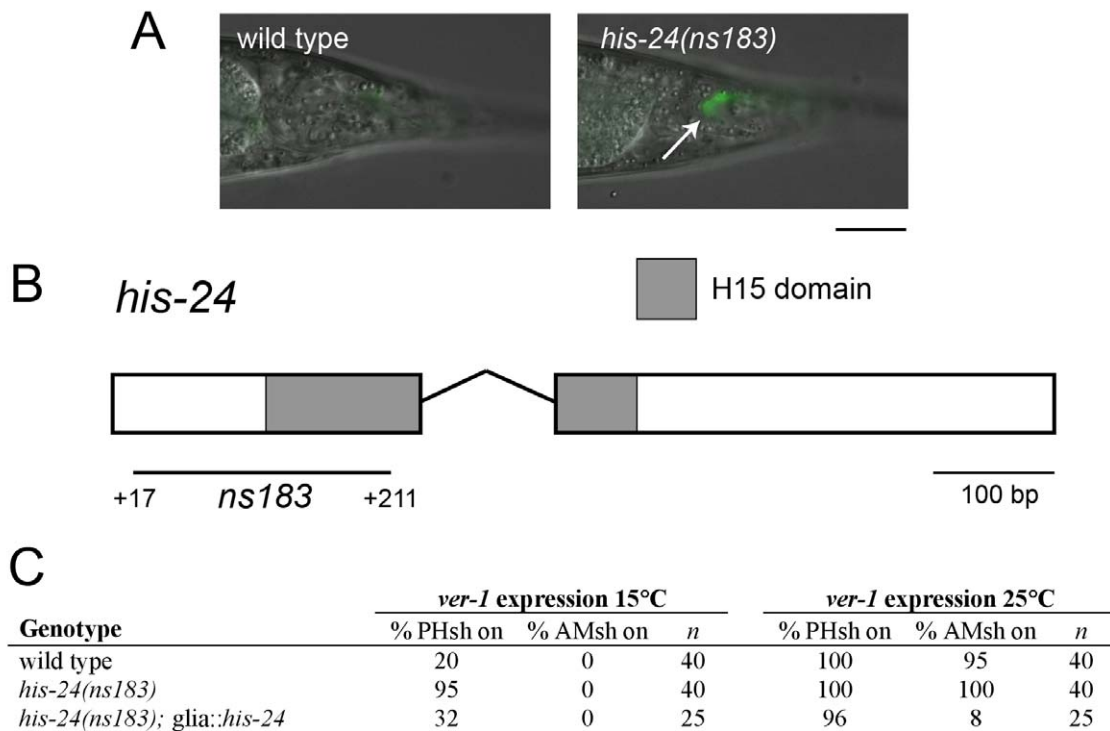


**Figure A4.7. A mutation in the linker histone *his-24* causes a weak increase in *ver-1* promoter::*gfp* expression. (A) DIC and fluorescence merged images of wild type (left) and *his-24(ns183)* (right) adult animals carrying a *ver-1* promoter::*gfp* reporter (*nsIs22*) at 15°C. Note weak GFP in the PHsh glia of *ns183* mutants (arrow). Anterior is left; scale bar, 20  $\mu$ m. GFP exposure, 200 ms. (B) A schematic of the *his-24* gene. Exons are represented by boxes; the linker histone H15 DNA-binding domain is shaded. The 195 bp deletion (and single base A insertion) of the *ns183* allele is shown. Coordinates are relative to the +1 start site of the coding sequence. (C) Restoring *his-24* cDNA expression specifically to the sheath glia rescues the *ns183* mutant phenotype. All strains carry the *ver-1* promoter::*gfp* transgene (*nsIs22*). The rescuing extrachromosomal array shown (*nsEx1590*) is representative of others.**

C44H4 at position 21512, an interval of ~126 kb. Within this region, a 195 bp deletion and single base A insertion was identified in the *his-24* linker histone gene (Figure A4.7B). Furthermore, glia-specific expression of a *his-24* cDNA rescued the *ver-1* promoter::*gfp* over-expression phenotype of *ns183* mutants (Figure A4.7C). *his-24* is likely expressed in all somatic cells and nuclear-localized, and may function as a general component of chromatin structure (Jedrusik and Schulze, 2001). Although linker histones share little sequence similarity with the winged-helix domain factors, the structure of the DNA-binding regions are conserved (Clark et al., 1993). This implies that *his-24* may act weakly through the same target genes as *fkh-9* to regulate *ver-1* promoter::*gfp* expression. Based on these observations, the gene was not pursued further.

## **Appendix 5: Dauer animals are repelled by isoamyl alcohol and benzaldehyde**

*daf-7(e1372)* dauers induced by cultivation at 25°C (60-72 h after laying) were tested in behavioral assays to the odorants benzaldehyde and isoamyl alcohol (IAA). In non-dauer adult animals, these odorants are sensed by the AWC neurons and mediate an attractive response (Bargmann et al., 1993). By contrast, we found that 1% IAA (Figure A5.1) and 0.5% benzaldehyde (data not shown) caused robust repulsion of *daf-7* dauers. Due to the small size and limited movement of dauer animals, we used a modified chemotaxis assay: animals were washed and plated onto the center of a 9 cm round chemotaxis plate, with three 1 µl drops of the odorant spotted equidistant on one side of the plate and three drops of ethanol vehicle control spotted on the other. 1 µl 0.1 M sodium azide was added to each spot. Animals were allowed to disperse from the center of the plate for 90 min, after which time they were fixed by addition of chloroform to the lid of the plate and the number of animals in each half of the plate counted. The chemotaxis index was calculated by subtracting the number of animals which moved in the direction away from the odorant from the number that went towards the odorant, divided by the total.

This difference between *daf-7* dauers and wild-type adults was not a result of AMsh glia fusion in dauers: *ttx-1(p767); daf-7(e1372)* (Figure A5.1) and *ttx-1(oy26); daf-7(e1372)* (data not shown) mutant dauers were also repelled by the odorant. Therefore, the switch in behavior of dauer animals from attraction towards IAA to repulsion may be a result of AWC circuit rewiring or, perhaps more likely, changes in odorant receptor expression between chemosensory neurons (for example, see Peckol et al., 2001).

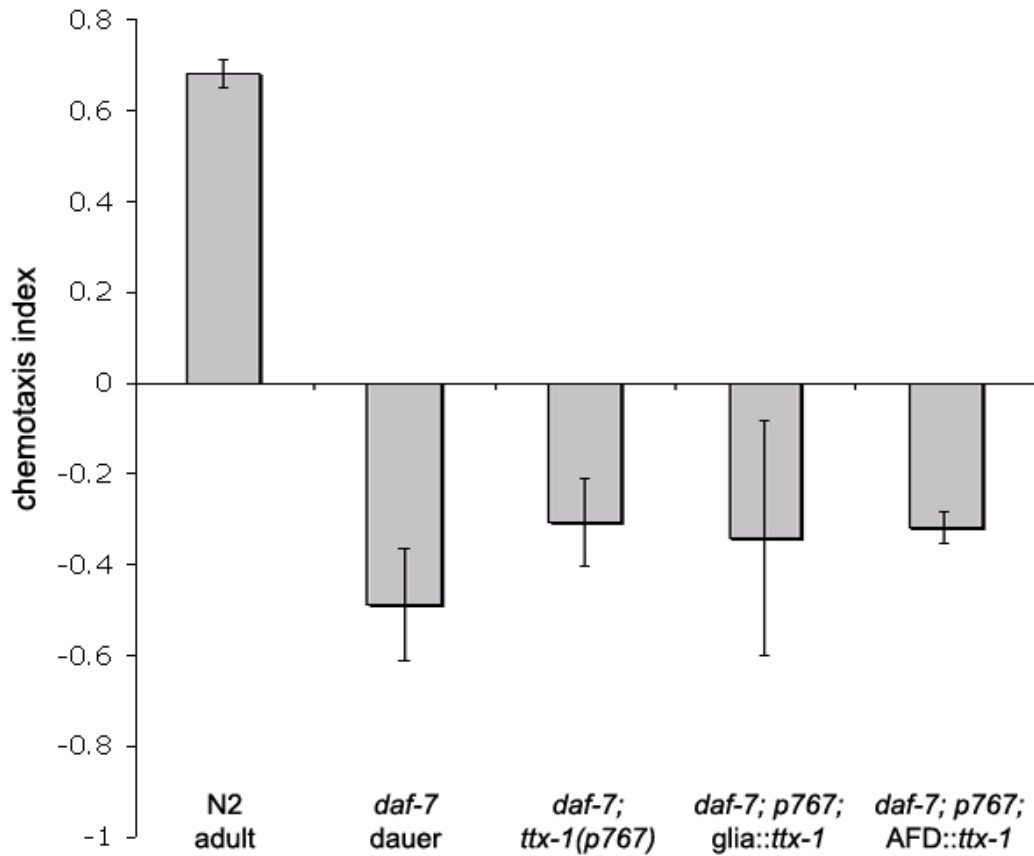


**Figure A5.1. *daf-7(e1372)* dauer animals are repelled by isoamyl alcohol (IAA).** Chemotaxis index of wild-type (N2) adult animals and *daf-7(e1372)* dauers cultivated at 25°C towards IAA (for method, see text). A negative index indicates repulsion. The cell-specific *ttx-1* rescue transgenes used were *nsIs219* (*glia::ttx-1*) and *nsIs99* (*AFD::ttx-1*). Results shown are averages of 4 assays, +/- s.d.

## **Appendix 6: *ttx-1* likely functions in AFD to regulate dauer exit of *daf-7(e1372)* mutants**

It was previously reported that *daf-7(e1372); ttx-1(p767)* mutants prematurely exit dauer compared to *daf-7(e1372)* single mutants (Satterlee et al., 2001). We rescued this phenotype using a transgene that restored *ttx-1* expression specifically to the AFD thermosensory neurons and not to the glia (Figure A6.1). Briefly, *daf-7* mutant strains were staged and grown at 25°C on OP50 bacteria. At 50 h, dauer animals were selected by 1% SDS treatment (see Chapter 6). Animals were cultivated for an additional 30 h and then scored as dauer or post-dauer by morphology. Due to the subtlety of the phenotype being scored (daurers vs recent post-daurers), we have been unable to rule out erroneous effects of the integrated transgenes on animal growth rates in these experiments.

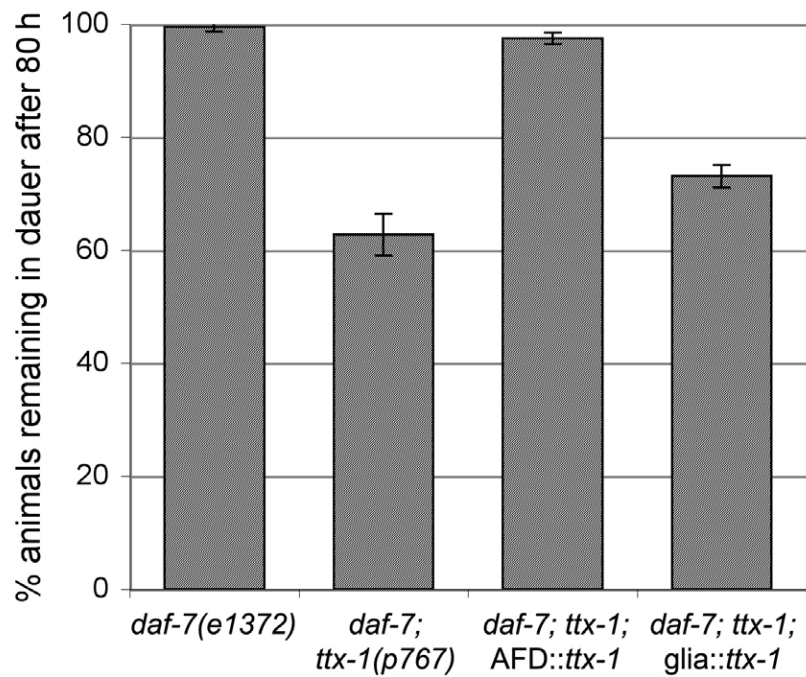


**Figure A6.1. *ttx-1* likely functions in AFD to regulate dauer exit of *daf-7(e1372)* mutants.** The percentage of animals of the indicated genotype remaining in dauer after 80 h at 25°C. Results are averages of 3 assays,  $n > 50$  each assay,  $\pm$  s.d. The *ttx-1* rescue transgenes used were *nsIs99* (*AFD::ttx-1*) and *nsIs101* (*glia::ttx-1*). All strains also carry *ver-1* promoter::*gfp* (*nsIs22*).

# References

**Acampora, D., Mazan, S., Avantaggiato, V., Barone, P., Tuorto, F., Lallemand, Y., Brulet, P. and Simeone, A.** (1996). Epilepsy and brain abnormalities in mice lacking the *Otx1* gene. *Nat Genet* **14**, 218-22.

**Aime, P., Duchamp-Viret, P., Chaput, M. A., Savigner, A., Mahfouz, M. and Julliard, A. K.** (2007). Fasting increases and satiation decreases olfactory detection for a neutral odor in rats. *Behav Brain Res* **179**, 258-64.

**Albert, P. S. and Riddle, D. L.** (1983). Developmental alterations in sensory neuroanatomy of the *Caenorhabditis elegans* dauer larva. *J Comp Neurol* **219**, 461-81.

**Antebi, A., Yeh, W. H., Tait, D., Hedgecock, E. M. and Riddle, D. L.** (2000). *daf-12* encodes a nuclear receptor that regulates the dauer diapause and developmental age in *C. elegans*. *Genes Dev* **14**, 1512-27.

**Anton, E. S., Kreidberg, J. A. and Rakic, P.** (1999). Distinct functions of  $\alpha 3$  and  $\alpha (v)$  integrin receptors in neuronal migration and laminar organization of the cerebral cortex. *Neuron* **22**, 277-89.

**Arad, Z., Goldenberg, S. and Heller, J.** (1989). Resistance to desiccation and distribution patterns in the land snail *Sphincterochila*. *Journal of Zoology* **218**, 353-364.

**Awasaki, T., Lai, S. L., Ito, K. and Lee, T.** (2008). Organization and postembryonic development of glial cells in the adult central brain of *Drosophila*. *J Neurosci* **28**, 13742-53.

**Bacaj, T., Tevlin, M., Lu, Y. and Shaham, S.** (2008). Glia are essential for sensory organ function in *C. elegans*. *Science* **322**, 744-7.

**Baehr, W., Wu, S. M., Bird, A. C. and Palczewski, K.** (2003). The retinoid cycle and retina disease. *Vision Res* **43**, 2957-8.

**Ballanyi, K., Panaitescu, B. and Ruangkittisakul, A.** (2010). Control of breathing by "nerve glue". *Sci Signal* **3**, pe41.

**Bargmann, C. I. and Avery, L.** (1995). Laser killing of cells in *Caenorhabditis elegans*. *Methods Cell Biol* **48**, 225-50.

**Bargmann, C. I., Hartweg, E. and Horvitz, H. R.** (1993). Odorant-selective genes and neurons mediate olfaction in *C. elegans*. *Cell* **74**, 515-27.

**Bargmann, C. I. and Horvitz, H. R.** (1991a). Chemosensory neurons with overlapping functions direct chemotaxis to multiple chemicals in *C. elegans*. *Neuron* **7**, 729-42.

**Bargmann, C. I. and Horvitz, H. R.** (1991b). Control of larval development by chemosensory neurons in *Caenorhabditis elegans*. *Science* **251**, 1243-6.

- Barker, A. J., Koch, S. M., Reed, J., Barres, B. A. and Ullian, E. M.** (2008). Developmental control of synaptic receptivity. *J Neurosci* **28**, 8150-60.
- Battye, R., Stevens, A. and Jacobs, J. R.** (1999). Axon repulsion from the midline of the Drosophila CNS requires slit function. *Development* **126**, 2475-81.
- Bernardos, R. L., Barthel, L. K., Meyers, J. R. and Raymond, P. A.** (2007). Late-stage neuronal progenitors in the retina are radial Muller glia that function as retinal stem cells. *J Neurosci* **27**, 7028-40.
- Biron, D., Wasserman, S., Thomas, J. H., Samuel, A. D. and Sengupta, P.** (2008). An olfactory neuron responds stochastically to temperature and modulates *Caenorhabditis elegans* thermotactic behavior. *Proc Natl Acad Sci U S A* **105**, 11002-7.
- Bok, D. and Hall, M. O.** (1971). The role of the pigment epithelium in the etiology of inherited retinal dystrophy in the rat. *J Cell Biol* **49**, 664-82.
- Boulant, J. A.** (2000). Role of the preoptic-anterior hypothalamus in thermoregulation and fever. *Clin Infect Dis* **31 Suppl 5**, S157-61.
- Bourne, J. N. and Harris, K. M.** (2008). Balancing structure and function at hippocampal dendritic spines. *Annu Rev Neurosci* **31**, 47-67.
- Breipohl, W., Laugwitz, H. J. and Bornfeld, N.** (1974). Topological relations between the dendrites of olfactory sensory cells and sustentacular cells in different vertebrates. An ultrastructural study. *J Anat* **117**, 89-94.
- Brenner, S.** (1974). The genetics of *Caenorhabditis elegans*. *Genetics* **77**, 71-94.
- Breunig, E., Manzini, I., Piscitelli, F., Gutermann, B., Di Marzo, V., Schild, D. and Czesnik, D.** (2010). The endocannabinoid 2-arachidonoyl-glycerol controls odor sensitivity in larvae of *Xenopus laevis*. *J Neurosci* **30**, 8965-73.
- Brock, T. D.** (1967). Micro-organisms adapted to high temperatures. *Nature* **214**, 882-5.
- Brock, T. D. and Brock, M. L.** (1966). Temperature optima for algal development in Yellowstone and Iceland hot springs. *Nature* **209**, 733-&.
- Butcher, R. A., Fujita, M., Schroeder, F. C. and Clardy, J.** (2007). Small-molecule pheromones that control dauer development in *Caenorhabditis elegans*. *Nat Chem Biol* **3**, 420-2.
- Cajal, S. R.** (1911). *Histologie du Système Nerveux de L'Homme et des Vertébrés. Maloine. Paris.*
- Campbell, A. L., Naik, R. R., Sowards, L. and Stone, M. O.** (2002). Biological infrared imaging and sensing. *Micron* **33**, 211-25.

- Cano, R. J. and Borucki, M. K.** (1995). Revival and identification of bacterial spores in 25- to 40-million-year-old Dominican amber. *Science* **268**, 1060-4.
- Carlson, S. D. and Saint Marie, R. L.** (1990). Structure and function of insect glia. *Annual Review of Entomology* **35**, 597-621.
- Carmona, M. A., Murai, K. K., Wang, L., Roberts, A. J. and Pasquale, E. B.** (2009). Glial ephrin-A3 regulates hippocampal dendritic spine morphology and glutamate transport. *Proc Natl Acad Sci U S A* **106**, 12524-9.
- Cassada, R. C. and Russell, R. L.** (1975). The dauerlarva, a post-embryonic developmental variant of the nematode *Caenorhabditis elegans*. *Dev Biol* **46**, 326-42.
- Chalasani, S. H., Chronis, N., Tsunozaki, M., Gray, J. M., Ramot, D., Goodman, M. B. and Bargmann, C. I.** (2007). Dissecting a circuit for olfactory behaviour in *Caenorhabditis elegans*. *Nature* **450**, 63-70.
- Chotard, C. and Salecker, I.** (2004). Neurons and glia: team players in axon guidance. *Trends Neurosci* **27**, 655-61.
- Christopherson, K. S., Ullian, E. M., Stokes, C. C., Mullowney, C. E., Hell, J. W., Agah, A., Lawler, J., Mosher, D. F., Bornstein, P. and Barres, B. A.** (2005). Thrombospondins are astrocyte-secreted proteins that promote CNS synaptogenesis. *Cell* **120**, 421-33.
- Chung, Y. D., Zhu, J., Han, Y. and Kernan, M. J.** (2001). *nompA* encodes a PNS-specific, ZP domain protein required to connect mechanosensory dendrites to sensory structures. *Neuron* **29**, 415-28.
- Clark, D. A., Biron, D., Sengupta, P. and Samuel, A. D.** (2006). The AFD sensory neurons encode multiple functions underlying thermotactic behavior in *Caenorhabditis elegans*. *J Neurosci* **26**, 7444-51.
- Clark, K. L., Halay, E. D., Lai, E. and Burley, S. K.** (1993). Co-crystal structure of the HNF-3/fork head DNA-recognition motif resembles histone H5. *Nature* **364**, 412-20.
- Coburn, C. M. and Bargmann, C. I.** (1996). A putative cyclic nucleotide-gated channel is required for sensory development and function in *C. elegans*. *Neuron* **17**, 695-706.
- Colbert, H. A., Smith, T. L. and Bargmann, C. I.** (1997). OSM-9, a novel protein with structural similarity to channels, is required for olfaction, mechanosensation, and olfactory adaptation in *Caenorhabditis elegans*. *J Neurosci* **17**, 8259-69.
- Colon-Ramos, D. A., Margeta, M. A. and Shen, K.** (2007). Glia promote local synaptogenesis through UNC-6 (netrin) signaling in *C. elegans*. *Science* **318**, 103-6.

- Colosimo, M. E., Brown, A., Mukhopadhyay, S., Gabel, C., Lanjuin, A. E., Samuel, A. D. and Sengupta, P.** (2004). Identification of thermosensory and olfactory neuron-specific genes via expression profiling of single neuron types. *Curr Biol* **14**, 2245-51.
- Conradt, B. and Horvitz, H. R.** (1998). The *C. elegans* protein EGL-1 is required for programmed cell death and interacts with the Bcl-2-like protein CED-9. *Cell* **93**, 519-29.
- Cui, W., Allen, N. D., Skynner, M., Gusterson, B. and Clark, A. J.** (2001). Inducible ablation of astrocytes shows that these cells are required for neuronal survival in the adult brain. *Glia* **34**, 272-82.
- Czesnik, D., Schild, D., Kuduz, J. and Manzini, I.** (2007). Cannabinoid action in the olfactory epithelium. *Proc Natl Acad Sci U S A* **104**, 2967-72.
- Delaney, C. L., Brenner, M. and Messing, A.** (1996). Conditional ablation of cerebellar astrocytes in postnatal transgenic mice. *J Neurosci* **16**, 6908-18.
- Doherty, J., Logan, M. A., Tasdemir, O. E. and Freeman, M. R.** (2009). Ensheathing glia function as phagocytes in the adult *Drosophila* brain. *J Neurosci* **29**, 4768-81.
- Dunaevsky, A., Tashiro, A., Majewska, A., Mason, C. and Yuste, R.** (1999). Developmental regulation of spine motility in the mammalian central nervous system. *Proc Natl Acad Sci U S A* **96**, 13438-43.
- Elias, L. A., Wang, D. D. and Kriegstein, A. R.** (2007). Gap junction adhesion is necessary for radial migration in the neocortex. *Nature* **448**, 901-7.
- Eroglu, C., Allen, N. J., Susman, M. W., O'Rourke, N. A., Park, C. Y., Ozkan, E., Chakraborty, C., Mulinyawe, S. B., Annis, D. S., Huberman, A. D. et al.** (2009). Gabapentin receptor alpha2delta-1 is a neuronal thrombospondin receptor responsible for excitatory CNS synaptogenesis. *Cell* **139**, 380-92.
- Estevez, M., Attisano, L., Wrana, J. L., Albert, P. S., Massague, J. and Riddle, D. L.** (1993). The *daf-4* gene encodes a bone morphogenetic protein receptor controlling *C. elegans* dauer larva development. *Nature* **365**, 644-9.
- Fielenbach, N. and Antebi, A.** (2008). *C. elegans* dauer formation and the molecular basis of plasticity. *Genes Dev* **22**, 2149-65.
- Fischer, A. J. and Reh, T. A.** (2001). Muller glia are a potential source of neural regeneration in the postnatal chicken retina. *Nat Neurosci* **4**, 247-52.
- Fishell, G. and Hatten, M. E.** (1991). Astrotactin provides a receptor system for CNS neuronal migration. *Development* **113**, 755-65.
- Flock, A., Flock, B., Fridberger, A., Scarfone, E. and Ulfendahl, M.** (1999). Supporting cells contribute to control of hearing sensitivity. *J Neurosci* **19**, 4498-507.

- Franze, K., Grosche, J., Skatchkov, S. N., Schinkinger, S., Foja, C., Schild, D., Uckermann, O., Travis, K., Reichenbach, A. and Guck, J.** (2007). Muller cells are living optical fibers in the vertebrate retina. *Proc Natl Acad Sci U S A* **104**, 8287-92.
- Fraser, A. G., Kamath, R. S., Zipperlen, P., Martinez-Campos, M., Sohrmann, M. and Ahringer, J.** (2000). Functional genomic analysis of *C. elegans* chromosome I by systematic RNA interference. *Nature* **408**, 325-30.
- Furrer, M. P., Kim, S., Wolf, B. and Chiba, A.** (2003). Robo and Frazzled/DCC mediate dendritic guidance at the CNS midline. *Nat Neurosci* **6**, 223-30.
- Gao, F. B.** (2007). Molecular and cellular mechanisms of dendritic morphogenesis. *Curr Opin Neurobiol* **17**, 525-32.
- Georgi, L. L., Albert, P. S. and Riddle, D. L.** (1990). *daf-1*, a *C. elegans* gene controlling dauer larva development, encodes a novel receptor protein kinase. *Cell* **61**, 635-45.
- Golden, J. W. and Riddle, D. L.** (1984a). The *Caenorhabditis elegans* dauer larva: developmental effects of pheromone, food, and temperature. *Dev Biol* **102**, 368-78.
- Golden, J. W. and Riddle, D. L.** (1984b). A pheromone-induced developmental switch in *Caenorhabditis elegans*: Temperature-sensitive mutants reveal a wild-type temperature-dependent process. *Proc Natl Acad Sci U S A* **81**, 819-23.
- Gourine, A. V., Kasymov, V., Marina, N., Tang, F., Figueiredo, M. F., Lane, S., Teschemacher, A. G., Spyer, K. M., Deisseroth, K. and Kasparov, S.** (2010). Astrocytes control breathing through pH-dependent release of ATP. *Science* **329**, 571-5.
- Gracheva, E. O., Ingolia, N. T., Kelly, Y. M., Cordero-Morales, J. F., Hollopeter, G., Chesler, A. T., Sanchez, E. E., Perez, J. C., Weissman, J. S. and Julius, D.** (2010). Molecular basis of infrared detection by snakes. *Nature* **464**, 1006-11.
- Grueber, W. B., Jan, L. Y. and Jan, Y. N.** (2002). Tiling of the *Drosophila* epidermis by multidendritic sensory neurons. *Development* **129**, 2867-78.
- Hall, S. E., Beverly, M., Russ, C., Nusbaum, C. and Sengupta, P.** (2010). A cellular memory of developmental history generates phenotypic diversity in *C. elegans*. *Curr Biol* **20**, 149-55.
- Hartenstein, V. and Posakony, J. W.** (1989). Development of adult sensilla on the wing and notum of *Drosophila melanogaster*. *Development* **107**, 389-405.
- Hatten, M. E.** (2002). New directions in neuronal migration. *Science* **297**, 1660-3.
- Hedgecock, E. M. and Russell, R. L.** (1975). Normal and mutant thermotaxis in the nematode *Caenorhabditis elegans*. *Proc Natl Acad Sci U S A* **72**, 4061-5.

- Hegg, C. C., Irwin, M. and Lucero, M. T.** (2009). Calcium store-mediated signaling in sustentacular cells of the mouse olfactory epithelium. *Glia* **57**, 634-44.
- Heiman, M. G. and Shaham, S.** (2009). DEX-1 and DYF-7 establish sensory dendrite length by anchoring dendritic tips during cell migration. *Cell* **137**, 344-55.
- Hilliard, M. A., Bargmann, C. I. and Bazzicalupo, P.** (2002). *C. elegans* responds to chemical repellents by integrating sensory inputs from the head and the tail. *Curr Biol* **12**, 730-4.
- Holt, S. J. and Riddle, D. L.** (2003). SAGE surveys *C. elegans* carbohydrate metabolism: evidence for an anaerobic shift in the long-lived dauer larva. *Mech Ageing Dev* **124**, 779-800.
- Holtmaat, A. and Svoboda, K.** (2009). Experience-dependent structural synaptic plasticity in the mammalian brain. *Nat Rev Neurosci* **10**, 647-58.
- Hope, I. A., Mounsey, A., Bauer, P. and Aslam, S.** (2003). The forkhead gene family of *Caenorhabditis elegans*. *Gene* **304**, 43-55.
- Hsieh, J., Liu, J., Kostas, S. A., Chang, C., Sternberg, P. W. and Fire, A.** (1999). The RING finger/B-box factor TAM-1 and a retinoblastoma-like protein LIN-35 modulate context-dependent gene silencing in *Caenorhabditis elegans*. *Genes Dev* **13**, 2958-70.
- Huang, L. S., Tzou, P. and Sternberg, P. W.** (1994). The *lin-15* locus encodes two negative regulators of *Caenorhabditis elegans* vulval development. *Mol Biol Cell* **5**, 395-411.
- Inada, H., Ito, H., Satterlee, J., Sengupta, P., Matsumoto, K. and Mori, I.** (2006). Identification of guanylyl cyclases that function in thermosensory neurons of *Caenorhabditis elegans*. *Genetics* **172**, 2239-52.
- Ishitani, S., Inaba, K., Matsumoto, K. and Ishitani, T.** (2011). Homodimerization of Nemo-like kinase is essential for activation and nuclear localization. *Mol Biol Cell* **22**, 266-77.
- Iuchi, S.** (2001). Three classes of C2H2 zinc finger proteins. *Cell Mol Life Sci* **58**, 625-35.
- Jedrusik, M. A. and Schulze, E.** (2001). A single histone H1 isoform (H1.1) is essential for chromatin silencing and germline development in *Caenorhabditis elegans*. *Development* **128**, 1069-80.
- Kaplan, J. M. and Horvitz, H. R.** (1993). A dual mechanosensory and chemosensory neuron in *Caenorhabditis elegans*. *Proc Natl Acad Sci U S A* **90**, 2227-31.

- Kelley, C. G., Lavorgna, G., Clark, M. E., Boncinelli, E. and Mellon, P. L.** (2000). The Otx2 homeoprotein regulates expression from the gonadotropin-releasing hormone proximal promoter. *Mol Endocrinol* **14**, 1246-56.
- Kevany, B. M. and Palczewski, K.** (2010). Phagocytosis of retinal rod and cone photoreceptors. *Physiology (Bethesda)* **25**, 8-15.
- Kidd, T., Bland, K. S. and Goodman, C. S.** (1999). Slit is the midline repellent for the robo receptor in Drosophila. *Cell* **96**, 785-94.
- Kim, K., Sato, K., Shibuya, M., Zeiger, D. M., Butcher, R. A., Ragains, J. R., Clardy, J., Touhara, K. and Sengupta, P.** (2009). Two chemoreceptors mediate developmental effects of dauer pheromone in *C. elegans*. *Science* **326**, 994-8.
- Kim, S. and Chiba, A.** (2004). Dendritic guidance. *Trends Neurosci* **27**, 194-202.
- Kimble, J. and Hirsh, D.** (1979). The postembryonic cell lineages of the hermaphrodite and male gonads in *Caenorhabditis elegans*. *Dev Biol* **70**, 396-417.
- Kimura, K. D., Miyawaki, A., Matsumoto, K. and Mori, I.** (2004). The *C. elegans* thermosensory neuron AFD responds to warming. *Curr Biol* **14**, 1291-5.
- Kimura, K. D., Tissenbaum, H. A., Liu, Y. and Ruvkun, G.** (1997). *daf-2*, an insulin receptor-like gene that regulates longevity and diapause in *Caenorhabditis elegans*. *Science* **277**, 942-6.
- Komatsu, H., Mori, I., Rhee, J. S., Akaike, N. and Ohshima, Y.** (1996). Mutations in a cyclic nucleotide-gated channel lead to abnormal thermosensation and chemosensation in *C. elegans*. *Neuron* **17**, 707-18.
- Kuhara, A., Okumura, M., Kimata, T., Tanizawa, Y., Takano, R., Kimura, K. D., Inada, H., Matsumoto, K. and Mori, I.** (2008). Temperature sensing by an olfactory neuron in a circuit controlling behavior of *C. elegans*. *Science* **320**, 803-7.
- Kumar, S. V. and Wigge, P. A.** (2010). H2A.Z-containing nucleosomes mediate the thermosensory response in *Arabidopsis*. *Cell* **140**, 136-47.
- Kunitomo, H., Uesugi, H., Kohara, Y. and Iino, Y.** (2005). Identification of ciliated sensory neuron-expressed genes in *Caenorhabditis elegans* using targeted pull-down of poly(A) tails. *Genome Biol* **6**, R17.
- Landmann, F., Quintin, S. and Labouesse, M.** (2004). Multiple regulatory elements with spatially and temporally distinct activities control the expression of the epithelial differentiation gene *lin-26* in *C. elegans*. *Dev Biol* **265**, 478-90.
- Large, E. E. and Mathies, L. D.** (2010). *hunchback* and *Ikaros*-like zinc finger genes control reproductive system development in *Caenorhabditis elegans*. *Dev Biol* **339**, 51-64.

- Larsen, P. L., Albert, P. S. and Riddle, D. L.** (1995). Genes that regulate both development and longevity in *Caenorhabditis elegans*. *Genetics* **139**, 1567-83.
- Legan, P. K., Rau, A., Keen, J. N. and Richardson, G. P.** (1997). The mouse tectorins. Modular matrix proteins of the inner ear homologous to components of the sperm-egg adhesion system. *J Biol Chem* **272**, 8791-801.
- Lennon, G., Auffray, C., Polymeropoulos, M. and Soares, M. B.** (1996). The I.M.A.G.E. Consortium: an integrated molecular analysis of genomes and their expression. *Genomics* **33**, 151-2.
- Leung, C. T., Coulombe, P. A. and Reed, R. R.** (2007). Contribution of olfactory neural stem cells to tissue maintenance and regeneration. *Nat Neurosci* **10**, 720-6.
- Li, W., Kennedy, S. G. and Ruvkun, G.** (2003). *daf-28* encodes a *C. elegans* insulin superfamily member that is regulated by environmental cues and acts in the DAF-2 signaling pathway. *Genes Dev* **17**, 844-58.
- Lippman, J. J., Lordkipanidze, T., Buell, M. E., Yoon, S. O. and Dunaevsky, A.** (2008). Morphogenesis and regulation of Bergmann glial processes during Purkinje cell dendritic spine ensheathment and synaptogenesis. *Glia* **56**, 1463-77.
- Liu, J., Ward, A., Gao, J., Dong, Y., Nishio, N., Inada, H., Kang, L., Yu, Y., Ma, D., Xu, T. et al.** (2010). *C. elegans* phototransduction requires a G protein-dependent cGMP pathway and a taste receptor homolog. *Nat Neurosci* **13**, 715-22.
- Loomis, S. H.** (2010). Diapause and estivation in sponges. *Prog Mol Subcell Biol* **49**, 231-43.
- Loomis, S. H., Bettridge, A. and Branchini, B. R.** (2009). The effects of elevated osmotic concentration on control of germination in the gemmules of freshwater sponges *Eunapius fragilis* and *Anheteromeyana ryderi*. *Physiol Biochem Zool* **82**, 388-95.
- Lundquist, E. A., Reddien, P. W., Hartweg, E., Horvitz, H. R. and Bargmann, C. I.** (2001). Three *C. elegans* Rac proteins and several alternative Rac regulators control axon guidance, cell migration and apoptotic cell phagocytosis. *Development* **128**, 4475-88.
- Maeda, K. and Imae, Y.** (1979). Thermosensory transduction in *Escherichia coli*: inhibition of the thermoresponse by L-serine. *Proc Natl Acad Sci U S A* **76**, 91-5.
- Mallamaci, A., Di Blas, E., Briata, P., Boncinelli, E. and Corte, G.** (1996). OTX2 homeoprotein in the developing central nervous system and migratory cells of the olfactory area. *Mech Dev* **58**, 165-78.
- Matthews, B. J., Kim, M. E., Flanagan, J. J., Hattori, D., Clemens, J. C., Zipursky, S. L. and Grueber, W. B.** (2007). Dendrite self-avoidance is controlled by Dscam. *Cell* **129**, 593-604.

- McCarty, A. S., Kleiger, G., Eisenberg, D. and Smale, S. T.** (2003). Selective dimerization of a C2H2 zinc finger subfamily. *Mol Cell* **11**, 459-70.
- Mello, C. and Fire, A.** (1995). DNA transformation. *Methods Cell Biol* **48**, 451-82.
- Mello, C. C., Kramer, J. M., Stinchcomb, D. and Ambros, V.** (1991). Efficient gene transfer in *C.elegans*: extrachromosomal maintenance and integration of transforming sequences. *Embo J* **10**, 3959-70.
- Melvin, R. G. and Andrews, M. T.** (2009). Torpor induction in mammals: recent discoveries fueling new ideas. *Trends Endocrinol Metab* **20**, 490-8.
- Meyer-Franke, A., Kaplan, M. R., Pfrieder, F. W. and Barres, B. A.** (1995). Characterization of the signaling interactions that promote the survival and growth of developing retinal ganglion cells in culture. *Neuron* **15**, 805-19.
- Miller, M. R., Robinson, K. J., Cleary, M. D. and Doe, C. Q.** (2009). TU-tagging: cell type-specific RNA isolation from intact complex tissues. *Nat Methods* **6**, 439-41.
- Mizuno, T. and Imae, Y.** (1984). Conditional inversion of the thermoresponse in *Escherichia coli*. *J Bacteriol* **159**, 360-7.
- Mohler, W. A., Shemer, G., del Campo, J. J., Valansi, C., Opoku-Serebuoh, E., Scranton, V., Assaf, N., White, J. G. and Podbilewicz, B.** (2002). The type I membrane protein EFF-1 is essential for developmental cell fusion. *Dev Cell* **2**, 355-62.
- Molnar, A. and Georgopoulos, K.** (1994). The Ikaros gene encodes a family of functionally diverse zinc finger DNA-binding proteins. *Mol Cell Biol* **14**, 8292-303.
- Monne, M., Han, L., Schwend, T., Burendahl, S. and Jovine, L.** (2008). Crystal structure of the ZP-N domain of ZP3 reveals the core fold of animal egg coats. *Nature* **456**, 653-7.
- Moore, A. W., Jan, L. Y. and Jan, Y. N.** (2002). hamlet, a binary genetic switch between single- and multiple- dendrite neuron morphology. *Science* **297**, 1355-8.
- Moore, A. W., Roegiers, F., Jan, L. Y. and Jan, Y. N.** (2004). Conversion of neurons and glia to external-cell fates in the external sensory organs of *Drosophila* hamlet mutants by a cousin-cousin cell-type respecification. *Genes Dev* **18**, 623-8.
- Mori, I. and Ohshima, Y.** (1995). Neural regulation of thermotaxis in *Caenorhabditis elegans*. *Nature* **376**, 344-8.
- Motola, D. L., Cummins, C. L., Rottiers, V., Sharma, K. K., Li, T., Li, Y., Suino-Powell, K., Xu, H. E., Auchus, R. J., Antebi, A. et al.** (2006). Identification of ligands for DAF-12 that govern dauer formation and reproduction in *C. elegans*. *Cell* **124**, 1209-23.

- Mukhopadhyay, S., Lu, Y., Shaham, S. and Sengupta, P.** (2008). Sensory signaling-dependent remodeling of olfactory cilia architecture in *C. elegans*. *Dev Cell* **14**, 762-74.
- Murai, K. K., Nguyen, L. N., Irie, F., Yamaguchi, Y. and Pasquale, E. B.** (2003). Control of hippocampal dendritic spine morphology through ephrin-A3/EphA4 signaling. *Nat Neurosci* **6**, 153-60.
- Murakami, S. and Johnson, T. E.** (2001). The OLD-1 positive regulator of longevity and stress resistance is under DAF-16 regulation in *Caenorhabditis elegans*. *Curr Biol* **11**, 1517-23.
- Nicholson, W. L., Munakata, N., Horneck, G., Melosh, H. J. and Setlow, P.** (2000). Resistance of *Bacillus* endospores to extreme terrestrial and extraterrestrial environments. *Microbiol Mol Biol Rev* **64**, 548-72.
- Okkema, P. G., Harrison, S. W., Plunger, V., Aryana, A. and Fire, A.** (1993). Sequence requirements for myosin gene expression and regulation in *Caenorhabditis elegans*. *Genetics* **135**, 385-404.
- Oren-Suissa, M., Hall, D. H., Treinin, M., Shemer, G. and Podbilewicz, B.** (2010). The Fusogen EFF-1 Controls Sculpting of Mechanosensory Dendrites. *Science*.
- Panatier, A., Theodosis, D. T., Mothet, J. P., Touquet, B., Pollegioni, L., Poulain, D. A. and Oliet, S. H.** (2006). Glia-derived D-serine controls NMDA receptor activity and synaptic memory. *Cell* **125**, 775-84.
- Parrish, J. Z., Emoto, K., Kim, M. D. and Jan, Y. N.** (2007). Mechanisms that regulate establishment, maintenance, and remodeling of dendritic fields. *Annu Rev Neurosci* **30**, 399-423.
- Peckol, E. L., Troemel, E. R. and Bargmann, C. I.** (2001). Sensory experience and sensory activity regulate chemosensory receptor gene expression in *Caenorhabditis elegans*. *Proc Natl Acad Sci U S A* **98**, 11032-8.
- Peier, A. M., Moqrich, A., Hergarden, A. C., Reeve, A. J., Andersson, D. A., Story, G. M., Earley, T. J., Dragoni, I., McIntyre, P., Bevan, S. et al.** (2002a). A TRP channel that senses cold stimuli and menthol. *Cell* **108**, 705-15.
- Peier, A. M., Reeve, A. J., Andersson, D. A., Moqrich, A., Earley, T. J., Hergarden, A. C., Story, G. M., Colley, S., Hogenesch, J. B., McIntyre, P. et al.** (2002b). A heat-sensitive TRP channel expressed in keratinocytes. *Science* **296**, 2046-9.
- Perens, E. A. and Shaham, S.** (2005). *C. elegans* daf-6 encodes a patched-related protein required for lumen formation. *Dev Cell* **8**, 893-906.
- Perkins, L. A., Hedgecock, E. M., Thomson, J. N. and Culotti, J. G.** (1986). Mutant sensory cilia in the nematode *Caenorhabditis elegans*. *Dev Biol* **117**, 456-87.

- Popovici, C., Isnardon, D., Birnbaum, D. and Roubin, R.** (2002). Caenorhabditis elegans receptors related to mammalian vascular endothelial growth factor receptors are expressed in neural cells. *Neurosci Lett* **329**, 116-20.
- Porter, J. T. and McCarthy, K. D.** (1996). Hippocampal astrocytes in situ respond to glutamate released from synaptic terminals. *J Neurosci* **16**, 5073-81.
- Rakic, P.** (1971). Neuron-glia relationship during granule cell migration in developing cerebellar cortex. A Golgi and electronmicroscopic study in Macacus Rhesus. *J Comp Neurol* **141**, 283-312.
- Rakic, P.** (1972). Mode of cell migration to the superficial layers of fetal monkey neocortex. *J Comp Neurol* **145**, 61-83.
- Ramot, D., MacInnis, B. L. and Goodman, M. B.** (2008a). Bidirectional temperature-sensing by a single thermosensory neuron in *C. elegans*. *Nat Neurosci* **11**, 908-15.
- Ramot, D., MacInnis, B. L., Lee, H. C. and Goodman, M. B.** (2008b). Thermotaxis is a robust mechanism for thermoregulation in *Caenorhabditis elegans* nematodes. *J Neurosci* **28**, 12546-57.
- Ren, P., Lim, C. S., Johnsen, R., Albert, P. S., Pilgrim, D. and Riddle, D. L.** (1996). Control of *C. elegans* larval development by neuronal expression of a TGF-beta homolog. *Science* **274**, 1389-91.
- Rhinn, M., Dierich, A., Shawlot, W., Behringer, R. R., Le Meur, M. and Ang, S. L.** (1998). Sequential roles for *Otx2* in visceral endoderm and neuroectoderm for forebrain and midbrain induction and specification. *Development* **125**, 845-56.
- Riddle, D. L., Swanson, M. M. and Albert, P. S.** (1981). Interacting genes in nematode dauer larva formation. *Nature* **290**, 668-71.
- Rio, C., Dikkes, P., Liberman, M. C. and Corfas, G.** (2002). Glial fibrillary acidic protein expression and promoter activity in the inner ear of developing and adult mice. *J Comp Neurol* **442**, 156-62.
- Robitaille, R.** (1998). Modulation of synaptic efficacy and synaptic depression by glial cells at the frog neuromuscular junction. *Neuron* **21**, 847-55.
- Rodriguez, S., Sickles, H. M., Deleonardis, C., Alcaraz, A., Gridley, T. and Lin, D. M.** (2008). *Notch2* is required for maintaining sustentacular cell function in the adult mouse main olfactory epithelium. *Dev Biol* **314**, 40-58.
- Rosette, C. and Karin, M.** (1996). Ultraviolet light and osmotic stress: activation of the JNK cascade through multiple growth factor and cytokine receptors. *Science* **274**, 1194-7.

- Rothberg, J. M., Hartley, D. A., Walther, Z. and Artavanis-Tsakonas, S.** (1988). slit: an EGF-homologous locus of *D. melanogaster* involved in the development of the embryonic central nervous system. *Cell* **55**, 1047-59.
- Rothberg, J. M., Jacobs, J. R., Goodman, C. S. and Artavanis-Tsakonas, S.** (1990). slit: an extracellular protein necessary for development of midline glia and commissural axon pathways contains both EGF and LRR domains. *Genes Dev* **4**, 2169-87.
- Ryu, W. S. and Samuel, A. D.** (2002). Thermotaxis in *Caenorhabditis elegans* analyzed by measuring responses to defined Thermal stimuli. *J Neurosci* **22**, 5727-33.
- Sapir, A., Choi, J., Leikina, E., Avinoam, O., Valansi, C., Chernomordik, L. V., Newman, A. P. and Podbilewicz, B.** (2007). AFF-1, a FOS-1-regulated fusogen, mediates fusion of the anchor cell in *C. elegans*. *Dev Cell* **12**, 683-98.
- Satterlee, J. S., Sasakura, H., Kuhara, A., Berkeley, M., Mori, I. and Sengupta, P.** (2001). Specification of thermosensory neuron fate in *C. elegans* requires *ttx-1*, a homolog of *otd/Otx*. *Neuron* **31**, 943-56.
- Schackwitz, W. S., Inoue, T. and Thomas, J. H.** (1996). Chemosensory neurons function in parallel to mediate a pheromone response in *C. elegans*. *Neuron* **17**, 719-28.
- Schmidt-Nielsen, K., Taylor, C. R. and Shkolnik, A.** (1971). Desert snails: problems of heat, water and food. *J Exp Biol* **55**, 385-98.
- Schmitz, H. and Bleckmann, H.** (1998). The photomechanic infrared receptor for the detection of forest fires in the beetle *Melanophila acuminata* (Coleoptera : Buprestidae). *Journal of Comparative Physiology a-Sensory Neural and Behavioral Physiology* **182**, 647-657.
- Schummers, J., Yu, H. and Sur, M.** (2008). Tuned responses of astrocytes and their influence on hemodynamic signals in the visual cortex. *Science* **320**, 1638-43.
- Secor, S. M. and Lignot, J. H.** (2010). Morphological plasticity of vertebrate aestivation. *Prog Mol Subcell Biol* **49**, 183-208.
- Shaham, S.** (2005). Glia-neuron interactions in nervous system function and development. *Curr Top Dev Biol* **69**, 39-66.
- Shaham, S.** (2006). Glia-neuron interactions in the nervous system of *Caenorhabditis elegans*. *Curr Opin Neurobiol* **16**, 522-8.
- Shaham, S.** (2010). Chemosensory organs as models of neuronal synapses. *Nat Rev Neurosci.* **11**, 212-217.
- Shen, K. and Bargmann, C. I.** (2003). The immunoglobulin superfamily protein SYG-1 determines the location of specific synapses in *C. elegans*. *Cell* **112**, 619-30.

- Shen, K., Fetter, R. D. and Bargmann, C. I.** (2004). Synaptic specificity is generated by the synaptic guidepost protein SYG-2 and its receptor, SYG-1. *Cell* **116**, 869-81.
- Shen, W. L., Kwon, Y., Adegbola, A. A., Luo, J., Chess, A. and Montell, C.** (2011). Function of rhodopsin in temperature discrimination in *Drosophila*. *Science* **331**, 1333-6.
- Shimizu, H., Watanabe, E., Hiyama, T. Y., Nagakura, A., Fujikawa, A., Okado, H., Yanagawa, Y., Obata, K. and Noda, M.** (2007). Glial Nax channels control lactate signaling to neurons for brain [Na<sup>+</sup>] sensing. *Neuron* **54**, 59-72.
- Shostak, Y., Van Gilst, M. R., Antebi, A. and Yamamoto, K. R.** (2004). Identification of *C. elegans* DAF-12-binding sites, response elements, and target genes. *Genes Dev* **18**, 2529-44.
- Smale, S. T. and Dorshkind, K.** (2006). Hematopoiesis flies high with Ikaros. *Nat Immunol* **7**, 367-9.
- Sondell, M., Lundborg, G. and Kanje, M.** (1999). Vascular endothelial growth factor has neurotrophic activity and stimulates axonal outgrowth, enhancing cell survival and Schwann cell proliferation in the peripheral nervous system. *J Neurosci* **19**, 5731-40.
- Spacek, J.** (1985). Three-dimensional analysis of dendritic spines. III. Glial sheath. *Anat Embryol (Berl)* **171**, 245-52.
- Stanojevic, D., Hoey, T. and Levine, M.** (1989). Sequence-specific DNA-binding activities of the gap proteins encoded by hunchback and Kruppel in *Drosophila*. *Nature* **341**, 331-5.
- Steinberg, R. H., Wood, I. and Hogan, M. J.** (1977). Pigment epithelial ensheathment and phagocytosis of extrafoveal cones in human retina. *Philos Trans R Soc Lond B Biol Sci* **277**, 459-74.
- Story, G. M., Peier, A. M., Reeve, A. J., Eid, S. R., Mosbacher, J., Hricik, T. R., Earley, T. J., Hergarden, A. C., Andersson, D. A., Hwang, S. W. et al.** (2003). ANKTM1, a TRP-like channel expressed in nociceptive neurons, is activated by cold temperatures. *Cell* **112**, 819-29.
- Strauss, O.** (2005). The retinal pigment epithelium in visual function. *Physiol Rev* **85**, 845-81.
- Sun, L., Liu, A. and Georgopoulos, K.** (1996). Zinc finger-mediated protein interactions modulate Ikaros activity, a molecular control of lymphocyte development. *Embo J* **15**, 5358-69.
- Suzuki, Y., Takeda, M. and Farbman, A. I.** (1996). Supporting cells as phagocytes in the olfactory epithelium after bulbectomy. *J Comp Neurol* **376**, 509-17.

- Takayama, J., Faumont, S., Kunitomo, H., Lockery, S. R. and Iino, Y.** (2009). Single-cell transcriptional analysis of taste sensory neuron pair in *Caenorhabditis elegans*. *Nucleic Acids Res* **38**, 131-42.
- Taniguchi, H., Gollan, L., Scholl, F. G., Mahadomrongkul, V., Dobler, E., Limthong, N., Peck, M., Aoki, C. and Scheiffele, P.** (2007). Silencing of neuroligin function by postsynaptic neurexins. *J Neurosci* **27**, 2815-24.
- Tautz, D., Lehmann, R., Schnurch, H., Schuh, R., Seifert, E., Kienlin, A., Jones, K. and Jackle, H.** (1987). Finger protein of novel structure encoded by hunchback, a second member of the gap class of *Drosophila* segmentation genes. *Nature* **327**, 383-389.
- Theodosis, D. T. and Poulain, D. A.** (1993). Activity-dependent neuronal-glia and synaptic plasticity in the adult mammalian hypothalamus. *Neuroscience* **57**, 501-35.
- Timmons, L. and Fire, A.** (1998). Specific interference by ingested dsRNA. *Nature* **395**, 854.
- Tominaga, M., Caterina, M. J., Malmberg, A. B., Rosen, T. A., Gilbert, H., Skinner, K., Raumann, B. E., Basbaum, A. I. and Julius, D.** (1998). The cloned capsaicin receptor integrates multiple pain-producing stimuli. *Neuron* **21**, 531-43.
- Trachtenberg, J. T., Chen, B. E., Knott, G. W., Feng, G., Sanes, J. R., Welker, E. and Svoboda, K.** (2002). Long-term in vivo imaging of experience-dependent synaptic plasticity in adult cortex. *Nature* **420**, 788-94.
- Ullian, E. M., Sapperstein, S. K., Christopherson, K. S. and Barres, B. A.** (2001). Control of synapse number by glia. *Science* **291**, 657-61.
- Van De Bor, V., Walther, R. and Giangrande, A.** (2000). Some fly sensory organs are gliogenic and require glide/gcm in a precursor that divides symmetrically and produces glial cells. *Development* **127**, 3735-43.
- Ventura, R. and Harris, K. M.** (1999). Three-dimensional relationships between hippocampal synapses and astrocytes. *J Neurosci* **19**, 6897-906.
- Wadsworth, W. G., Bhatt, H. and Hedgecock, E. M.** (1996). Neuroglia and pioneer neurons express UNC-6 to provide global and local netrin cues for guiding migrations in *C. elegans*. *Neuron* **16**, 35-46.
- Wang, W. Y., Dong, J. H., Liu, X., Wang, Y., Ying, G. X., Ni, Z. M. and Zhou, C. F.** (2005). Vascular endothelial growth factor and its receptor Flk-1 are expressed in the hippocampus following entorhinal deafferentation. *Neuroscience* **134**, 1167-78.
- Wang, Y., Apicella, A., Jr., Lee, S. K., Ezcurra, M., Slone, R. D., Goldmit, M., Schafer, W. R., Shaham, S., Driscoll, M. and Bianchi, L.** (2008). A glial DEG/ENaC channel functions with neuronal channel DEG-1 to mediate specific sensory functions in *C. elegans*. *Embo J* **27**, 2388-99.

- Ward, D. M., Ferris, M. J., Nold, S. C. and Bateson, M. M.** (1998). A natural view of microbial biodiversity within hot spring cyanobacterial mat communities. *Microbiol Mol Biol Rev* **62**, 1353-70.
- Ward, S., Thomson, N., White, J. G. and Brenner, S.** (1975). Electron microscopical reconstruction of the anterior sensory anatomy of the nematode *Caenorhabditis elegans*. *J Comp Neurol* **160**, 313-37.
- White, J. G., Southgate, E., Thomson, J. N. and Brenner, S.** (1986). The structure of the nervous system of the nematode *Caenorhabditis elegans*. *Philos Trans R Soc Lond B Biol Sci* **314**, 1-340.
- Wicks, S. R., Yeh, R. T., Gish, W. R., Waterston, R. H. and Plasterk, R. H.** (2001). Rapid gene mapping in *Caenorhabditis elegans* using a high density polymorphism map. *Nat Genet* **28**, 160-4.
- Woolley, C. S., Gould, E., Frankfurt, M. and McEwen, B. S.** (1990). Naturally occurring fluctuation in dendritic spine density on adult hippocampal pyramidal neurons. *J Neurosci* **10**, 4035-9.
- Xuan, S., Baptista, C. A., Balas, G., Tao, W., Soares, V. C. and Lai, E.** (1995). Winged helix transcription factor BF-1 is essential for the development of the cerebral hemispheres. *Neuron* **14**, 1141-52.
- Yoshimura, S., Murray, J. I., Lu, Y., Waterston, R. H. and Shaham, S.** (2008). *mls-2* and *vab-3* Control glia development, *hlh-17/Olig* expression and glia-dependent neurite extension in *C. elegans*. *Development* **135**, 2263-75.
- Young, R. W. and Bok, D.** (1969). Participation of the retinal pigment epithelium in the rod outer segment renewal process. *J Cell Biol* **42**, 392-403.
- Yu, R. Y., Nguyen, C. Q., Hall, D. H. and Chow, K. L.** (2000). Expression of *ram-5* in the structural cell is required for sensory ray morphogenesis in *Caenorhabditis elegans* male tail. *Embo J* **19**, 3542-55.